AD

RSIC-670

INTEGRATION OF NASA-SPONSORED STUDIES ON ALUMINUM WELDING

by

Koichi Masubuchi
Battelle Memorial Institute
505 King Avenue
Columbus, Ohio 43201

Contract No. DA-01-021-AMC-14693(Z)

September 1967

REDSTONE SCIENTIFIC INFORMATION CENTER
REDSTONE ARSENAL, ALABAMA

JOINTLY SUPPORTED BY

U.S. ARMY MISSILE COMMAND

GEORGE C. MARSHALL SPACE FLIGHT CENTER

DISPOSITION INSTRUCTIONS

Destroy this report when no longer needed. Do not return it to the originator.

DISCLAIMER

The findings in this report are not to be construed as an official Department of the Army position unless so designated by other authorized documents.

28 September 1967 RSIC-670

INTEGRATION OF NASA-SPONSORED STUDIES ON ALUMINUM WELDING

by

Koichi Masubuchi
Battelle Memorial Institute
505 King Avenue
Columbus, Ohio 43201

Contract No. DA-01-021-AMC-14693(Z)

Research Branch
Research and Development Directorate
Redstone Scientific Information Center
U. S. Army Missile Command
Redstone Arsenal, Alabama 35809

ABSTRACT

This report analyzes and integrates the findings of NASA-sponsored studies on the welding of aluminum alloys. It covers information received through 15 February 1967. On this basis, nine of the eleven research programs currently sponsored by NASA on welding aluminum are covered. The following subjects are discussed:

1) Effects of shielding-gas contamination on porosity

2) Effects of base- and filler-metal contamination on porosity

3) Mechanisms of porosity formation

4) Scavenger elements to reduce porosity

5) Effects of porosity on weld-joint performance

6) Time-temperature effects and control

7) Transferability of welding parameters in the gas tungsten-arc process

8) Development of arc shaper and puddle stirrer

9) Material preparation.

Major findings obtained in the nine programs on welding aluminum are described, analyzed, and integrated. Recommendations are presented for future work and for application of the integrated findings to the fabrication of structural components of Saturn V rockets.

FOREWORD

This is a report of a program to analyze and integrate data generated from NASA-sponsored studies on the welding of aluminum alloys.

Information in this report comes from the Marshall Space Flight Center, from visits to the Lockheed-Georgia Company, Marietta, Georgia; the Martin Company, Denver, Colorado; the Douglas Missile and Space Systems Division, Santa Monica, California; Harvey Aluminum, Incorporated, Torrance, California; The Boeing Company, Seattle, Washington; the Illinois Institute of Technology Research Institute, Chicago, Illinois; and the Air Reduction Company, Incorporated, Murray Hill, New Jersey.

CONTENTS

CONTENTS (Continued)

CONTENTS(Continued)

CONTENTS (Concluded)

ILLUSTRATIONS

ILLUSTRATIONS (Continued)

ILLUSTRATIONS (Concluded)

Section I. INTRODUCTION

Although this report is concerned only with the welding of aluminum structures, it is important to understand that this is only one phase of the fabrication of a complex structure such as the Saturn V rocket, and must eventually be related to a much greater whole. The Saturn V structure requires a very complex system of design and fabrication composed of many phases. These phases include design, material selection, stress analysis, cutting, machining, forming, joining, and inspection. Each phase is closely related to and dependent upon the others. For example, the material selection must be made not only on the basis of mechanical properties but also with regard to forming and joining the material. The design must be made so that a structure with sufficient reliability can be fabricated with a tolerable dimensional accuracy. There are also many factors within each phase of design and fabrication. For example, the quality of a weld depends upon such factors as the cleanliness of the metal surface, purity of the shielding gas, and the welding conditions. To improve the structural reliability of a space vehicle, we must know more about each phase, the relationship of factors within it, the relationship of any one phase to other phases, and, ultimately, the importance of each phase to the final product. With this knowledge, time and money can be spent most effectively to improve the product. NASA has recognized the importance of conducting several aluminum welding studies and integrating the results in this report. It is equally important that studies of the phases outlined above be made and that the results be integrated in a like manner.

Welding is used extensively in the fabrication of space vehicles. NASA has selected high-strength aluminum alloys, primarily 2014 and 2219. Table I gives some characteristics of these alloys. Gas tungsten-arc (GTA) and gas metal-arc (GMA) processes are being used for the fabrication of some components, including fuel tanks. However, fusion welding of high-strength, heat-treated aluminum alloys presents the following reliability problems:

1) Possibility of obtaining defects in welds

2) Undesirable thermal effects due to welding heat

Aluminum alloys are subject to certain types of weld defects, especially porosity. Every attempt should be made to minimize porosity, but it has become especially important because of the limited effectiveness of presently available inspection techniques. Among various nondestructive inspection techniques, visual and X-ray (and sometimes ultrasonic) inspections are used to examine structural welds. However, none of these techniques is completely satisfactory. The usefulness of visual inspection is limited. X-ray

TABLE I. CHARACTERISTICS OF 2014 AND 2219 ALUMINUM ALLOYS

2014 ALLOY		
Type	Wrought, heat treatable aluminum alloy	
Nominal composition	Al-4.4Cu-0.8Mn-0.8Si-0.4Mg	
Availability	Bare and clad sheet and plate, rod, bar, wire, tube, extruded shapes, forgings and forging stock	
Typical physical properties	Density	2.815 g/cm^3 at RT
	Thermal conductivity	0.46 cal/cm sec °C (O temper) 0.37 cal/cm sec °C (T6 temper)
	Thermal expansion	(20-100C), 22.5 × 10^{-6} in./in./°C
	Specific heat	0.23 cal/g cm at 100°C
	Electrical resistivity	3.45 μ ohm-cm at RT (O temper) 4.31 μ ohm-cm at RT (T6 temper)
Typical mechanical properties	Ultimate tensile strength	27,000 psi (O temper) 70,000 psi (T6 temper)
	0.2% Tensile yield strength	14,000 psi (O temper) 60,000 psi (T6 temper)
	Elongation (2-in.)	18% (O temper) 13% (T6 temper)
	Modulus of elasticity (tension)	10.6 × 10^6 psi

TABLE I. (Continued)

Fabrication characteristics	Weldability	Good (fusion and resistance methods) if proper procedures are used
	Formability	Good in the annealed condition difficult to form in T6 temper
	Machinability	Good in the T6 temper
Comments	A high-strength aluminum alloy which is often used for heavy-duty structures	
2219 ALLOY		
Type	Wrought, heat treatable aluminum alloy	
Nominal composition	Al-6.3Cu-0.3Mn-0.18Zr-0.1V-0.06T1	
Availability	Bare and clad sheet, plate, forgings, extrusions, drawn tube, rod and bar	
Typical physical properties	Density	2.82 g/cm^3 at RT
	Thermal conductivity	0.41 cal/cm sec °C (O temper) 0.30 cal/cm sec °C (T62 temper)
	Thermal expansion	(20-100°C), 22.3 in./in./°C
	Electrical resistivity	3.90 μ ohm-cm at RT (O temper) 5.23 μ ohm-cm at RT (T62 temper)
Typical mechanical properties	Ultimate tensile strength	25,000 psi (O temper) 68,000 psi (T87 temper)
	0.2% Tensile yield strength	10,000 psi (O temper) 56,000 psi (T87 temper)

TABLE I. (Concluded)

	Elongation (2-in.)	20% (O temper) 10% (T87 temper)
	Modulus of elasticity	10.6×10^6 psi
Fabrication characteristics	Weldability	Excellent (fusion and resistance methods)
	Formability	Slightly superior to 2014 alloy
	Machinability	Good in annealed condition
Comments	Alloy has good mechanical properties at cryogenic temperatures and at elevated temperatures up to 600°F. Recommended for applications requiring high-strength weldments.	

inspection is usually two-dimensional, and three-dimensional distributions of defects are not determined.

The intense heat generated by the welding arc causes various undesirable thermal effects. Metallurgical structures of the weld metal and the heat-affected zone differ from those of the original base metal. A welded joint is composed of many zones with different structures and mechanical properties. It is known that the ultimate tensile strength of a welded joint in high-strength heat-treated aluminum alloy decreases with increasing heat input, i.e., the amount of heat energy supplied per inch of weld length. Welding heat also causes residual stresses and distortion. Because there is no reliable non-destructive technique to determine the strength of a welded structure, it is essential to control the manufacturing process so that the fluctuation in behavior of welded structures can be minimized and limited to a certain range.

The ultimate purpose of the NASA welding research program is to improve the performance and reliability of space vehicles. This can be done by investigating each of the problems involved and then determining how best to utilize the information obtained. Results obtained in some of the investigations may be contradictory; for example, a welding process using a certain set of parameters found to be very effective in reducing porosity may be undesirable because of large thermal effects. It is important, therefore, to integrate results obtained in the individual investigations. Such integration of data will provide a basis of recommendations for design and fabrication of space vehicles.

The welding process is a dynamic whole, an entirety. It is a series of interrelated, interdependent events. We are not able to minutely analyze the dynamic whole, but must arbitrarily select restricted areas for study, which might be considered fragments of the map of welding. The studies listed herein are such fragments which collectively represent a major portion of welding technology. The time comes, however, when the fragments must be integrated and the whole map constructed, if we are to understand welding and if we are to formulate process control. The present report is a first step in the integration of individual, independent studies.

Process control is the final objective: quantitative limits of the major variables which can be expressed in manufacturing specifications. Such specifications will supplement inspection in the assurance of weld-joint reliability.

Section II. OBJECTIVE AND PROCEDURES OF THE PRESENT STUDY

1. Objective

The objective of the present study is to analyze and integrate several interrelated studies conducted by various organizations for Marshall Space Flight Center. These studies are intended to improve current aluminum welding techniques. The studies which are to be or have been integrated are listed below:

1) Gas Analysis Study by The Boeing Company under Contract NAS8-20168 - a quantitative study of the role of gas contaminants as a source of defects in welds.

2) Base Metal Studies (Phases I and II) by Battelle Memorial Institute under Contracts NAS8-11445 and NAS8-20303 - a study of effects of chemistry, internal and external impurities, and hydrogen content of base metal on porosity in welds.

3) Mechanisms of Porosity by Douglas Aircraft Company under Contract NAS8-11332 - an effort to find methods of porosity arrest and inhibition through a study of how it nucleates and grows.

4) Gas Scavenger Study by Southern Research Institute under Contract NAS8-20307 - a study seeking an element with affinity for porosity-forming gases that would tie them up in a harmless way or wash them out of the molten pool.

5) Defects Versus Joint Performance by Martin Company under Contract NAS8-11335 - a study to formulate realistic weld quality standards by quantitatively analyzing the effect of defects on weld strength.

6) Time-Temperature Control by Harvey Aluminum, Incorporated, under Contract NAS8-11930 - a study for formulating methods of producing and controlling time-temperature gradients in fusion welding that will yield optimum responses, i.e., ultimate strength, yield strength, elongation, X-ray quality, etc.

7) Data Transfer by Lockheed-Georgia Company under Contract NAS8-11435 - a study consisting of arranging welding variables in order of importance and devising instrumentation and control that will insure accurate transfer from laboratory to production.

8) Arc Shaper and Molten Puddle Stirrer by Air Reduction Company under Contract NAS8-11954 - a study to increase power density of the GTA arc and agitation of the molten puddle.

9) Material Preparation by Illinois Institute of Technology Research Institute under Contract NAS8-20363 - a study to identify the surface of the material to be welded, i.e., identifying organic material, hydrogen, etc.

10) Welding Power Supply Output Wave Shape on Weld Joint Performance by Air Reduction Company under Contract NAS8-20338 - an investigation of the effect of AC, DC, and a combination of AC and DC, various wave shapes, and frequencies on the weld joint.

11) Nonvacuum Electron-Beam Welding by Westinghouse Electric Corporation under Contract NAS8-11929 - analysis of welding parameters, energy input, and shielding gas with defect level and mechanical properties as major responses.

This report also integrates information generated in studies, conducted at Marshall Space Flight Center, of the time-temperature relationship in welding aluminum alloys.

The present report covers information received up to 15 February 1967.

2. Procedures of the Present Study

The major source of information used for the present study was documents supplied by the Marshall Space Flight Center, Manufacturing Engineering Laboratory, NASA. These documents include (1) proposals, monthly reports, and interim, summary, and/or final reports prepared for the above 11 NASA-sponsored programs, and (2) reports and memorandums on the NASA in-house program on time-temperature relationship.

On the basis of the progress of the NASA-sponsored research programs, as of 15 February 1967, it was decided that the present report should cover thoroughly the following nine programs:

1) gas analysis

2) base metal

3) mechanisms of porosity

4) gas scavenger

5) defects versus joint performance

6) time-temperature control

7) data transfer

8) arc shaper and molten puddle stirrer

9) material preparation .

The remaining studies had not been completed and will be covered in future reports.

Titles of the final reports and the interim report on the nine programs covered in this report are listed in Literature Cited.[3-14] Information on welding time-temperature effect has been supplied by the Marshall Space Flight Center, NASA.[15]

Conclusions given in the final reports and the interim reports on the nine programs are summarized in the Appendix. These conclusions were drawn by the investigators working on the programs and do not necessarily agree with the conclusions and opinions given in the main body of the present report.

Section III. GENERAL DESCRIPTION OF THE NASA RESEARCH PROGRAMS ON ALUMINUM WELDLING

Figure 1 illustrates the relationships between problems in fusion welding of high-strength heat-treated aluminum alloys and the current NASA-sponsored research programs. The ultimate objective of the whole NASA effort is to develop a system of controlling weld quality to improve performance and reliability of space vehicles. Many problems need to be solved before this ultimate objective is reached. The current programs are directed toward the following three major problems:

1) Reduction of porosity and its effect on the behavior of weldments

2) Reduction of thermal effects of welding on the behavior of weldments

3) Improvements of weld-joint properties.

1. Weld Porosity

Weld porosity has been a major problem in the use of high-strength aluminum alloys for structural components of space vehicles that must operate under severe loading conditions. Many of the current NASA-sponsored programs are concerned with the porosity problem. Subjects that are being investigated or considered for future investigation include:

1) Reduction of porosity

   a) Sources of porosity. What causes the porosity contamination attributed to shielding gas, unclean joint surfaces, improper composition of base plate or filler metal? How can these causes be removed? How can we find whether these causes are removed?

   b) Mechanisms of porosity. How is porosity formed?

   c) Effects of welding parameters and processes. How do welding parameters affect the size and distribution of porosity? What combinations of welding parameters produce less porosity -- high current and low travel speed or low current and high travel speed? Which welding process is suitable for reducing porosity--GTA, GMA, or a new process? What are the effects of power supply--D-C or A-C, straight or reverse polarity?

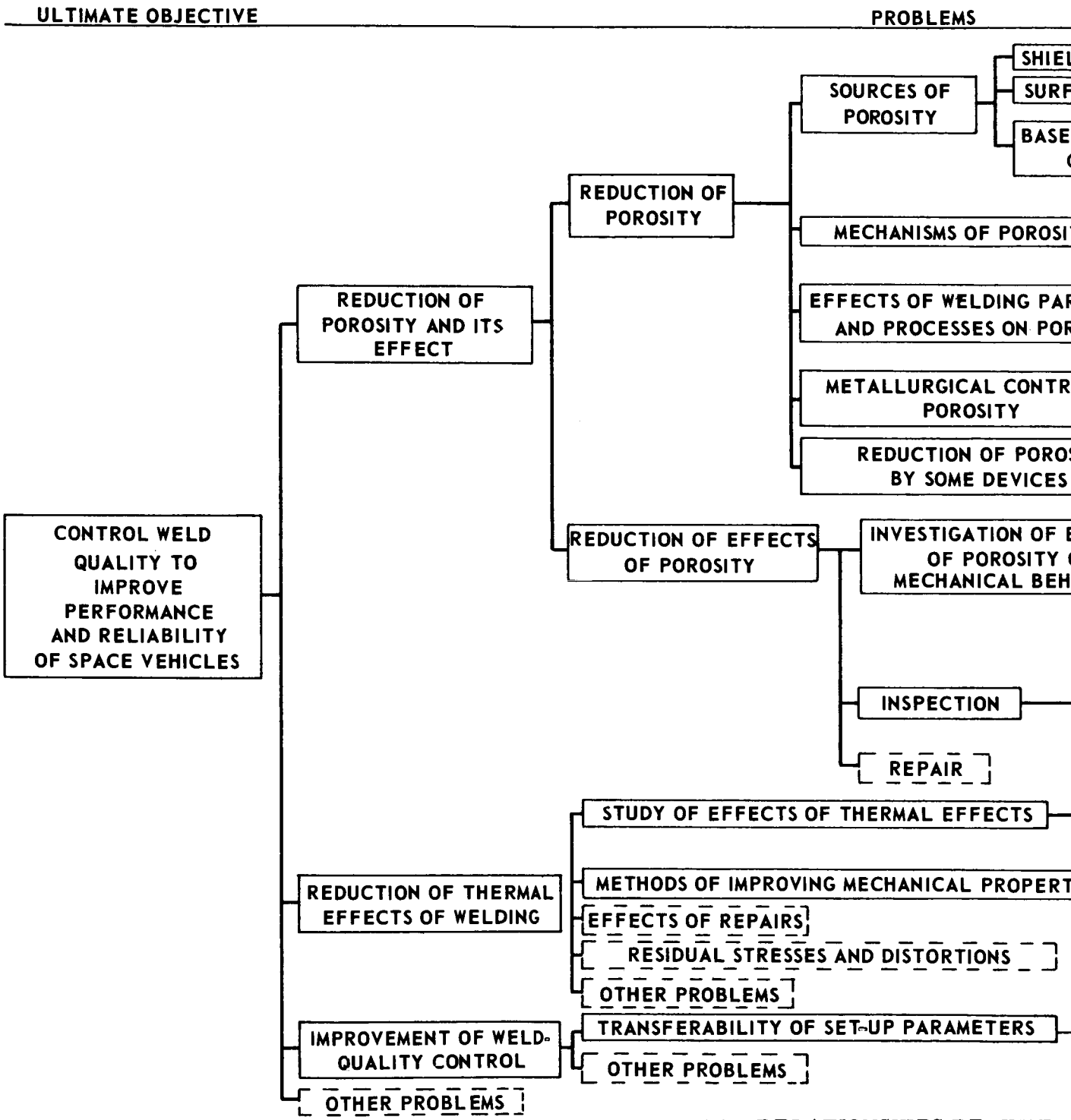

FIGURE 1. RELATIONSHIPS BETWEEN
ALUMINUM ALLOYS AND THE CURREN

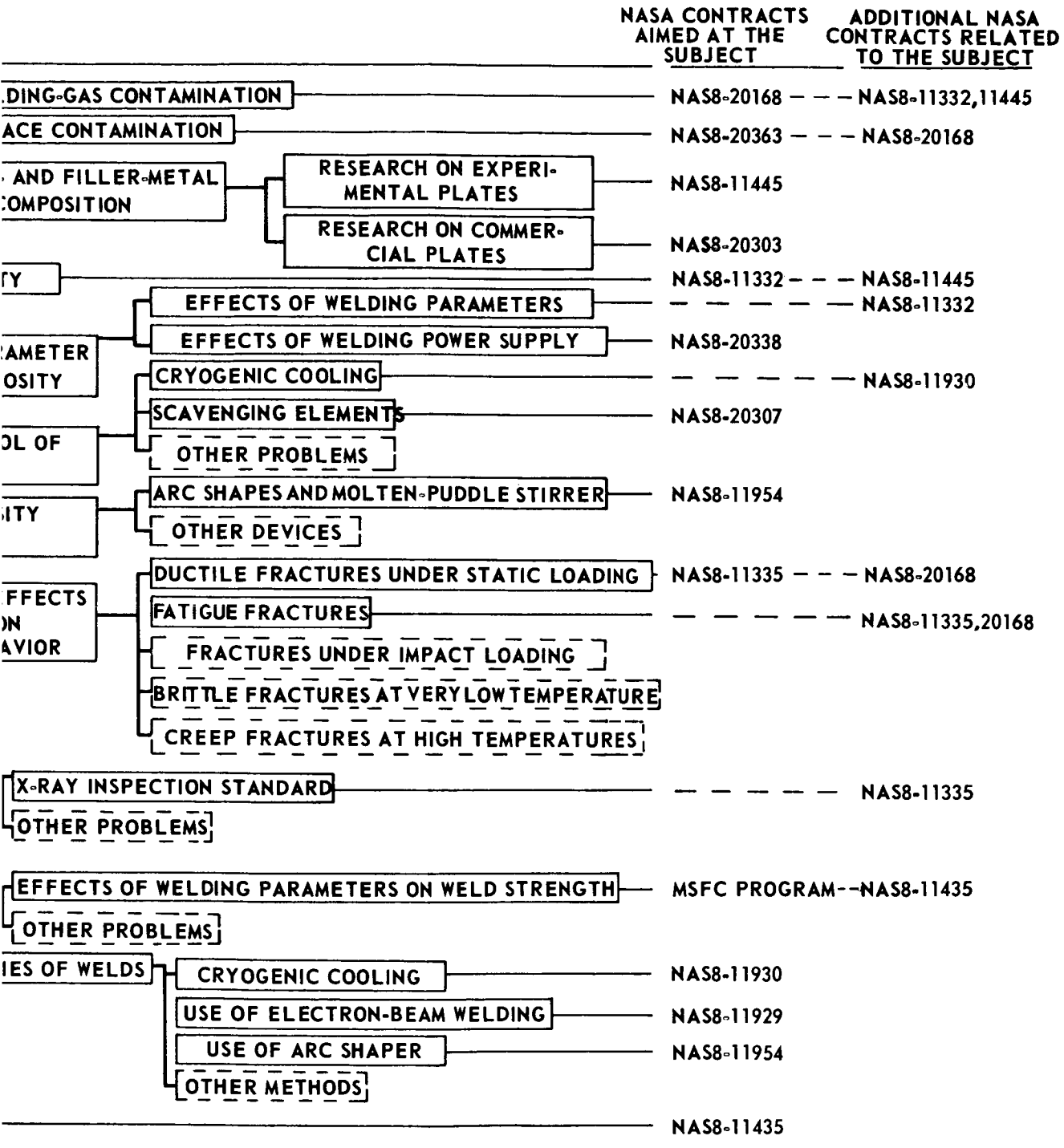

PROBLEMS IN FUSION WELDING HIGH-STRENGTH HEAT-TREATED
T NASA-SPONSORED RESEARCH PROGRAMS

d) Metallurgical control of porosity. Is there any way to reduce porosity metallurgically? Should we cool the molten metal faster or more slowly? Is it feasible to add some elements to reduce hydrogen by chemical reactions in the molten metal?

e) Reduction of porosity by mechanical devices. Is it feasible to reduce porosity by such a device as a molten puddle stirrer?

2) Effects of porosity

a) Investigation of effects of porosity on mechanical behavior. How does porosity affect the mechanical behavior of weldments under static, impact, or repeated loading? What about the effects of porosity on the strength of welds at very low or high temperatures? How much porosity can be accepted under what conditions?

b) Inspection. How can we inspect for porosity? How can we set an acceptance standard?

c) Repair. If a weld contains porosity that is unacceptable, how can the weld be repaired with minimum detrimental effects?

Many of these questions are being answered in the current programs. Programs at Boeing, Battelle, and IITRI were aimed at studying sources of porosity. The objective of the Boeing work was to establish a quantitative relationship between atmospheric contaminants in the arc-shielding medium and the magnitude and frequency of porosity in 2219-T87 aluminum GTA weldments. Welds were made in an atmospheric control chamber filled with helium containing various levels of contaminants including oxygen, hydrogen, nitrogen, and water vapor. Information on the effects of shielding-gas contamination on porosity also has been obtained under contracts with Douglas and Battelle. The objective of the IITRI study was to establish standardized methods of assuring high-quality surface preparation for the welding of aluminum-alloy Saturn V components. Information on the effects of surface contamination on porosity also has been obtained in the Boeing study. Effects of base- and filler-metal composition on porosity were studied at Battelle. Welds made with experimental base and filler metals and welds in commercial plates were studied.

The problem of porosity formation in aluminum-base alloy welds and castings has been the subject of numerous other investigations.[16-23] These and additional studies have shown that hydrogen is the principal, if not the sole, cause of porosity. However, little is known of the kinetics of porosity

formation. An understanding of the kinetics is especially important in welding, where the range of heating and cooling cycles can produce important effects. Work at Douglas was directed toward studying mechanisms responsible for porosity in aluminum welds in terms of metallurgical phenomena as well as welding parameters.

Studies at Southern Research Institute and Air Reduction Company were directed toward developing techniques for reducing porosity. At Southern Research Institute, a study was made to determine the feasibility of reducing porosity by a metallurgical method involving the use of scavenging elements for eliminating hydrogen porosity in the weld metal. The scavenging elements were to be capable of combining with the hydrogen gas and forming relatively harmless compounds that would have insignificant effects on the mechanical properties of the weld. At AIRCO, a study was made to reduce porosity by using some device such as a magnetic arc shaper and a molten-puddle stirrer.

It is believed that information pertinent to the reduction of porosity can be obtained in several other programs. The primary objective of a program at Harvey Aluminum was to improve mechanical properties of a weldment by reducing the thermal effect. They investigated the possibility of reducing porosity by rapidly cooling the weldment during welding with a cryogenic liquid. At AIRCO, a study is being made to assess the relative merits of the output wave shape of the welding power supply and its effects on weld-joint quality and performance.

The Martin Company conducted a study on the effect of porosity on the performance of welded joints. The objective of this program was to enable an inspector to describe a weld defect in terms that allow a precise prediction of a joint's expected mechanical properties. This requires a defect classification system that can predict the mechanical behaviors of interest. Static tensile tests were made on transverse- and longitudinal-weld specimens containing various levels of porosity. A limited study also was made of fatigue strength of welds containing porosity. The study at Boeing provided data on the effect of porosity on the static and fatigue strengths of welded joints.

2. Thermal Effects of Welding

The second major problem in the current NASA research on aluminum welding is the reduction of thermal effects of welding on the behavior of weldments. A research program is being conducted at the Manufacturing Engineering Laboratory of Marshall Space Flight Center, NASA, on the effects of welding heat input on the mechanical properties of aluminum welds.[5]

Figure 2, which summarizes the test results, shows the relationship between the following two variables.

1) Welding heat input per unit plate thickness

$$\frac{V.I \times 60}{s \times T}, \text{ joules/in.}^2, \tag{1}$$

where

V = arc voltage, v

I = welding current, amp

s = arc travel speed, ipm

T = plate thickness, in.

2) Ultimate tensile strengths of transverse-weld specimens prepared from weldments in 2219-T81 and -T87 alloys 0.224 to 2.25 in. thick made by GTA, GMA, and electron-beam welding processes.

Figure 2 shows that the ultimate tensile strengths of welded joints decreased as welding heat input increased, regardless of the welding process or the material thickness. The higher weld strength obtained by using low heat input is believed to be due to (1) a reduced thermal effect and (2) the geometrical effect of a narrow weld. A reduction in weld heat input appears to result in a heat-affected zone with higher-strength metallurgical structures. A joint with a very narrow weld-metal area, but with a heat-affected zone that has lower strengths than the base metal, still has nearly the same fracture strength as the base metal. This is because the plastic deformation in the weld metal and the heat-affected zone is restricted by the surrounding base metal. NASA is conducting a study of physical metallurgy on aluminum weldments in an attempt to determine the mechanisms of why welded joint strength increases as heat input decreases.

A study is needed on how the information shown in Figure 2 can be used for designing specific components. For example, when the major stress acting on a joint is parallel to the joint, it is obvious that the ultimate tensile strength across the weld joint has little effect on the strength of that particular structural element. Consequently, there is no actual benefit from reducing heat input for such joints. However, there may be cases where the increase in strength by reducing heat input is critical. These areas need to be more closely defined.

In the current programs, studies were made of electron-beam (EB) welding and cryogenic cooling as possible means of improving weld strength. Since the heat generated during electron-beam welding is highly concentrated in the weld area, a joint can be made with a very narrow weld-metal area and heat-affected zone. A limited investigation conducted at the Marshall Space Flight Center has shown that successful welds can be made by the EB process with much lower heat input than required by ordinary GTA and GMA processes, and that the ultimate strengths of EB welds are much higher than those of GTA and GMA welds, as shown in Figure 2. However, with the present EB process the weld must be made in a vacuum chamber; consequently, use of the electron-beam process has been limited to the joining of small parts. Westinghouse is conducting a NASA program to develop a practical, nonvacuum EB-welding unit capable of penetrating 1-in. thick 2219 aluminum alloy. This would enable electron-beam welding to be used for the fabrication of large structural components. However, the program was not completed as of 15 February 1967; therefore, it is not covered in this report.

It was thought the same effect as the reduction of welding heat input could be obtained by absorbing the heat conducted into the base plate during welding. The absorption of heat could be achieved by forced cooling of the base plate by impingement of cryogenic liquids, such as liquid CO_2 and liquid nitrogen. At Harvey Aluminum, a study was of the effect of cryogenic cooling during welding on properties of weldments.

3. Weld Quality Control

It is recognized that there are a number of quality-control problems in welding. Consider, for example, the size and shape of the weld. The depth of penetration is not always uniform; it fluctuates along the weld, especially when the weld is made with certain types of welding equipment. When welds are made with machines having different characteristics, the sizes and shapes of welds may differ to some extent, even though the welds are made with the same welding parameters, including welding current, arc voltage, and travel speed.

Ideally, welds should have the same configuration (depth of penetration, weld area, etc.) and quality no matter where or when they are made (by different fabricators at different times); provided the same type of equipment, tooling, and joint design, and the same welding parameters are used. To attain this objective, the following problems are being investigated or considered for future investigation:

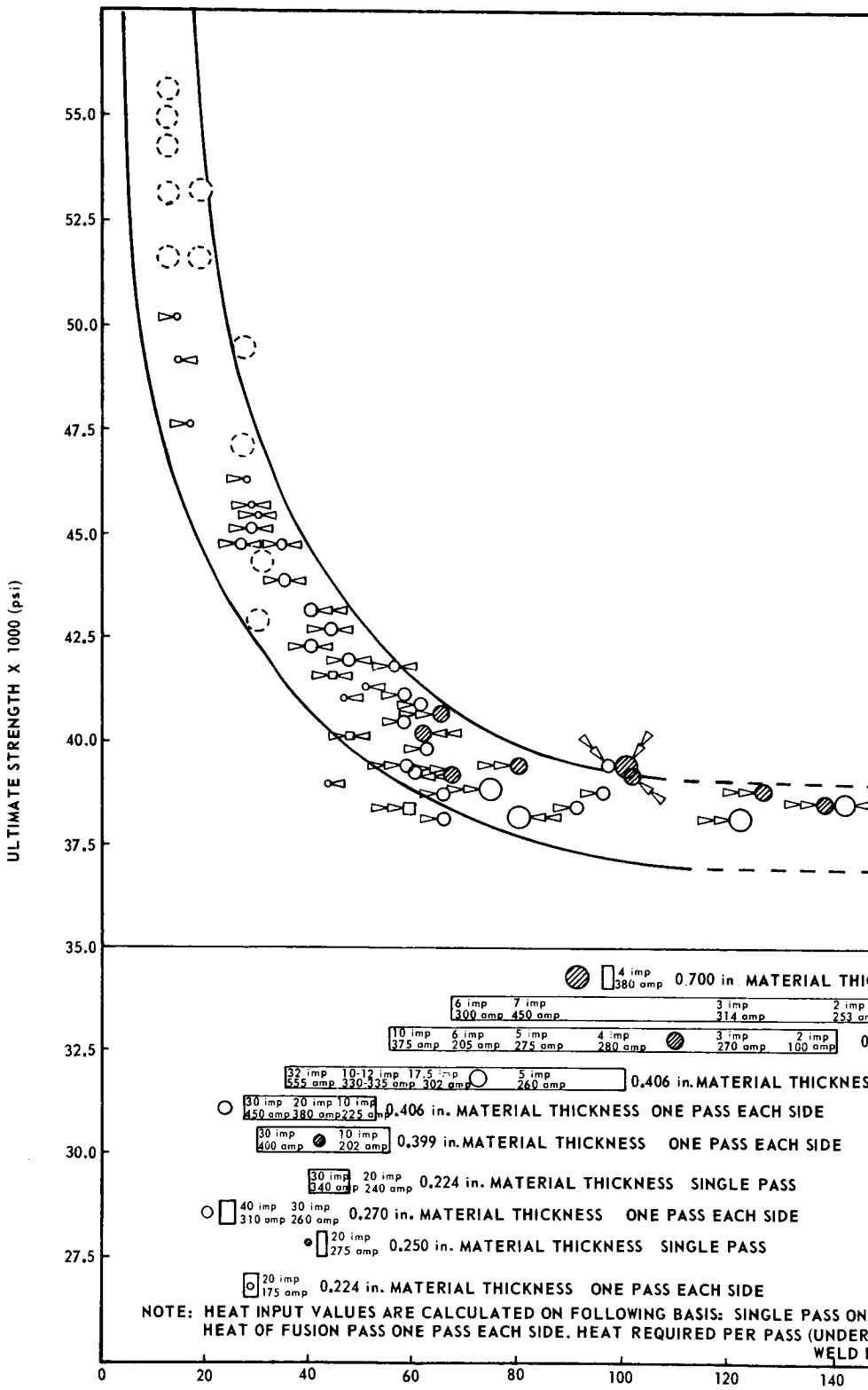

FIGURE 2. HEAT INPUT VERSUS ULTIMAT

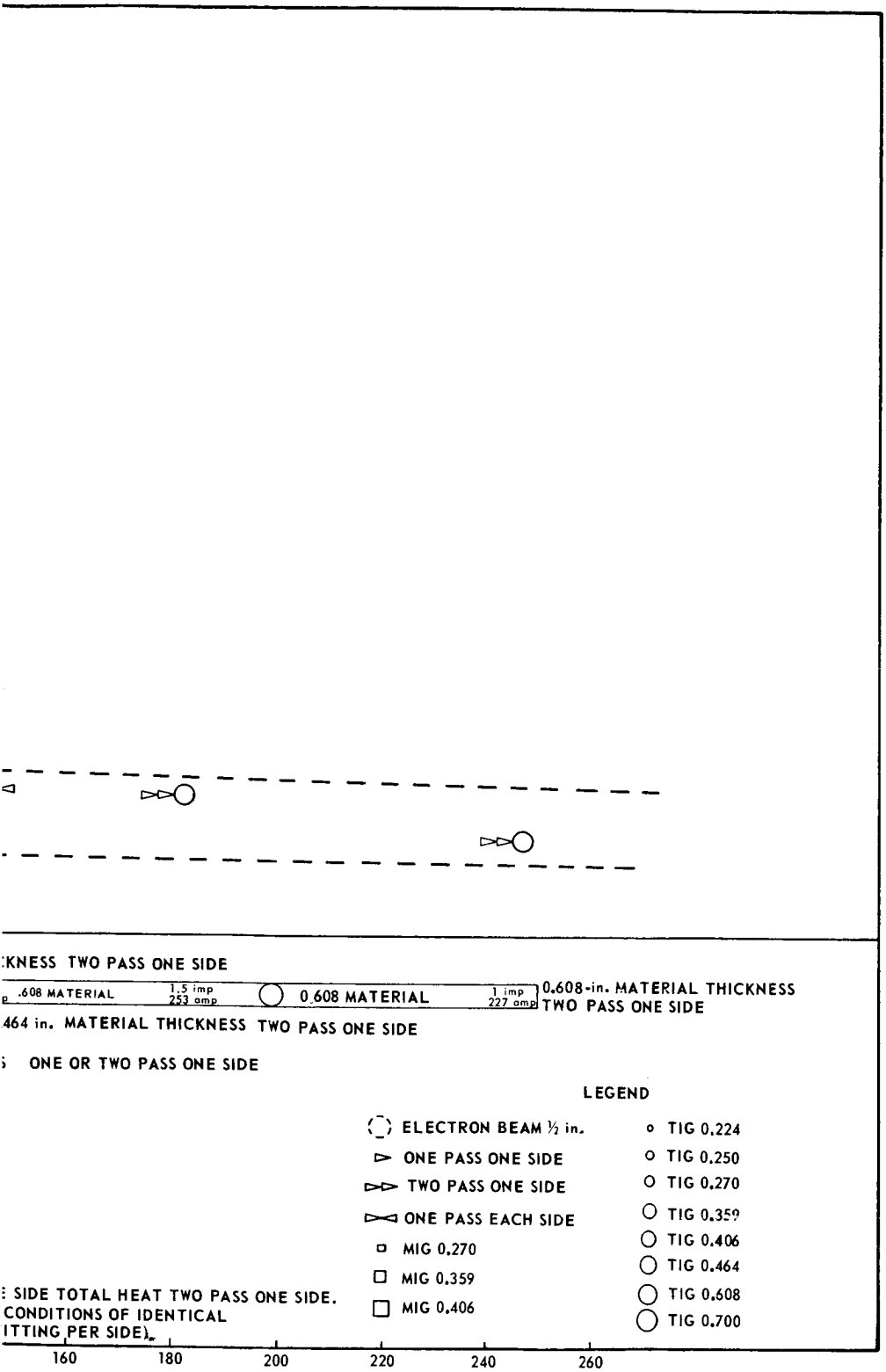

E STRENGTH, 2219-T87 AND T81 ALUMINUM ALLOYS

1) What type of welding equipment (with what types of voltage, current, and electrode-position control systems) is most suitable to obtain consistent welds?

2) What weld-quality characteristics are likely to fluctuate--depth of penetration, size and shape of weld, metallurgical and mechanical properties of welds? How are they affected by different welding parameters?

3) How are weld-quality characteristics changed when welding equipment is changed? How should we transfer welding parameters from one welding setup to another to obtain welds with the same quality?

The objective at Lockheed-Georgia was to study the transferability of setup parameters for inert-gas welding. To accomplish this, attempts were made to determine (1) the significant variables and (2) the degree of control that can be achieved.

Section IV. SUMMARY OF INTEGRATION STUDY AND RECOMMENDATIONS

This section summarizes major findings in the nine NASA programs covered in this report. The following areas of investigation are discussed:

1) Sources of porosity

2) Mechanisms of porosity

3) Methods for reducing porosity

4) Effects of porosity level on weld-joint performance

5) Welding time-temperature control

6) Transferability of welding machines and parameters.

The major findings in each area are discussed briefly and the integrator's recommendations are made for application to Saturn V fabrication and for future research. Following these discussions, general recommendations for the selection of weld parameters and for weld inspection and repair are presented.

1. Sources of Porosity

Sources of porosity in aluminum weldments can be classified as: (1) contamination of shielding gas, (2) contamination of the joint or filler-metal surfaces, and (3) composition of base plate and filler metal.

a. Shielding-Gas Contamination

It has been found that shielding-gas contamination can be one of the major sources of porosity in aluminum weldments. However, it also has been found that commercial shielding gas is normally acceptably pure as received. In the NASA-sponsored programs conducted at Boeing,[3] Battelle,[4,5] Douglas,[6] and Martin,[9] investigators reported that it was always necessary to intentionally contaminate the shielding gas to produce an appreciable amount of porosity. Welds made in the laboratory did not contain appreciable amounts of porosity when they were made with proper procedures, i.e., when plates were cleaned properly and commercially pure shielding gas was used.

The effect of individual gas contaminants were studied by making welds in an atmospheric-control chamber containing various levels of gas contamination.[3] The metal studied was 1/4-in. thick, 2219-T87 aluminum alloy, welded in the horizontal position by the GTA process using 1/16-in. diameter, 2319 aluminum-alloy filler wire. The following results were obtained:

1) Increasing hydrogen concentration increased porosity.

2) Increasing water vapor increased porosity.

3) Increasing oxygen did not increase porosity; in some cases, a slight decrease in porosity was observed.

4) Increasing nitrogen had little effect on porosity.

The Boeing investigators presented Figure 3 as a guide for controlling shielding-gas contamination.[3] The contamination levels shown indicate where occurrence of a weld-quality change is initially observed. The figure indicates that 250 ppm of either hydrogen or water vapor was necessary before significant quality changes were observed. As shown in Figure 3, shielding-gas contamination caused various effects including surface discoloration, undercut, and reduction in arc stability. Such phenomena also were observed in other programs.[4,5,6,9]

Figure 4 gives the calculated relationship, as determined by the Boeing investigators, between percent of water-saturated air in the base gas and resulting hydrogen concentration.[3] The figure indicates that at 70°F, for example, an addition of 0.6 percent saturated air to pure helium would result in 250 ppm hydrogen in the shielding gas.

On the basis of experience gained in the current programs, the integrator believes that there is no reason to change the present NASA specification (MSFC-364A) for shielding gas. Normal commercial gases which meet this specification are believed to have sufficient purity.

However, gas contamination can occur within the bottle, or sometimes between the bottle and the torch nozzle. Contamination could occur in a partially empty bottle, for instance. Or, it could occur due to defective connections in the tubing system. For these reasons, it might be advisable to devise a means of checking the purity of shielding gas at the torch nozzle rather than in the bottle. In such checking, Figure 3 could be used as a guide in determining the acceptance purity level. However, it should be only a guide, remembering that these data are based on welds made in an atmospheric-control chamber. Results for production welds, made under open conditions,

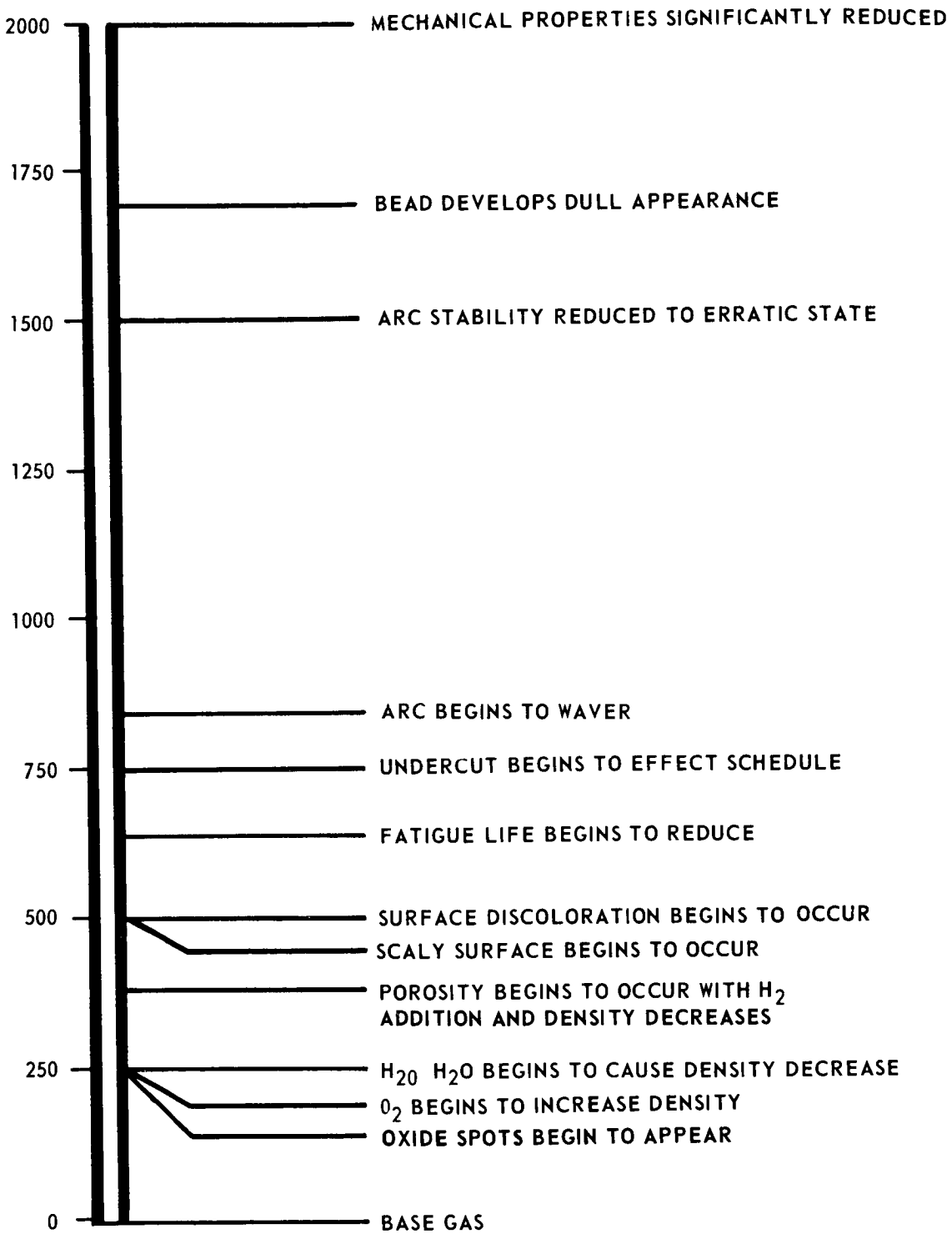

FIGURE 3. CONTAMINATION CONCENTRATION LEVELS AT WHICH SIGNIFICANT CHANGES OCCUR IN WELD QUALITY

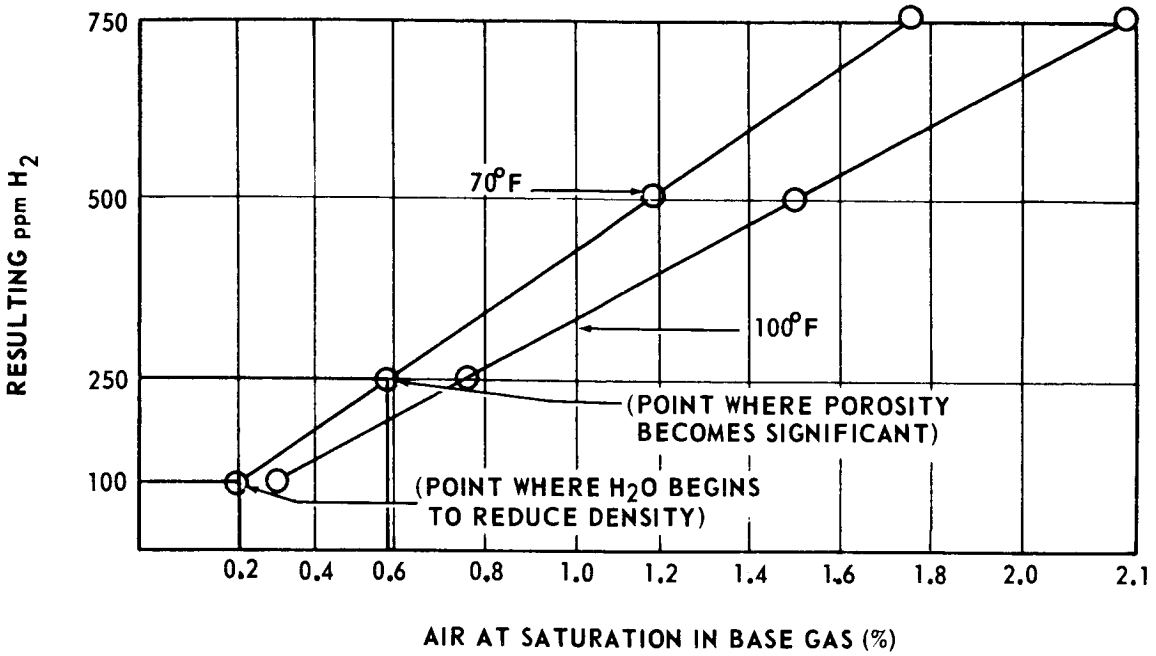

FIGURE 4. VOLUME OF WATER AVAILABLE TO WELDMENT FROM SATURATED AIR CONTAMINATION

could be expected to differ from these. Further experimental studies of open-air conditions would be needed to determine exact shielding-gas purity levels for production welds.

b. Surface Contamination

In all of the current NASA programs, except the IITRI work, metal surfaces were cleaned and surface contaminations were kept at the minimum. The IITRI work, in which effects of base-metal surface contamination on weld porosity were studied, was not completed as of 15 February 1967. Consequently, the following comments are temporary and subject to changes in the future.

Surface Contamination as a Source of Porosity. It is believed that contamination of the base metal and the filler metal is an important factor causing porosity.

Figure 5 shows results of calculation by the Boeing investigators on the amount of hydrogen gas available by decomposition of hydrocarbon on the weld groove.[3] It is assumed that hydrocarbon will decompose completely to gases by the welding arc and they will become gaseous contaminants. According to

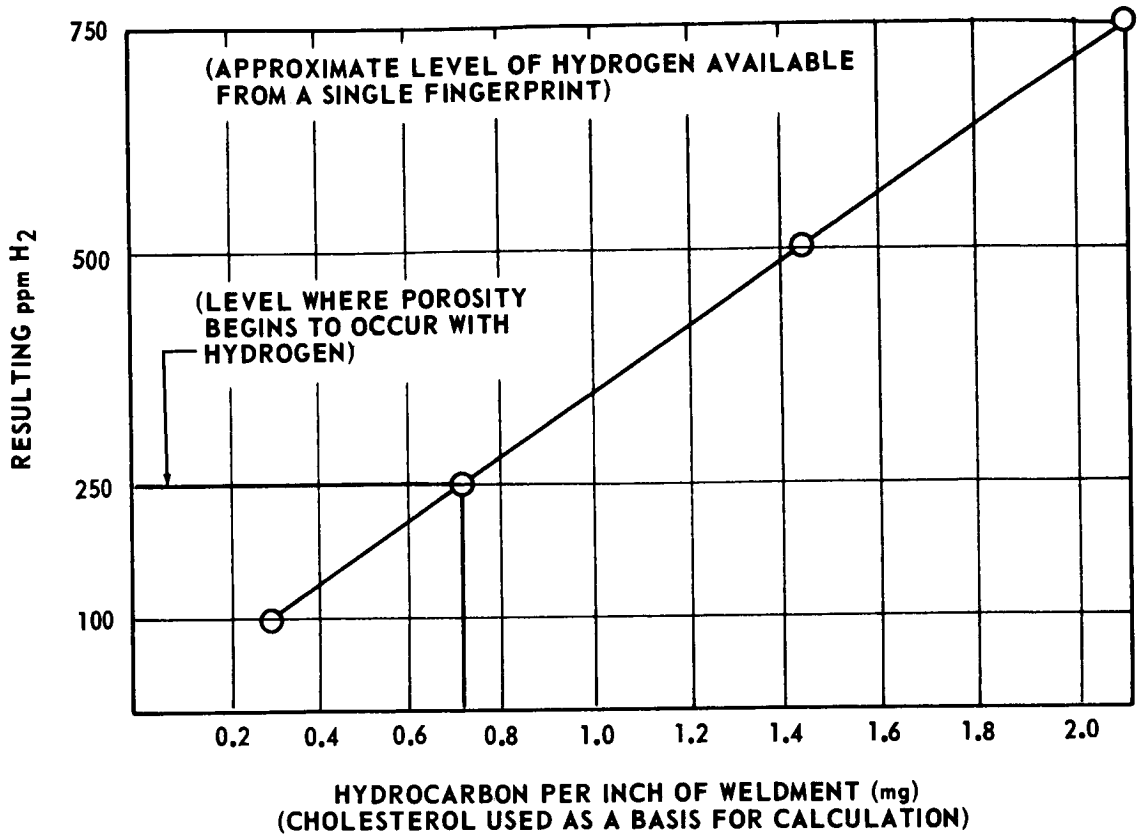

FIGURE 5. CALCULATED VOLUME OF HYDROCARBON AVAILABLE TO WELDMENT FROM HYDROCARBON CONTAMINATION

their calculation, it requires less than 1 mg of hydrocarbon per inch of weld to continuously generate 250 ppm hydrogen in the shielding gas. It is estimated that a single fingerprint would result in a 750-ppm hydrogen increase in the area contamined. By comparing Figures 3 and 5, the Boeing investigators estimated that a single fingerprint would cause a significant increase in porosity. The estimation was based on the assumption that hydrocarbons on the surface of the weld joint would have the same effect as an equivalent amount of hydrogen being introduced as a contaminant in the shielding gas.

A simple weld test was conducted at IITRI on the weld-defect potential of several surface preparations.[14] The experiments were made on 2014-T651 alloy plates. The results are shown in Figure 6 as a weld-defect potential. In this study, all the machined-only surfaces had a zero weld-defect potential. All other types of surface preparation produced some degree of porosity. Conventional surface treatments such as solvent degreasing, chemical cleaning, and water rinsing promote the formation of porosity. The IITRI investigators

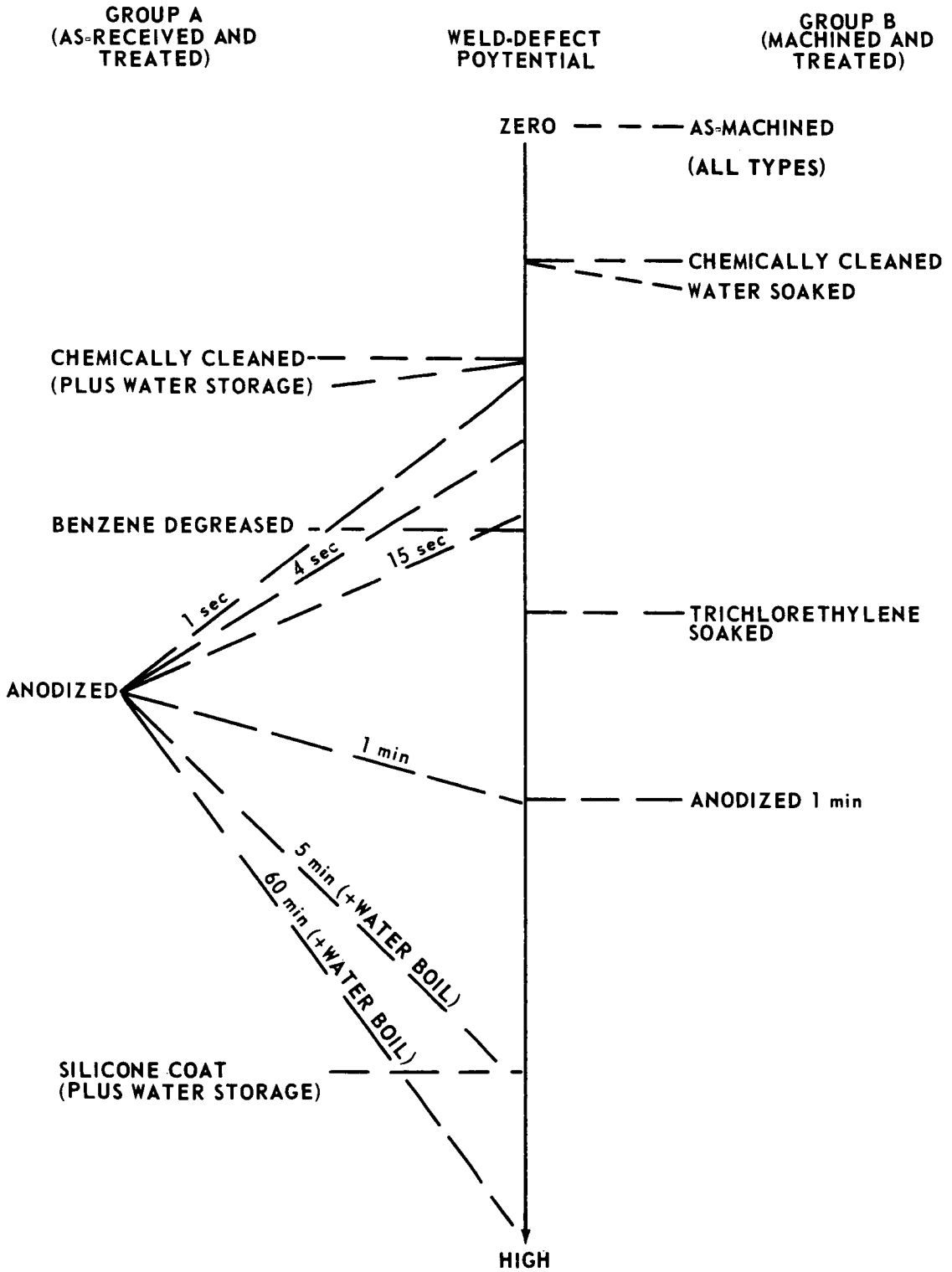

FIGURE 6. SCALE OF WELD-DEFECT POTENTIAL
OF VARIOUS SURFACE PREPARATIONS

believe that porosity is formed due to adsorbed solvent, hydrogen, and water. Anodizing and silicone coating produce extremely detrimental conditions for welding. In Figure 6, the treatments tested are divided in two groups: Group A (as-received and treated) and Group B (machined and treated).

An important finding obtained at IITRI is that an extended exposure to moist air prior to welding did not result in porosity in the as-machined specimens. However, other types of contamination can occur on the machined surface, and therefore, machining immediately before welding will be a desirable method of surface preparation.

Analysis of Surface Cleanliness. During the work which is still in progress, several techniques for measuring surface cleanliness have been evaluated.[14] These include radioactive evaporation (Meseran), spectral reflectance, mass spectrometry, gas chromatography, and spark emission spectroscopy. These techniques and others are still being evaluated in Phase II of the program. Each of them is quite sophisticated and will require closely controlled conditions and highly trained personnel to operate. To date, none of these techniques has proven completely satisfactory and none of them appears very practical for a production application.

Recommendations. Further studies need to be made of the defect potential of various surface preparations and of various contaminations, such as fingerprints. Studies need to be continued on techniques of evaluating surface cleanliness. Perhaps of most importance is a means of machining surfaces immediately before welding to insure a clean surface.

c. Composition of Base Plate and Filler Metal

An investigation was made of the effects of four factors on porosity.[4,5] The four factors, listed in the order of their influence on porosity level, are:

1) Shielding-gas moisture content

2) Alloying elements

3) Metallic impurities

4) Internal hydrogen content.

The program was conducted in two phases, the first phase using experimental base metals and filler metals, and the second phase using commercial materials. The results indicate that base-plate and filler-metal compositions are not likely to be significant sources of porosity as long as (1) shielding-gas and surface contamination are controlled at low levels and (2) base plates and filler metals are carefully prepared to meet the present specification with no gross hydrogen contamination. It has been hypothesized that there is a synergistic effect of alloy and metal impurity content, and external contamination (shielding gas and surface), which causes significant porosity. This has not yet been substantiated.

Because of these findings, the integrator recommends no changes in the present NASA specification for base-plate and filler-metal compositions.

2. Mechanisms of Porosity

A study was made of the effects of welding parameters on the nucleation and growth of porosity.[6] However, there appear to be reasons for questioning the reliability of some of the equations used in the statistical analysis. More studies are needed before conclusive statements can be made on the mechanisms of porosity formation.

3. Methods for Reducing Porosity

It has been shown that hydrogen contamination can be reduced or eliminated through proper surface preparation, cleanliness precautions during the handling of the materials, and welding procedures. However, carefully these procedures are observed, though, some hydrogen may still be present in the molten puddle. Thus, it is desirable to devise a means within the welding process to eliminate or neutralize hydrogen that may be present, and thus reduce porosity. Three separate means of doing this were studied in different programs.

a. Hydrogen Getters

It is known that certain elements will act as scavengers of hydrogen, either eliminating it or combining with it in a harmless form. The problem is how to introduce these elements to the welding process. At Southern Research Institute, experiments were made of studying the use of scavenging elements including Ti, Zr, Ce and Ca. In the work conducted so far, no significant reduction in porosity was obtained through use of powders as

scavenger elements, and in some cases the severity of porosity was increased. The results, however, do not necessarily mean that the theory of scavenger elements is wrong. Further work should be done to develop other methods of using these elements.

b. Magnetic Arc Shaper and Molten-Puddle Stirrer

Another possible method of reducing porosity is the use of mechanical devices that either agitate the puddle or oscillate or shape the plasma. Both puddle stirring and plasma oscillation have proved successful in reducing the level of porosity, although the percent reduction was relatively small. However, attaining this reduction requires the addition of complicated equipment to the welding torch.

c. Cryogenic Cooling

The results obtained at Harvey Aluminum have shown that porosity could be reduced by cryogenic cooling during welding. However, the percentage of porosity reduction was relatively small. The use of this method introduces the risk of contaminating the weld and further complicates the welding process. More study is needed before conclusive statements can be given on this subject.

4. Effects of Porosity Level on Weld-Joint Performance

The following tests were made on specimens prepared from welds containing various levels of porosity:[3,9]

1) Static tensile tests of transverse-weld specimens

2) Static tensile tests of longitudinal-weld specimens

3) Fatigue tests of transverse-weld specimens.

a. Static Tensile Strength of Transverse-Weld Specimens

It was observed in the programs at Martin[9] and Boeing[3] that the ultimate tensile strength of a transverse-weld specimen decreases with increasing porosity. Theoretically, this loss in strength should be approximately proportional to the loss of sectional area due to porosity. However,

this was not the case in experimental results at Martin.[9] In these experiments, a 5 percent loss of sectional area caused as much as 30 percent reduction in strength. The Martin investigators felt that a large number of very fine pores, which were not counted (only pores 1/64 in. in diameter and larger were counted in figuring loss of sectional area), were the prime cause of the marked decrease in strength. If the loss of sectional area due to these fine pores were added, the total loss in sectional area would be closer to the loss in strength. Additional analysis by the investigators supports this conclusion. However, it is the integrator's opinion that the inclusion of the fine pores may not be the only factor that caused the great loss of strength. These welds were made using highly contaminated gas, and some material degradation may have taken place.

Before conclusions are drawn from these results, experiments should be made, if possible, on production welds, or Boeing specimens should be analyzed in the same manner as the Martin specimens. It might also be well to run metallurgical tests on the Martin specimens to determine what degradation may have occurred.

b. Static Tensile Strengths of Longitudinal-Weld Specimens

Results of these studies indicated that mechanical properties of longitudinal-weld specimens are much less affected by porosity than are those of a transverse-weld specimen because the weld metal represents only a fraction of the specimen area.

c. Fatigue Tests of Transverse-Weld Specimens

It has been found in the two programs that fatigue life decreases with porosity. However, more research is needed to measure these effects quantitatively.

5. Welding Time-Temperature Control

It is known that the transverse strength of a weldment increases as welding heat input decreases, as shown in Figure 2. This has been observed in welds in different thicknesses made by the GTA, GMA, and EB welding processes. Consequently, welding of high-strength heat-treated aluminum alloy such as 2014 and 2219 should be made using low heat input. A study was made at Harvey Aluminum[10] of cryogenic cooling as a means of shortening thermal cycles and thus improving tensile properties of aluminum weldments. General increases of 4 to 10 percent in yield strength were obtained by cryogenic

cooling. The ultimate tensile strength also increased to some extent by cryogenic cooling. The ultimate tensile strengths of the unchilled welds, as reported by Harvey, were in the vicinity of 40 ksi. This appears to be only the start of the upswing of the heat input-strength curve (Figure 2). Much higher strengths are yet available by further reducing heat input. The effectiveness of cryogenic cooling may become greater as the weld heat input decreases.

The cryogenic cooling technique may prove to be a useful means of reducing weld distortion. However, to attain these improvements, a risk is taken of contaminating the weld, either by the cooling jet or by condensation on the surface. Further studies are needed to obtain conclusive results on this subject.

6. Transferability of Welding Machine and Parameters

It was found that duplicate trace recordings of six basic GTA welding variables indicate duplicate welds, if weld-joint preparation, tooling, and welding position have been duplicated. The six variables, in order of importance, are travel speed, electrode tip position, current, voltage, gas purity, and electrode tip diameter. On the basis of experimental results conducted on GMA welds, the regression analyses used were not considered reliable and no final conclusions have been made.

Experimental data were statistically analyzed to determine analytical relationships among welding parameters and weld properties including penetration, nugget shape, and mechanical properties of the joint. However, these results are not completely satisfactory. Further study needs to be made of the physical meanings of the equations used.

7. Selection of Welding Parameters

Selecting proper welding parameters has been an important problem for welding engineers. When fusion welding high-strength heat-treated aluminum alloys, the following two major problems need to be considered in selecting parameters: (1) mechanical properties of weldments and (2) porosity. Other problems such as susceptibility for weld cracking also need to be considered.

In order to improve the mechanical properties of weldments, it is recommended that welding parameters that produce small heat input be used. A lower welding current and a higher arc travel speed produce smaller heat

input. Figure 2 can be used as a guide for evaluating the effect of heat input on the strength of a welded joint.

The selection of proper welding parameters to control porosity requires more analyses. The use of high heat input with slow cooling tends to cause a small number of large pores; loss of cross-sectional area may be low, but the loss of strength due to welding thermal effect is great. Use of a small heat input with fast cooling tends to cause a large number of fine pores; loss of sectional area due to porosity may be high. More study is needed to develop a technique for scientifically selecting welding parameters.

8. Recommendations for Weld Inspection and Repair

a. Inspection of Weld Defects

Recommendations for the revision of the current inspection standards is outside the scope of this report. However, it seems essential to review some points that are suggested by the current programs and are pertinent to these standards. Only general conclusions are given here.

Small Pores. A large number of fine pores, say less than 0.03 in. in diameter, can cause significant reduction of cross-sectional area, resulting in considerable loss of strength. However, present inspection standards tend to place inadequate emphasis on the importance of the fine pores that are often found in aluminum welds. Further study should be made to determine more exactly the importance of these pores.

Stress State of a Joint. Welds that are loaded parallel to the welding direction are less sensitive in their mechanical behavior to defects than welds that are loaded transverse to the weld direction. Consequently, different acceptance levels of porosity might be used, depending upon the location of a weld and the direction of the weld relative to the direction of load expected during service.

Improved Nondestructive Testing. Improved nondestructive testing techniques should be developed for determining the total cross-sectional area of flaws in the expected fracture plane. Multiple X-ray shots appear to offer the best promise.

b. Repair Welds

It is known that repair welds, unless they are made very carefully, may have properties inferior to normal welds. The repair welds can create high residual stresses and additional distortion. Failures in various structures have been traced directly to repair welds. In many cases, porosity does not cause high stress concentration, and loss of strength due to porosity is rather minor. It is recommended that weld repairs be kept to a minimum. In some cases where defects are not critical, welds might better be left unrepaired.

Section V. ANALYSIS AND EVALUATION OF THE NASA-SPONSORED PROGRAMS COVERED IN THIS REPORT

1. Materials and Welding Processes Studied

The nine NASA-sponsored research programs that are covered in the present report deal primarily with welds made in the following materials and by the following processes:

1) Base Plate: 2014-T6 and 2219-T87 supplied by NASA-MSFC

2) Plate thickness: 1/4, 1/2, and 3/4 in.

3) Welding process: GTA processes, D-C, straight polarity

4) Filler wire (when used): 4043 for welding 2014-T6, and 2319 for 2219-T87, 1/16 in. in diameter

5) Shielding gas: helium

2. Effects of Shielding-Gas Contamination on Porosity

Three programs, at Boeing, Battelle, and Douglas, consisted of research on the effects of shielding-gas contamination on porosity. In all of these programs, it was found that the shielding-gas contamination had a much more significant effect on porosity than did the other factors investigated.

Section V-2 describes the results obtained at Boeing under Contract NAS8-20168. The other work at Battelle and Douglas is described in Sections V-3 and V-4, respectively, immediately following.

a. Research Procedures Under Contract NAS8-20168

The study was performed in two phases as follows:

Phase I. Determination of the ranges for which a relationship exists between contaminants (O_2, N_2, H_2, and H_2O) in arc-shielding helium and weldment defects.

Phase II. A quantitative determination of the shielding-gas contamination effects on porosity, mechanical properties, and metallurgical characteristics of 2219-T87 aluminum weldments.

Welding Procedures. 2219-T87 aluminum alloy plates 1/4-in. thick, 12-in. long, and 10-in. (Phase I) or 11-in. (Phase II) wide were butt-welded along the 12-in. long edges. Welds were made in an atmosphere-control chamber by the GTA process, D-C, straight polarity. The following welding schedule was used for all panels:

Joint design: square butt, no gap

Welding current: 240 amp

Arc voltage: 13 v

Wire feed speed: 36 ipm

Travel speed: 12 ipm

Work temperature: 70-78°F

Helium-gas flow rate: 15 ft^3/hr in Phase I
80 ft^3/hr in Phase II

The higher shielding-gas flow rate was used in Phase II to better simulate production conditions.

Weldment Evaluation. Following radiographic analysis, each weldment panel was machined to obtain two gravimetric, two tensile, and three fatigue samples and one metallographic sample.

Statistical Analyses. Statistical analyses were used extensively in the design of experimental programs and the analysis of experimental data. The 2^4 factorial analysis was used to design experimental programs for studying effects of the four contaminating gases (oxygen, hydrogen, nitrogen, and water vapor). Experimental results were analyzed on the basis of the factorial analysis. The data were then analyzed to obtain regression equations relating the levels of contamination to each measure of weld quality. The following model was used for the stepwise regression analysis:

$$Y_i = b_0 + B_1X_1 + \ldots\ldots\ldots + b_4X_4$$
$$+ b_{12}X_1X_2 + \ldots\ldots\ldots + b_{34}X_3X_4$$
$$+ b_{123}X_1X_2X_3 + \ldots\ldots\ldots + b_{234}X_2X_3X_4$$
$$+ b_{1234}X_1X_2X_3X_4 + b_{11}X_1^2 + \ldots\ldots + b_{44}X_4^2, \qquad (2)$$

where

Y_i = weld quality

X_1 = oxygen

X_2 = hydrogen

X_3 = nitrogen

X_4 = water vapor

b_0, b_1, ... b_4, b_{12} ...., b_{44} = coefficients.

Further definition of the terms used in the regression equations are shown in Tables II and III.

In the regression analysis in Phase II, the cubic centimeters of contaminant available per gram of weld bead formed, C_i, also were used. The value X_i was replaced by C_i for each contaminant in the regression model shown in Equation (2):

C_1 = (cc of oxygen)/(g of weld metal)

C_2 = (cc of hydrogen)/(g of weld metal)

C_3 = (cc of nitrogen)/(g of weld metal)

C_4 = (cc of water vapor)/(g of weld metal).

TABLE II. MEASURES OF WELD QUALITY FOR REGRESSION EQUATIONS

Radiographic Analysis

Y_1 = defects per inch of weld bead (porosity sizes up to 0.024 in.)
Y_2 = defects per inch of weld bead (porosity sizes 0.025 to 0.049 in.)
Y_3 = defects per inch of weld bead (porosity sizes 0.050 to 0.150 in.)
Y_4 = total defects per inch of weld bead (porosity sizes up to 0.150 in.)
Y_5 = defects per gram of weld bead (porosity sizes up to 0.024 in.)
Y_6 = defects per gram of weld bead (porosity sizes 0.025 to 0.049 in.)
Y_7 = defects per gram of weld bead (porosity sizes 0.050 to 0.150 in.)
Y_8 = total defects per gram of weld bead (porosity sizes up to 0.150 in.)

Density

Y_9 = weld bead density
Y_{10} = base metal density, weld bead density

Metallographic Analysis

Y_{11} = volume percent porosity

Static Tensile Test

Y_{12} = longitudinal weld, ultimate tensile strength (psi)
Y_{13} = longitudinal weld, yield strength (psi)
Y_{14} = longitudinal weld, elongation on 2-in. gage length (%)
Y_{15} = transverse weld, ultimate tensile strength (psi)
Y_{16} = transverse weld, yield strength (psi)
Y_{17} = transverse weld, elongation 2-in. gage length (%)

Fatigue Test

Y_{18} = transverse weld, cycles to failure

Notes: 1) Y_5 through Y_8 were obtained by dividing Y_1 through Y_4 by the weight of the weld bead (g/in.) for each panel to eliminate any effect due to variations in the weld bead between panels.

2) Y_{10} was obtained as the difference between the density of the base metal and the weld bead to eliminate any effect due to variations between panels.

TABLE III. LOGARITHMIC FUNCTIONS USED IN REGRESSION EQUATIONS

For expressing X_i, indicating the contamination level, logarithmic functions were used in Phase I, as follows:

1) Oxygen - $X_1 = (\log O_2 - 3.1505)/1.1505$

2) Nitrogen - $X_2 = (\log N_2 - 2.3495)/1.3495$

3) Hydrogen - $X_3 = (\log H_2 - 3.1505)/1.1505$

4) Water vapor - $X_4 = (\log H_2O - 3.0)/1.0$,

where O_2, N_2, H_2, H_2O are levels in ppm of oxygen, nitrogen, hydrogen, and water vapor, respectively.

In Phase II, linear functions were used, as follows:

1) Oxygen - $X_1 = (O_2 - 500)/250$

2) Nitrogen - $X_2 = (N_2 - 500)/250$

3) Hydrogen - $X_3 = (H_2 - 500)/250$

4) Water vapor - $X_4 = (H_2O - 500)/250$

b. Results Obtained Under Contract NAS8-20168

Porosity Data and Statistical Analyses. Table IV shows an example of test results obtained in Phase II. Shown in the table are (1) contamination levels of the four gases, (2) results of the radiographic analysis, and (3) porosity, in volumetric fraction percent, determined from the weld-density.

Table V shows, as an example of the statistical analyses, results of the regression analysis on the data obtained in Phase II. Values of regression coefficient b_0, b_1, ..., b_4, b_{12}, ..., b_{44} for various weld quality measures, Y_1, Y_2, ..., Y_{17}, are shown. Y_1 through Y_{11} are weld quality measures related to porosity, while Y_{12} through Y_{17} are related to mechanical properties. Also shown are coefficient of determination, R^2; coefficient of correlation, R; standard error of the test S_{yi}; and degree of freedom, DF. Good correlations

TABLE IV. ALUMINUM INERT GAS WELDMENT EFFECTS STUDY POROSITY ANALYSIS DATA

Panel Number	Levels of Contamination Experimental Design Phase II				Radiographic Analysis Y = defects per gram of weld bead				Metallographic Porosity vol. frac. %
	O_2	H_2	N_2	H_2O	0.024 in.	0.049 in.	0.150 in.	Total	
1205-854-03	250	250	250	250	3.316	0.122	0.025	3.463	0.5
1203-857-04	750	250	250	250	0.213	0.196	0.025	0.434	0.5
1105-853-03	250	750	250	250	1.823	0.078	0.000	1.901	0.5
1404-853-06	750	750	250	250	0.037	0.044	0.022	0.103	0.5
1104-352-03	250	250	750	250	2.282	0.068	0.015	2.365	1.0
1009-857-02	750	250	750	250	0.008	0.067	0.122	0.197	0.0
1405-854-05	250	750	750	250	4.982	0.082	0.022	5.086	3.0
1203-352-04	750	750	750	250	0.102	0.097	0.040	0.239	0.5
1006-854-06	250	250	250	750	2.688	0.064	0.016	2.768	2.0
1005-854-01	750	250	250	750	3.526	0.335	0.171	4.032	1.0
1209-853-04	250	750	250	750	9.674	0.275	0.030	9.979	2.0
1010-358-02	750	750	250	750	5.081	0.180	0.008	5.269	1.0
1003-852-02	250	250	750	750	5.025	0.148	0.045	5.218	1.0
1310-859-05	750	250	750	750	1.530	0.046	0.031	1.607	0.5
1204-853-04	250	750	750	750	7.474	0.116	0.008	7.598	1.0

TABLE IV. (Concluded)

Panel Number	Levels of Contamination Experimental Design Phase II				Radiographic Analysis Y = defects per gram of weld bead				Metallographic Porosity vol. frac. %
	O_2	H_2	N_2	H_2O	0.024 in.	0.049 in.	0.150 in.	Total	
1202-851-01	750	750	750	750	24.422	1.943	0.086	26.451	2.0
1107-854-02	5	500	500	500	10.014	0.105	0.030	10.149	10.0
1207-856-04	250	500	500	500	1.508	0.090	0.023	1.621	1.0
1206-855-03	750	500	500	500	15.451	0.144	0.015	15.610	1.0
1409-857-06	500	5	500	500	0.970	0.150	0.022	1.142	0.5
1110-858-03	500	250	500	500	1.560	0.047	0.008	1.615	1.0
1107-855-02	500	750	500	500	13.218	0.233	0.024	13.475	2.0
1403-852-06	500	500	5	500	0.153	0.039	0.000	0.192	1.0
1309-858-05	500	500	250	500	3.950	0.032	0.008	3.990	1.0
1406-855-05	500	500	750	500	26.996	0.343	0.032	27.371	1.0

were obtained between gas-contamination levels and the porosity measures. In addition to main factors, interactions of different gases also were found to be significant in some cases.

Effects of Shielding-Gas Contamination on Porosity. In general, the observed effects of the gaseous contaminants studied in Phases I and II were the same. However, the levels of contamination used in Phases I and II could not be compared because of the difference in torch flow rates for the shielding gas (15 cfh in Phase I and 80 cfh in Phase II). The level of contamination required to cause visual surface defects was considerably lower in Phase II. To study the contamination effects on a comparable basis, the level of contamination was changed from parts per million (ppm) to cubic centimeters (cc) per inch of weld.

Figure 7 plots individual gaseous contaminant effects on total defects per inch of weld in Phase II welds when all other gaseous contaminants are kept at 5 ppm.[3] Curves in the figure are determined from results of the statistical analysis shown in Table IV. Addition of either hydrogen or water vapor increased porosity. Hydrogen caused the greatest increase, becoming significant above 250 ppm. Additions of oxygen and nitrogen did not change the porosity level. Figures similar to Figure 7 were obtained to show effects of adding one gas while other gases were kept at constant levels, such as 250 and 500 ppm.

The Boeing investigators summarized the results of increasing individual gas contaminants as follows:

1) Oxygen. Increasing the oxygen level did not increase porosity. In some cases, a slight decrease in porosity was observed; however, because the welds made with no contamination present contained little or no porosity, there was not much chance for improvement. Increasing the oxygen caused an increase in the density of the weld bead in Phase II. This was not observed in Phase I where the maximum level of oxygen was less than half that in Phase II.

2) Hydrogen. Increasing the hydrogen concentration increased the level of porosity and decreased the density of the weld bead.

3) Nitrogen. Increasing nitrogen had little effect on porosity or density.

4) Water vapor. Increasing water vapor increased porosity and decreased density.

TABLE V. REGRESSION

Regression Coefficients	Radiographic Analysis								D
	Y = defects per inch of weld bead				Y = defects per gram of weld bead				
	To 0.024 in.	To 0.049 in.	To 0.150 in.	Total	To 0.024 in.	To 0.049 in.	To 0.150 in.	Total	Weld Bead Density
Constant b_0	27.581	0.629	0.0948	28.474	7.137	0.163	0.0237	7.002	2.818654
$X_1 = O_2$ b_1	- 3.897	0.381		- 3.977	-1.016	0.103	0.0080	-0.991	0.003317
$X_2 = H_2$ b_2	17.255	0.379		18.032	4.590	0.101		4.824	-0.008300
$X_3 = N_2$ b_3	14.166	0.316		14.738	3.757	0.085		3.958	
$X_4 = H_2O$ b_4	15.533	0.495	0.0488	16.444	4.148	0.130	0.0108	4.776	-0.008671
X_1X_2 b_{12}	- 3.606	0.439	-0.0252	- 3.754	-0.945	0.119	-0.0070	-0.932	
X_1X_3 b_{13}		0.445				0.123	0.0073		
X_1X_4 b_{14}		0.413				0.112	0.0036		0.001364
X_2X_3 b_{23}	8.876	0.443		9.613	2.400	0.120		2.678	
X_2X_4 b_{24}	11.400	0.382		11.991	3.034	0.103		3.060	-0.002597
X_3X_4 b_{34}	11.880	0.448		12.510	3.158	0.121		3.240	
$X_1X_2X_3$ b_{123}		0.448				0.121			
$X_1X_2X_4$ b_{124}		0.443				0.120			
$X_1X_3X_4$ b_{134}		0.305	-0.0137			0.084			0.000991
$X_2X_3X_4$ b_{234}	7.433	0.386		8.009	2.005	0.104		2.181	-0.001419
$X_1X_2X_3X_4$ b_{1234}		0.280				0.075			
X_1^2 b_{11}		0.116				0.032			
X_2^2 b_{22}	2.783	-0.059	0.0132	2.749	0.740	-0.016	0.0034	0.710	
X_3^2 b_{33}									
X_4^2 b_{44}	- 2.594	0.110	0.0214	- 2.265	-0.617	0.030	0.0060		
Coefficient of determination, R^2	0.927	0.879	0.650	0.930	0.928	0.881	0.650	0.929	0.878
Coefficient of correlation, R	0.963	0.938	0.806	0.964	0.963	0.939	0.806	0.964	0.936
Standard error of the test, S_{yi}	12.090	0.418	0.129	12.064	3.210	0.111	0.035	3.206	0.0063
Degrees of freedom, DF	54	47	60	54	54	47	58	55	58

Code for contamination level, X_i

$$X_1 = \frac{O_2(\text{ppm}) - 500}{250} \qquad X_3 = \frac{N_2(\text{ppm}) - 500}{250}$$

$$X_2 = \frac{H_2(\text{ppm}) - 500}{250} \qquad X_4 = \frac{H_2O(\text{ppm}) - 500}{250}$$

ANALYSIS (ppm)

nsity		Tensile Strength						Fatigue
Base Metal Minus Weld Bead Density	Metallographic Porosity Vf (%)	Longitudinal			Transverse			Transverse
		Ultimate (psi)	Yield (psi)	Elongation 2.0 in. (%)	Ultimate (psi)	Yield (psi)	Elongation 2.0 in. (%)	Cycles to Failure
0.019943	1.230	43,511.9	21,930.2	14.29	35,661.3	24,053.9	2.911	155,001.3
-0.002452	-0.350	202.5			374.1		0.150	
0.008408		- 516.4		- 0.75	- 1,653.9		-0.444	- 36,003.2
					458.5	213.2	0.149	50,195.2
0.008944	0.145	- 629.7	- 442.6	- 0.98	- 903.9	- 203.9	-0.164	- 16,301.9
	-0.040			0.38			0.825	22,350.3
	-0.243		105.1	- 0.77	175.8		0.671	- 29,597.9
	-0.196		- 294.7					
				0.21				
0.002826		- 251.1		- 0.46	- 652.1	- 126.2	-0.191	
0.000895	0.382		- 269.9					
	0.206		195.3					
0.000726	0.272					70.3		- 24,832.8
			- 126.0	- 0.19				
0.000830	-0.079	- 71.7	- 136.3			- 153.5		- 17,585.0
	0.085		43.0					- 11,819.5
	0.801		221.0			122.7	0.888	
		- 59.5			- 145.9			16,447.2
	-0.333		89.9	0.40	277.0			57,576.4
	-0.383	- 207.9	- 305.1		491.0		0.168	
0.885	0.695	0.502	0.249	0.670	0.770	0.161	0.684	0.515
0.941	0.834	0.709	0.499	0.818	0.877	0.402	0.827	0.717
0.0060	1.064	1.037	0.972	1.607	1.422	0.890	0.495	184,545.0
58	52	58	54	57	56	59	56	55

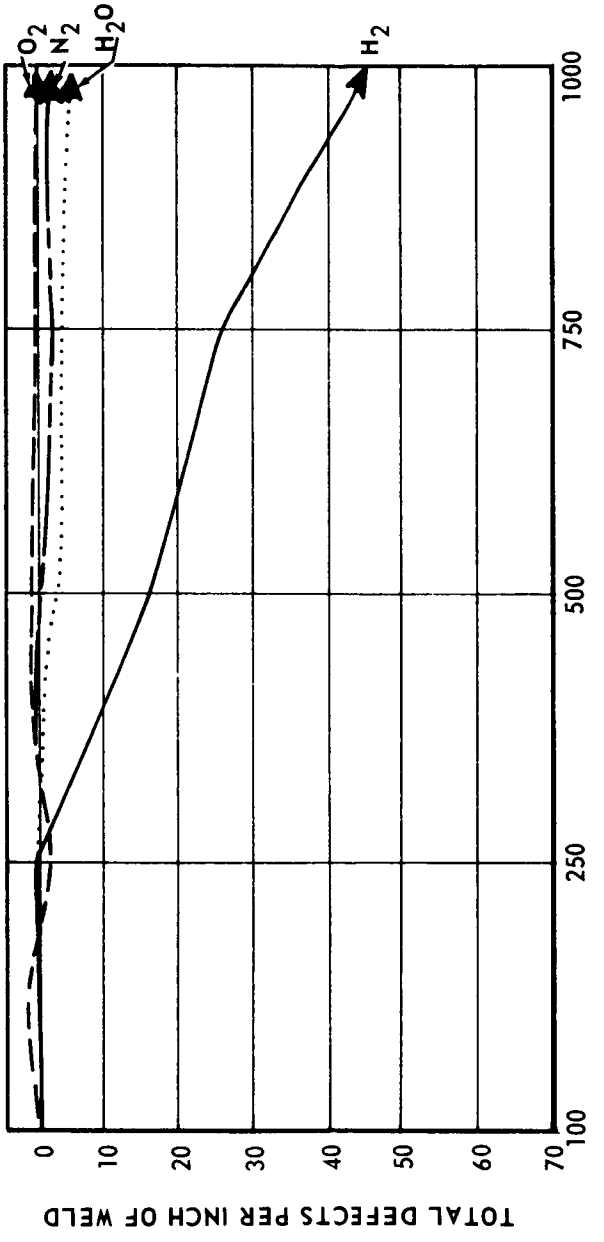

FIGURE 7. EFFECT OF INDIVIDUAL GASES CAUSING WELD BEAD DEFECTS

Metallographic Evaluation. The metallographic specimens were cross sectioned and examined in the polished and etched conditions. Increases in hydrogen and water vapor caused an increase in porosity, while oxygen and nitrogen had little effect on porosity.

In general, the porosity was localized in the weld metal along each side of the weld bead. The shielding-gas contamination had little effect on the microstructures of the welds.

Visual Effects. One of the most significant effects of contamination was changes in surface condition forming undercut, discoloration, and roughness. Surface variations caused by the individual gases were summarized as follows:

1) 500-ppm total contamination was necessary to cause an appearance change which could be considered cause for weldment rejection.

2) 100-ppm H_2O caused yellowish surface appearance fading to grayish, with roughening of the surface at 500 ppm.

3) Oxygen gave a silvery to grayish appearance and increased the undercut with increasing concentration.

4) Nitrogen gave a blackish appearance along the edge of the weld bead. This discoloration increased in intensity with increasing contamination from 100 to 500 ppm; the surface in the center of the bead began to yellow at 500 ppm.

5) Hydrogen gave a grayish rough appearance and decreased undercut was observed as concentration was increased; at hydrogen levels greater than 250 ppm no undercut was observed.

Increased surface effects were noted with the mixed gases, because for most of the conditions, the total contamination was in excess of 500 ppm. Between 750 and 1000 ppm total contamination, the arc began to wander leaving a wavy bead. At 1500 ppm total contamination, the arc became erratic and unstable.

c. Analysis and Evaluation of the Boeing Study on Shielding-Gas Effects

The conclusions drawn by the Boeing investigators are summarized in the Appendix. The integrator's discussion and evaluation of significant findings in their study follows.

On the basis of experimental findings, the Boeing investigators presented Figure 3, which shows contamination concentration levels at which significant changes in weld quality occur. This figure can be used as a guide for engineers who are engaged in the fabrication of space vehicles. It must be mentioned, however, that the figure was prepared on the basis of results obtained on welds made in an atmosphere control chamber, not in the open air in which most large structural components are fabricated.

Figure 4 shows calculated relationships between the percent of air at saturation in the base gas and the resulting hydrogen concentration. The figure indicates that at 70°F, the addition of 0.6 percent air, saturated with water vapor, to pure helium would result in 250 ppm of hydrogen in the shielding gas.

The Boeing investigators presented Figure 5 to estimate the amount of surface contamination necessary to produce a certain amount of shielding contamination. This figure plots the relationship of grams of surface hydrocarbon to level of hydrogen generated. Also shown is the estimated level of hydrogen generated by welding through a single fingerprint. These estimates are based on the assumption that hydrocarbons on the surface of the weld joint would have the same effect as an equivalent amount of hydrogen being introduced as a contaminant in the shielding gas. The figure shows that less than 1 mg/in. would be necessary to generate 250-ppm hydrogen in the shielding gas. A single fingerprint would cause 750-ppm hydrogen increase in the shielding gas. These calculations indicate that very small amounts of organic materials can be a significant cause of porosity.

3. Effects of Base- and Filler-Metal Composition on Porosity

The composition of the base metal and filler metal used in welded high-strength aluminum-alloy fabrication had been suspected as a possible cause of weld defects, especially porosity, and the objective of the work conducted at Battelle was to determine what influence, if any, variations in the composition of 2014-T651 and 2219-T87 aluminum alloys had on porosity in GTA welds. This work was sponsored under Contracts NAS8-1145 and NAS8-20303.

a. Research Procedures

Materials Investigated. The effect of aluminum-alloy composition upon resultant weld quality was studied using two different materials. The materials first used required fabrication of eight different compositions each

of experimental X2014-T6* and X2219-T87 base plates in 1/4- and 3/4-in. thicknesses, and of X4043 and X2319 filler wire. A total of 48 separate experimental compositions were prepared. The second set of materials used in later work were heats of available commercially-prepared 2014-T651 and 2219-T87 alloys with 1/4- and 3/4-in. thickness.

The procedure followed with the experimental and the commercial alloys was essentially the same. GTA welds were made on plates in the horizontal position with close control of welding conditions. The welding was conducted in a vacuum-purged chamber filled with helium to which water vapor could be added as a welding-arc contaminant.

Factors Investigated. The studies of the experimental and of the commercial materials were made in slightly different ways. The composition of 2014 and 2219 aluminum alloys was specified as follows:

Composition (percent by weight)

Alloy	Alloying Content (range)	Metallic Impurities (maximum)**
2014	3.9-5.0Cu, 0.4-1.2Mn, 0.5-1.2Si, 0.2-0.8Mg	1.0Fe, 0.25Zn, 0.15Ti, 0.10Cr
2219	5.8-6.8Cu, 0.2-0.4Mn, 0.02-0.10Ti, 0.05-0.15V, 0.10-0.25Zr	0.30Fe, 0.10Zn, 0.20Si, 0.02Mg

The initial study of experimental materials was planned to investigate four factors at two levels. The factors were alloying content, metallic impurities, internal hydrogen content, and arc shielding-gas water content. The alloying content was composed of those elements for which a range was specified, whereas metallic impurities were those elements specified only as a maximum allowable. Internal hydrogen content was the hydrogen content of the interior of the plate as measured by the tin-bath, vacuum-fusion process. The arc shielding-gas water content was the measured dewpoint of the helium in the welding chamber. The two levels selected were high and low. For example, at the low level, the alloying elements were near the specified minimum while the impurity elements were almost nonexistent. The initial plan called for a study of only one-half the 16 possible combinations of four variables at two levels for each thickness of X2014-T6 and X2219-T87. Because the level of each factor could not be controlled independently, the welding of

*"X" denotes alloys cast and fabricated by Battelle.

**Other elements, 0.05 percent maximum each, other elements total, 0.15 percent maximum.

X4043 on commercial 2014-T651 and X2319 on commercial 2219-T87 was conducted with a high level of arc shielding-gas water content. This deletion of one variable increased the number of observations that could be made.

The final study of commercial materials utilized a computer stepwise regression analysis of each specified element and of the internal hydrogen content of 2014-T651 and 2219-T87 alloys 1/4- and 3/4-in. thick. The quantity of different heats of material found for the investigation was limited as follows:

Number of Heats

Alloy	1/4-in. Thick	3/4-in. Thick
2014-T651	16	5
2219-T87	7	6

The range of composition of the materials obtained was limited to the central portion of the specified range as Figure 8 shows for the 2014-T651 heats.[5] The ranges of composition of the commercial alloys that were studied

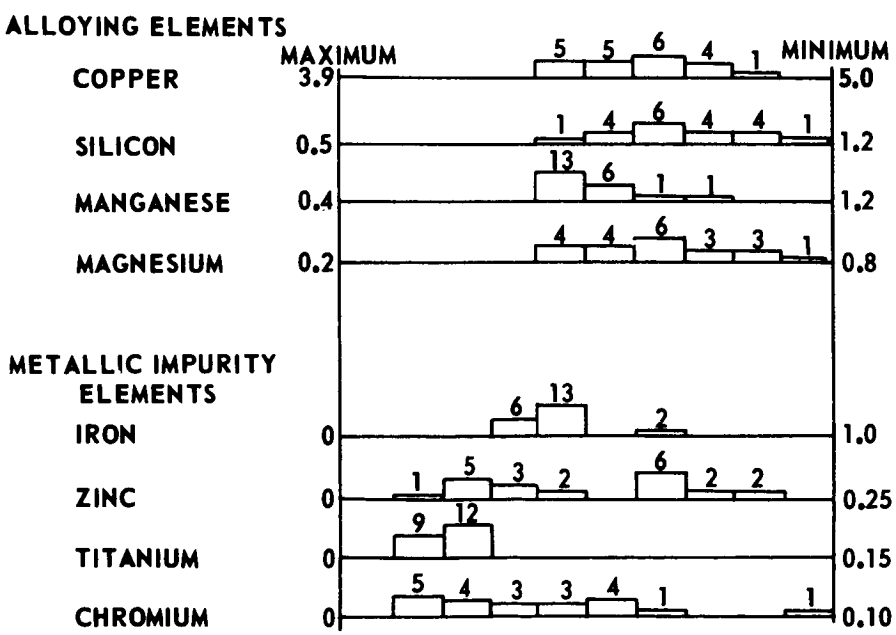

FIGURE 8. RANGES OF COMPOSITION FOR 2014-T651 BASE PLATE PLATE WELDED (Numerical indicates number of heats that fall within each interval.)

were typical of the composition range normally found in these alloys. The composition range of the experimental alloys was much broader than the range of the commercial alloys.

Welding. All of the welding was GTA straight polarity using a voltage-regulated automatic head in a helium-filled vacuum chamber. Welding was conducted in the horizontal position making 36-in. long bead-on-plate welds both with and without filler-wire addition. All plates were chemically cleaned immediately prior to welding. Any statistical analyses were for welds made with the same voltage, current, travel, and wire-feed speed. There were minor changes made in the settings to obtain complete penetration with a minimum of undercut. The welding conditions used for the analysis of commercial material are typical and are listed in Table VI. The moisture dewpoint of the helium arc shielding gas was about -60°F for low dewpoints and 0 to 5°F for high dewpoints.

TABLE VI. WELDING CONDITIONS EMPLOYED

Alloy	Plate Thickness (in.)	Voltage (v)	Current (amp)	Arc Travel (ipm)	Wire Feed (ipm)
2014-T651	1/4	11.5	180	11.6	-
2014-T651	3/4	12.4	260	10.3	-
2219-T87	1/4	13.2	150	11.6	-
2219-T87	3/4	13.2	260	10.3	-
2014-T651	1/4	11.5	210	11.6	45
2219-T87	1/4	13.2	210	11.6	45

All welds were bead-on-plate in the horizontal position using the D-C straight-polarity, GTA welding process. Arc shielding gas was helium. Wire was fed in the forehand position.

Weld Defect Analyses. A total of over 300 3-ft long welds were prepared for detailed study. All of the welds were first X-ray radiographed following MIL-STD-453 and graded to ABMA-PD-R-27A. The only defects observed were pores. Although some of the porosity found was graded in the worst classification, most of the welds contained a minimal amount of radiographically visible porosity. The programs relied on microscopic inspection of transverse weld sections to supply numbers for analysis. Point counting techniques were used to determine the volume percent porosity of the weld metal. About 1000 transverse weld cross sections were cut at random points, polished, etched, and photographed for point counting. The volume percent

porosity varied from 0 to 25 percent but the majority of the welds contained 1 to 8 volume percent porosity.

b. Results Obtained

Experimental Materials. The planned fractional factorial analysis was not used to analyze the results because the internal hydrogen content of the X2014 and X2219 could not be controlled independently of the composition. In addition, almost all the welds made with a helium dewpoint of -60°F were free of porosity. An analysis was conducted of the welds made at a helium dewpoint of about 5°F. For the four factors studied, the following general ranking was established. The most significant factor is listed first.

1) Arc shielding-gas water content. This factor, when changed from a dewpoint of -60°F to +5°F, was the most significant factor related to the occurrence of weld porosity.

2) Alloying content. In general, for the experimental materials studied, increasing the weight percent of the alloying elements from the minimum to the maximum specified was associated with minor increases in the occurrence of weld porosity.

3) Internal impurities. In general, the relationship of internal impurities to weld porosity was similar but less strong than that between porosity and alloying content.

4) Internal hydrogen content. Increasing amounts of base plate hydrogen content from 0.1 to 1.8 ppm (by weight) and of the wire total hydrogen content from 1.4 to 4.0 ppm was found to have a minor influence on increasing weld porosity. However, one heat of X2014 which had been grossly contaminated with hydrogen during pouring had very high weld porosity, indicating that gross contamination of aluminum with hydrogen might cause weld porosity.

Commercial Materials. The portion of the program that used commercial materials was analyzed by stepwise regression techniques to yield an equation linking the weld porosity to base metal composition. The results of the analyses for each thickness of the 2014-T651 and 2219-T87 alloys were combined and are presented in Table VII.[5] Increasing amounts of magnesium, manganese, titanium, and internal hydrogen contents were all related to decreasing porosity in 2014-T651. For 2219-T87, increasing amounts of zinc, magnesium, zirconium, internal hydrogen, and titanium were all related to

TABLE VII. VARIABLES STUDIED WHICH MOST SIGNIFICANTLY AFFECTED WELD POROSITY

Base Plate Alloy	Variable	Relative Strength of Relationship	Coefficient Sign*
2014-T651	Mg × Mn	1 or 2	-
2014-T651	Mn × Ti	1 or 2	-
2014-T651	$(Fe)^3$	3	+
2014-T651	$(H_2)^2$	4	-
2219-T87	Zn	1	-
2219-T87	Mg	2, 3, or 4	-
2219-T87	Mn × Fe	2, 3, or 4	+
2219-T87	Zr	2, 3, or 4	-
2219-T87	$(H_2)^3$ or $(H_2)^2$	5 or 6	-
2219-T87	Mg × Ti	5 or 6	-

*The coefficient sign indicates whether increasing amounts of the variable were associated with increasing (+) or decreasing (-) weld porosity.

decreasing weld porosity. For both alloys, increasing iron content was related to increasing weld porosity. Copper and silicon were not found to be significant factors for weld porosity. These observations were all made for welds that contained a "base-line" amount of hydrogen porosity due to the shielding gas dewpoint of 0°F.

c. Observations

During the program, a large number of observations were made that were of interest. The most important are summarized below.

A tendency for the pores to line up along certain planes was noted, both in the experimental and commercial materials. Figure 9a shows a transverse cross section that contained pores lined up along bands of segregation.[4] Figure 9b shows a longitudinal section of the weld with the pores again occurring preferentially in bands.

A second observation was the formation of voids within the base plate due to the heat of welding. Figure 10a shows the typical structure of a full-penetration weld bead in 2014-T651 plate.[5] Voids are visible beyond the fusion zone of the plate. In another weld, when the welding arc was maintained with

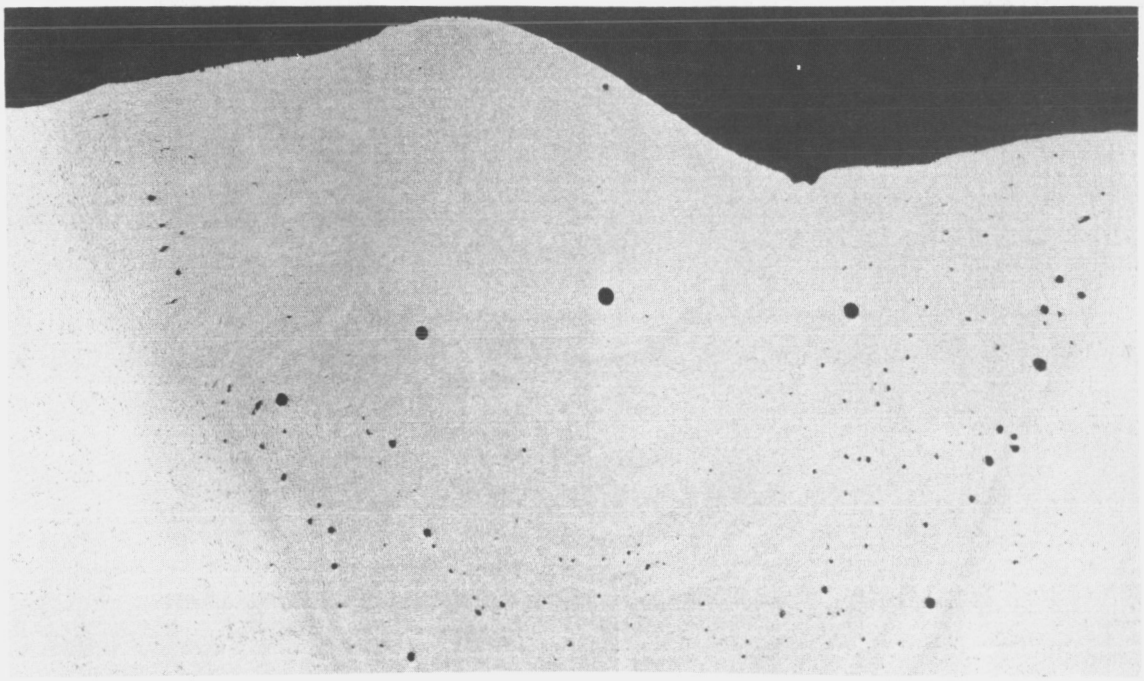

20X ETCH POLISHED RM 40635

a. TRANSVERSE SECTION SHOWING SOLUTE SEGRATION

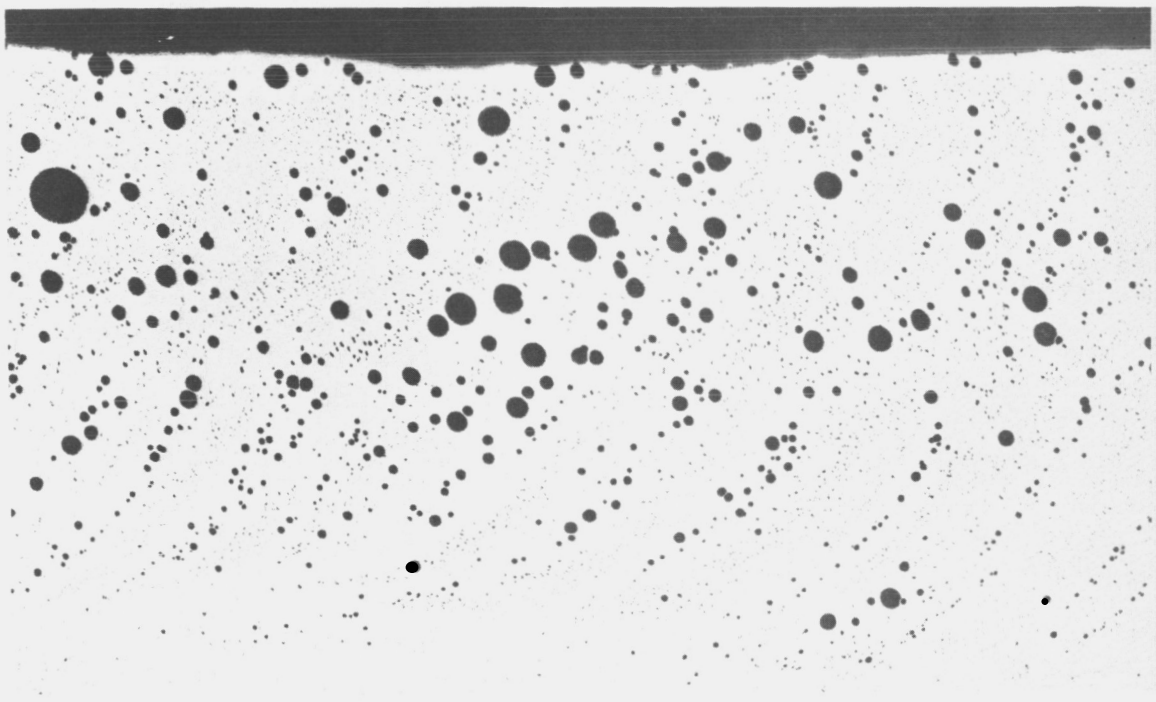

20X AS POLISHED RM 41860

b. LONGITUDINAL SECTION

FIGURE 9. PREFERENTIAL PORE OCCURRENCE

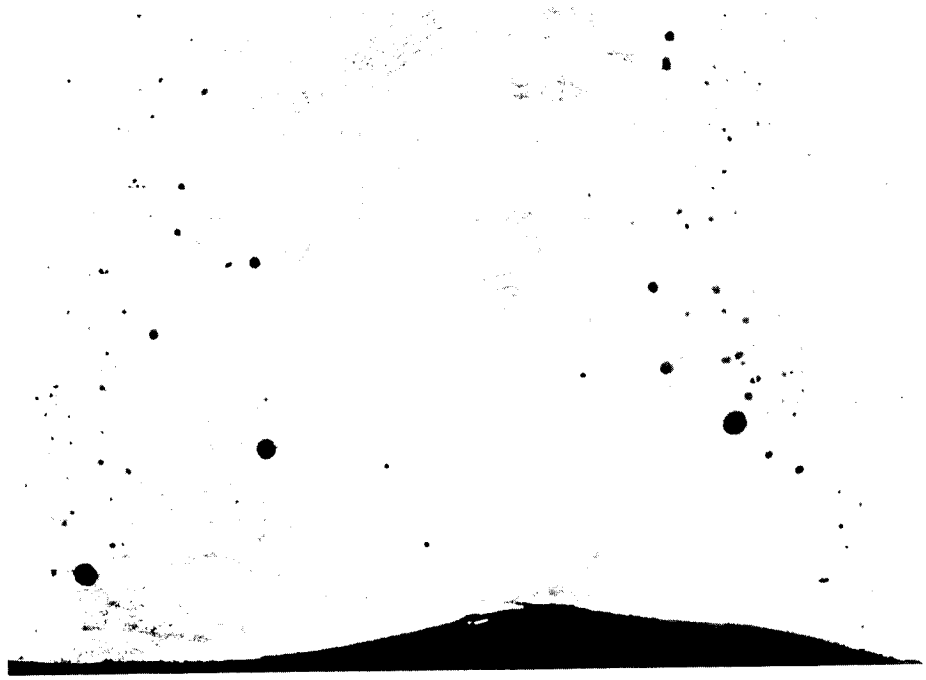

20X

6A852

a. TYPICAL TRANSVERSE SECTION

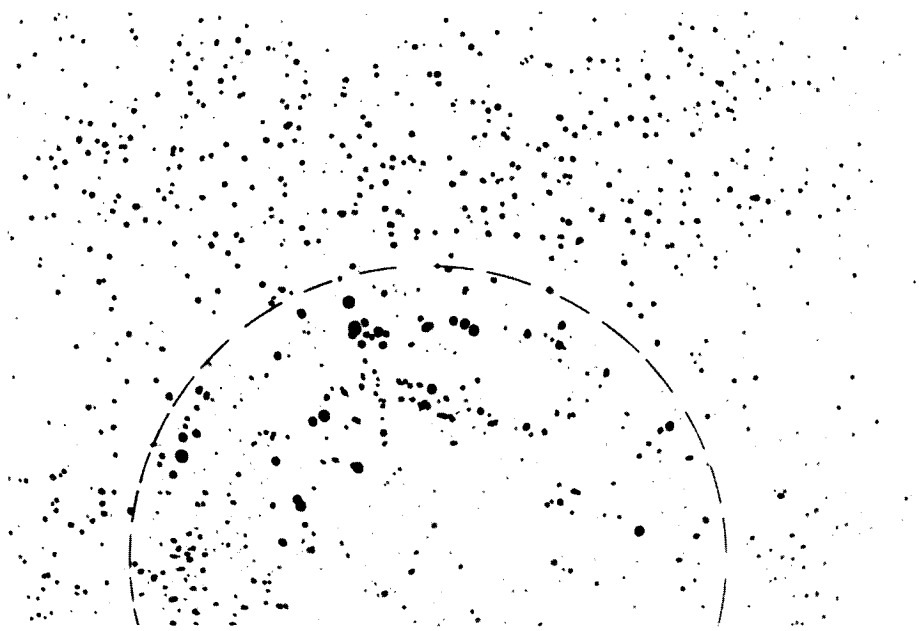

20X

AS POLISHED

3A982

b. BASE METAL VOIDS FORMED BY EXCESSIVE HEAT INPUT

FIGURE 10. BASE PLATE VOIDS IN 2014-T651 PLATE

no travel movement for about 15 sec, very large base-metal voids formed for some distance beyond the weld as shown in Figure 10b. The weld fusion zone is enclosed by a dotted line.

Figure 10a also shows the structure containing growth twins found in the weld center. Interestingly, these grains did not form until about 6 in. of weld had been made. No hardness differences in the weld center were detected when this structure appeared.

One composition of 2014-T651 had a fine-grained structure that was unlike the typical 2014 weld structure shown in Figure 10a. The cause for the structure difference was not determined.

Autoradiography was studied to determine whether radioactive hydrogen could be introduced into a weld to study the occurrence of hydrogen in solution. Several welds were made in helium containing tritiated water vapor at a dew-point of 25°F. The radioactivity of the tritiated water vapor was 10 mCi/grain. The activity of the tritiated water was not high enough to reveal much information on a micro or macro scale. The procedure used was feasible and would probably have yielded more results if more active tritiated water vapor could have been used.

During welding, it was also observed that oscillographic traces of arc voltage and arc current developed sharp inflections whenever the shielding gas was contaminated by water vapor. It was suggested that this could be a useful method of detecting arc contamination.

d. Analysis and Evaluation of the Battelle Study on Base- and Filler-Metal Composition on Porosity

The conclusions drawn by the Battelle investigators are summarized in the Appendix. The integrator's discussion of important findings follows.

The major conclusion obtained in this two-phase study is that the alloying elements, impurity elements, and internal hydrogen contents in the ranges studied had little significant influence on weld-metal porosity. When moisture was added to the shielding gas, certain compositions formed more weld porosity than others, but there were no large variations from the average. The Battelle investigators recommended that no changes be made in the composition of 2014-T651 and 2219-T87 to make the alloys less sensitive to weld

porosity, because their composition was no more than a secondary factor in the formation of weld porosity. On the basis of experimental data obtained, the conclusions and recommendations given by the Battelle investigators appear to be valid and soundly based.

4. Mechanisms of Porosity Formation

Mechanisms of porosity formation were studied at Douglas under Contract NAS8-11332.

a. Background and Technical Approach

A previous work by Saperstein, et al.[21] provides important background on this subject. This study investigated the effects of various factors on porosity. These included moisture content of helium-argon shielding gas, travel speed, and arc length. Welds were made in Type 3003 plate by the GMA process.

Figure 11 shows the effect of shielding-gas dewpoint on porosity formation, as determined in this study.[21] Each data point represents a single test weld, except where otherwise noted. The dewpoint threshold for porosity formation was approximately -40°F for both travel speeds. Porosity content seemed to increase exponentially as the dewpoint increased above -40°F.

An effort was made to correlate welding parameters to porosity. The mathematical analysis of heat flow in weldments developed by Rosenthal[24] and Adams[25] was used. Adams developed expressions for weld-cooling rates in the case of two-dimensional heat flow from a point heat source moving linearly with constant velocity in a flat plate. The cooling rate at the fusion interface (on the solid side) is given by the following expression:

$$P = \text{cooling rate parameter} = \left(\frac{10^3\,Vt}{EI}\right)^2 \left(\frac{\text{in.}^2}{\text{w, min}}\right). \qquad (3)$$

The cooling rate on the solid side of the fusion-line interface is directly proportional to the solidification time per unit volume on the liquid side. (Solidification time is the elapsed time between the liquidus and solidus temperature.) Since pores form during solidification, the cooling-rate parameter represents a convenient measure of porosity.

Many test welds were made to establish a correlation between the cooling-rate parameter and porosity. Figure 12 shows a typical dependence between percent porosity and the cooling-rate parameter.[21]

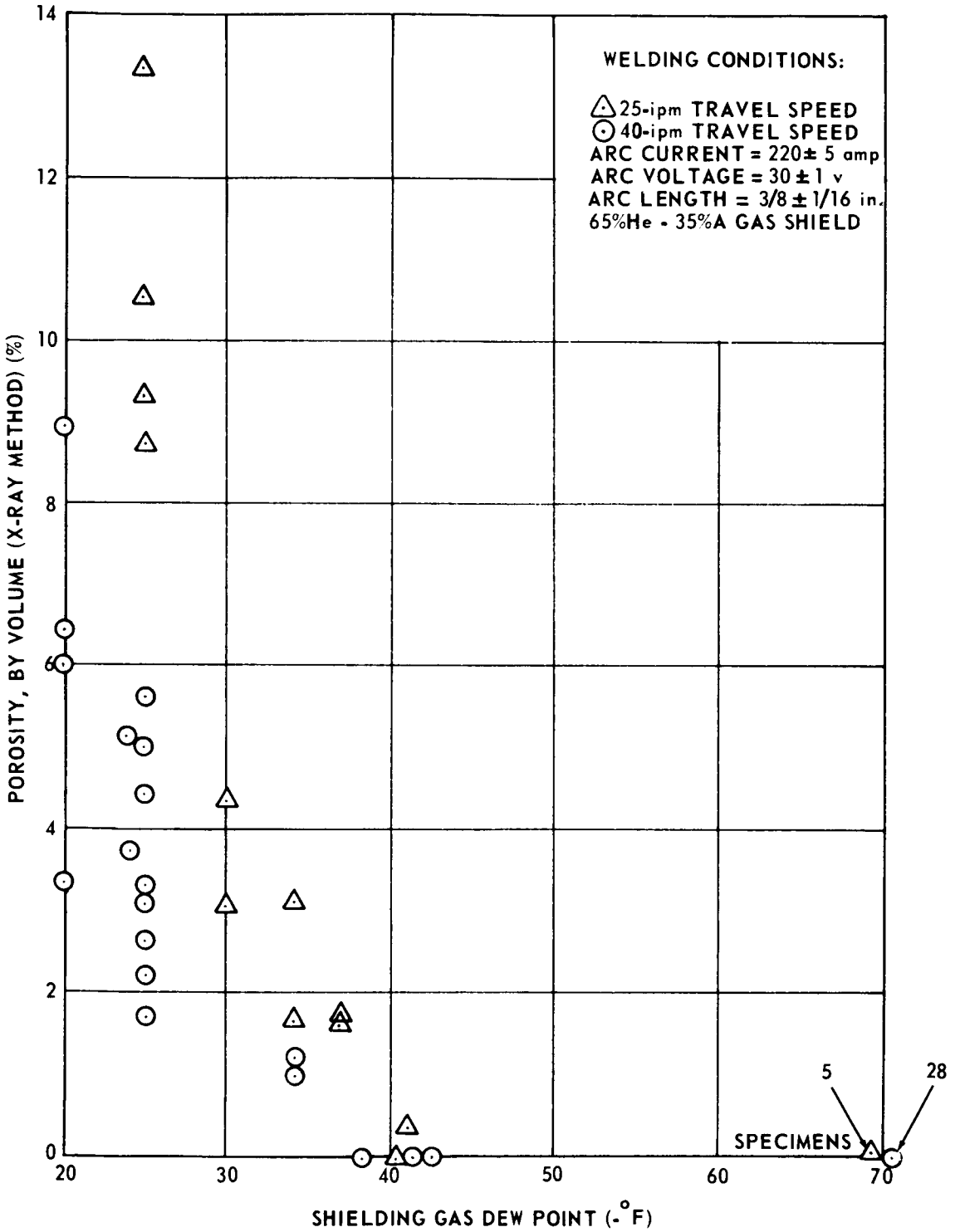

FIGURE 11. EFFECT OF SHIELDING-GAS DEWPOINT ON POROSITY FORMATION

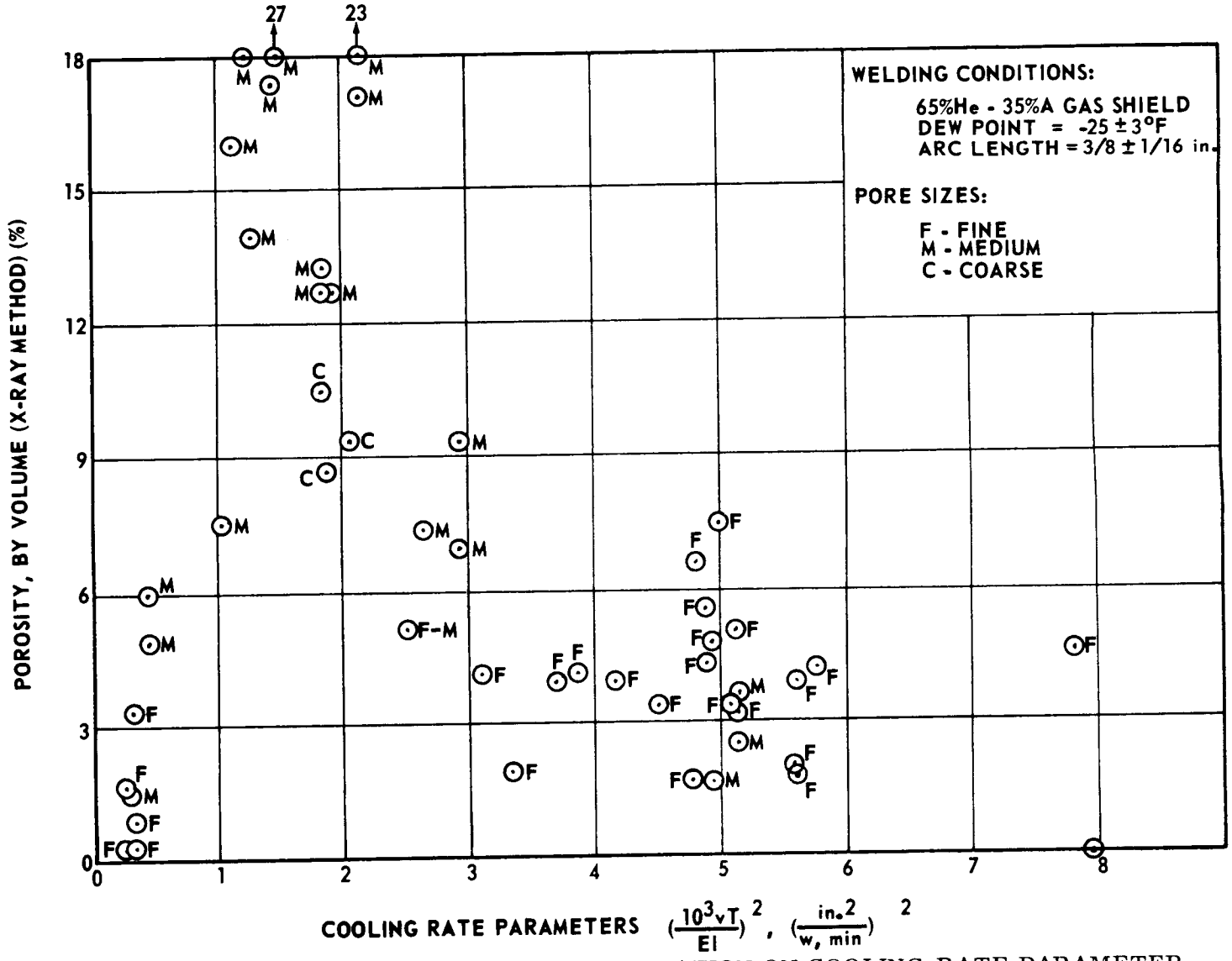

FIGURE 12. DEPENDENCE OF POROSITY FORMATION ON COOLING-RATE PARAMETER, HELIUM/ARGON WELDS

c. Results Obtained

Experimental data were analyzed statistically by the Douglas investigators. For data on 2219-T87 static welds made in Phase I, the following regression equations were obtained:*

$$Y_1 = 0.4 + 0.0124\, X_1 \tag{5}$$

$$Y_2 = 6.2 - 0.024\, X_1 + 0.000048\, X_1^2 \tag{6}$$

$$Y_3 = -161.8 + 1.590\, X_1 - 0.451\, X_2 + 22.05\, X_3 - 0.735\, X_4 - 355.8\, X_5 - 0.00282\, X_1X_2 - 0.0882\, X_1X_3 + 2.23\, X_2X_5 + 1.47\, X_4X_5 \tag{7}$$

$$Y_5 = 64,420 + 1200\, X_1 - 2.4\, X_1^2 \tag{8}$$

where

Y_1 = porosity determined gravimetrically, percent

Y_2 = time to reach the thermal arrest, or solidification time, sec

Y_3 = hydrogen content in the weld metal, ppm

Y_5 = number of pores in a volume equivalent of 1 g of weld metal

X_1 = water vapor present in the shielding gas, ppm

X_2 = measured arc current, amp

X_3 = measured arc voltage, v

X_4 = arc-exposure time, sec

X_5 = thickness of base plate, in.

Figure 13 was prepared by combining Eq. (6) and (8).[6] Shown in the figure is the relationship between the inverse square of solidification time, $(1/Y_2^2)$, and Y_5/Y_2, which was considered as the pore nucleation rate, N.

*It was found that the dendrite spacing, Y_4, was not a function of the independent variables.

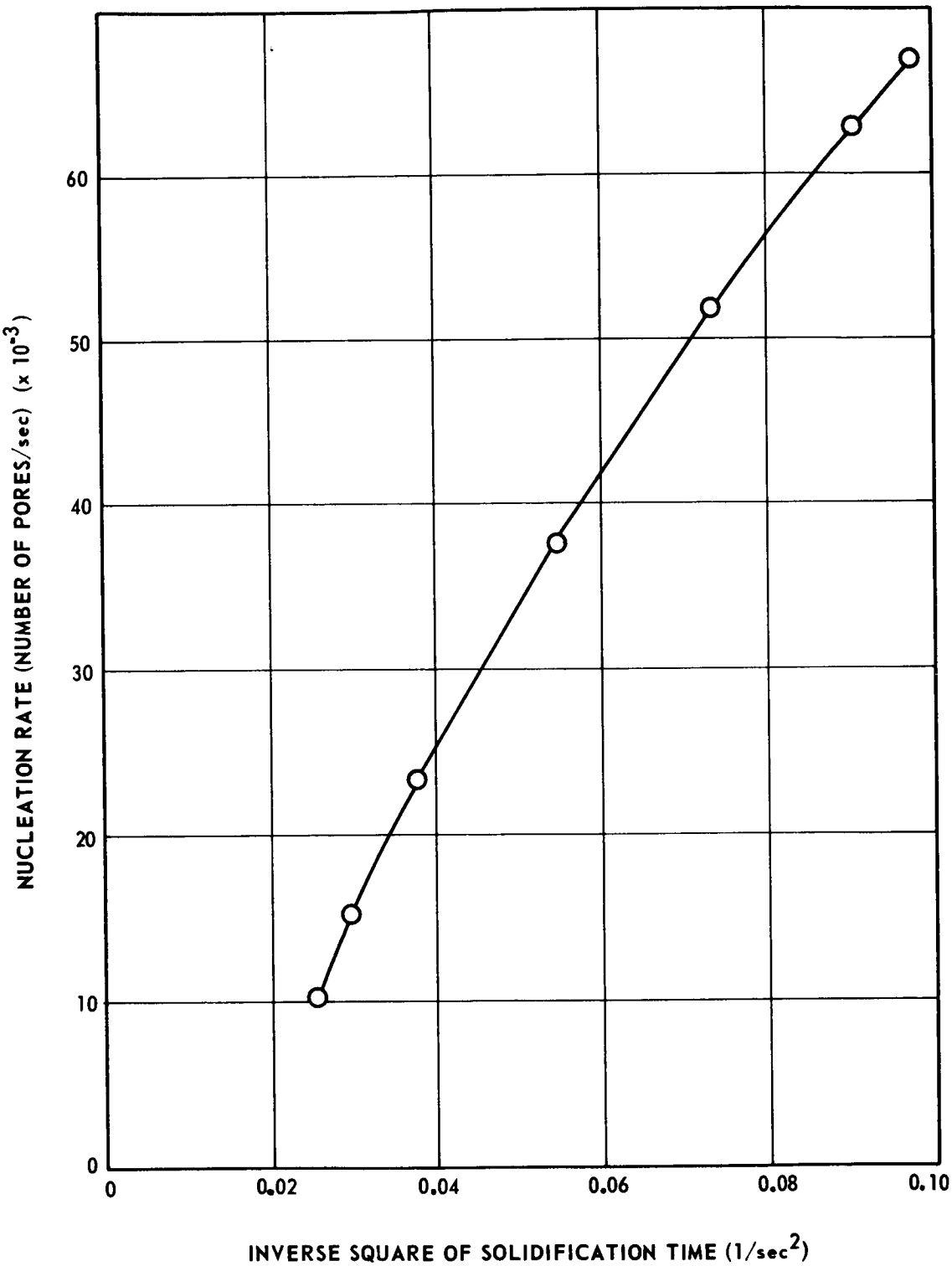

FIGURE 13. NUCLEATION RATE AS A FUNCTION OF THE INVERSE SQUARE OF SOLIDIFICATION TIME, PHASE I

Figure 14 was prepared by combining Eq. (5), (6), and (8).[6] Shown in the figure is the relationship between the square of solidification time, (Y_2^2), and $\frac{Y_1}{Y_5} \times \frac{1}{Y_2}$ which was considered as the pore growth rate, G.

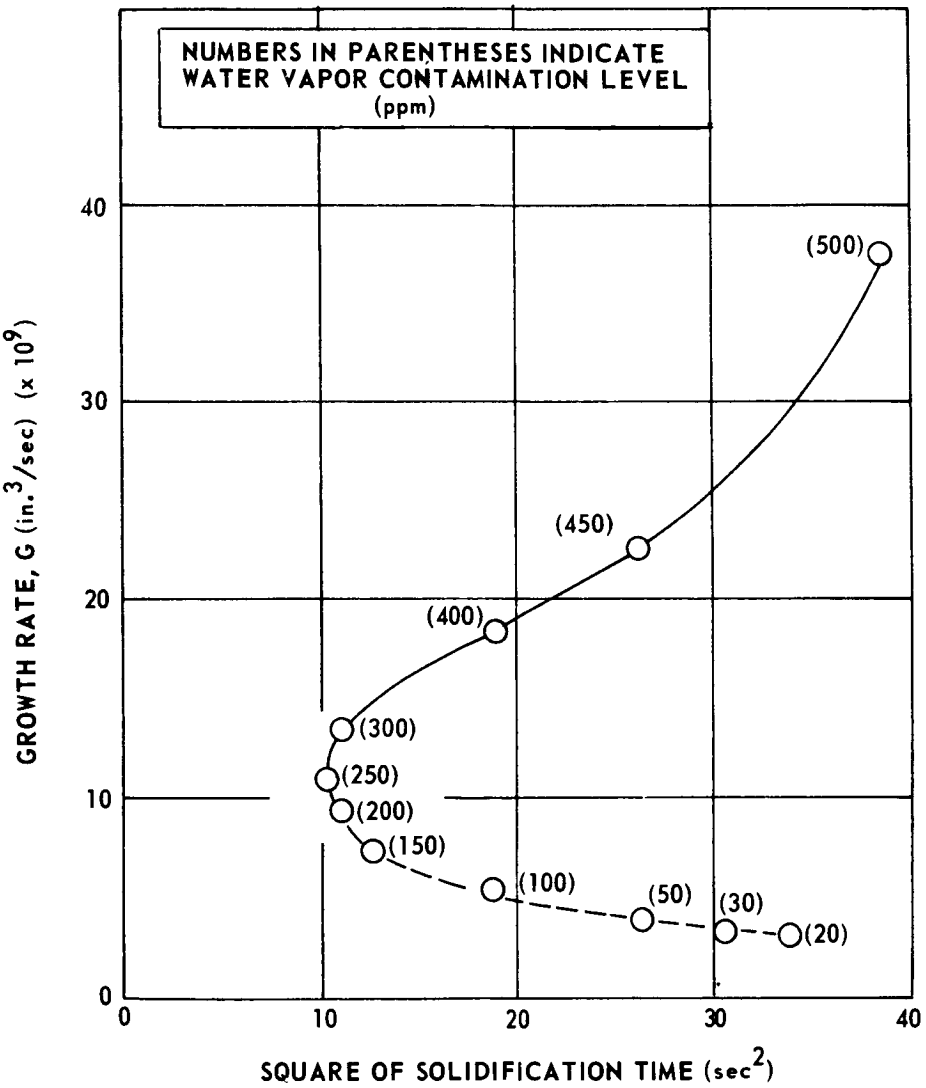

FIGURE 14. GROWTH RATE AS A FUNCTION OF THERMAL ARREST FOR VARIOUS WATER VAPOR CONTAMINATION LEVELS, PHASE I

Similar statistical analyses were conducted on data for bead-on-plate welds made in Phase II.

d. Analysis and Evaluation of the Douglas Study on Mechanisms of Porosity Formation

The conclusions drawn by the Douglas investigators are summarized in the Appendix.

During the course of this study, questions were raised about the way conclusions were being drawn from experimental data. The conclusions reached by the Douglas investigators have been considered questionable, and they are not used in any conclusions or recommendations for this report.

5. Use of Hydrogen Getters for Reducing Porosity

A literature study and welding experiments were performed at Southern Research Institute under Contract NAS8-20307 to determine the feasibility of using various elements as hydrogen getters during the gas tungsten-arc and gas metal-arc welding of aluminum alloys.

The project was originally divided into the following four phases:

Phase I. Literature and theoretical study to select the most promising elements to be used as getters.

Phase II. Preliminary evaluation of the selected elements by means of rapid melting operations simulating weld heating cycles.

Phase III. Evaluation of methods for applying the promising elements, using arc spot welds made with GTA and GMA welding techniques.

Phase IV. Evaluation of the most promising elements and application methods on 36-in. long welds.

However, Phases II and IV were discontinued. Therefore, this report covers Phases I and III only.

a. Phase I. Literature and Theoretical Study

It was determined from a survey of the literature[26-29] that hydrogen is chemically able to combine with almost every element to form binary compounds. These compounds are divided into three groups: the covalent hydrides, the saline hydrides, and the transition-metal hydrides.

The covalent hydrides are formed by the elements B, C, N, O, F, Si, P, S, Cl, Ge, As, Se, Br, Sn, Sb, Te, I, Pb, Bi, and Po. The elements Cu, Ag, Au, Zn, and Hg form an intermediate type of hydride that is neither pure ionic nor metallic bonded but tends to have the characteristics of the covalent hydrides. Therefore, this type hydride was included with the covalent hydrides for consideration in this study. In their natural state covalent hydrides are usually in either liquid or gaseous form. Since it was considered likely that liquid or gaseous hydrides would be detrimental if mixed into the weld puddle, these elements were eliminated from further consideration.

The saline hydrides are ionic in their bonding and form stoichiometric compounds. The elements included in this classification are Li, Na, Mg, Al, K, Ca, Rb, Sr, Cs, Ba, and Ra. It is probable that the rare earths are also included in the saline-hydride group.

The transition-metal hydrides are formed by Ti, Zr, Hf, Th, V, Cb, Ta, Pa, Cr, Mo, W, U, Pu, Fe, Ru, Os, Rh, Ir, Ni, Pd, Co, and Pt. These hydrides exhibit metallic bonding and nonstoichiometric compositions depending upon the exposure time to hydrogen, temperature of reaction, and past history of the element.

It was decided to select four of the promising elements for experimental investigation of their hydrogen-getting abilities, one from the saline group, two from the transition metals, and a rare earth. Calcium was chosen to represent the saline group because it was more readily available and presented less stringent handling requirements than Ba and Sr. Of the transition metals, Ti and Zr were chosen because of their availability and lower cost in comparison to Hf. Mischmetal, a mixture consisting of approximately 50 percent cerium and other rare-earth metals (principally lanthanum and neodymium), was chosen to represent the rare earths.

b. Phase III. Evaluation in Arc Spot Welds

The specimens used for evaluation were 1-1/2 by 3-in. rectangles of 2014 and 2219 alloy plates 3/4-in. thick. On most specimens, a GTA spot weld was made at the center of the specimen.

The procedures used in connection with the getters varied depending upon the methods used for applying the getters. Six different series of welds were made, vehicle series, small-hole series, depression series, butt-joint series, first slurry series, and second slurry series. With the exception of calcium, the getters were received in forms that necessitated drying procedures prior to application of the powders. Cerium (Mischmetal), which was received under kerosene, was given repeated rinses in hexane and allowed to dry following the final rinse. The titanium and zirconium powders were received in a moisturized condition to protect them from oxidation. This moisture was removed by keeping the powders in a continuously evacuated dessicator for a period of 24 hr. The dried powders were stored in dessicators under argon atmosphere.

Vehicle Series. The vehicle series of welds was made to determine whether some materials that might be used to bond the getter material to the workpiece surface would, in themselves, provide a source of moisture or hydrogen and contribute to porosity. The vehicles examined were epoxy resin, Duco cement, lime paste, and ethyl alcohol. These vehicles, alone and in combination with Ti powder, were applied to the freshly scraped surfaces of a series of specimens and fusion spot welded. In general, all specimens were welded at 150 or 200 amp, 14 v, and 53 CFH helium gas flow. Welding times varied depending upon the time necessary to achieve deep penetration into the workpiece. The helium gas in the dry condition (no moisture added) had a dew point of -35°F and consistently produced pore-free arc spot welds. On the basis of preliminary experiments to produce welds with easily detectable porosity, the moisturized gas was standardized at a + 50°F dew point. When the specimens had been welded, they were sectioned through the center of the nugget, wet-ground with silicon-carbide papers through 500 grit fineness, and visually examined for porosity. The visual results were negative; the addition of the powder did not result in reduction of porosity. Consequently, it was decided that the vehicle series would not be subjected to quantitative examination.

Small Hole Series. The small-hole series was made in an effort to apply the getters without vehicles and to assure that the getter material would be incorporated in the molten puddle during welding. In this procedure, eight 0.073-in. diameter holes were drilled to a depth approximately 3/4 the thickness of the plate at approximately equally spaced locations on the circumference of a 1/2-in. diameter circle surrounding the center of the location of the subsequent spot weld. Prior to the welding operation, the specimens were scraped and the getter materials packed into the small holes. The welding and inspection procedures were the same as those used for the vehicle series. All of the welds made with getters were porous even though made with dry gas. Since some specimens retained unfused portions of the original drilled holes, it is likely that much of the porosity was caused by entrapped air from the holes.

Depression Series. The depression series was made in an effort to avoid the use of vehicles and yet apply the getter without installing it into the deep interior of the specimens. Accordingly, the getters were packed into a shallow depression made with a 1/4-in. diameter drill to approximately a 1/8-in. depth. This depression was located at the center of the subsequent weld location. The same welding and inspection procedures used for the two previous series were used on these welds. Welds in this series were made with dry gas first with inconclusive results. The welds made with moist gas were all porous. However, the results could not be considered conclusive because the arcs struck directly on the getters were erratic, and there was some doubt about whether the getters remained in position long enough to be effective.

Butt-Joint Series. The specimens were cut in half along the transverse centerline and then rejoined with an arc spot weld. The getters were placed on the end faces to be butted together and were held in place by clamping the two pieces tightly together in the vise. An additional getter, barium, was included in this series to determine whether it might react more favorably than calcium. Although all but two specimens were welded with dry helium, only one specimen appeared to be relatively pore free. In addition, it was difficult, especially with Ti, to fuse the joint together. The arc tended to melt the aluminum on either side of the getter layer but the molten material would not penetrate through the unmolten getter to form the joint.

The First Slurry Series. The first slurry series was planned in an attempt to overcome the problems that had prevented the attainment of uniform welding conditions in the previous experiments. As a first criterion, it was decided that the getter should be applied only to the scraped surface and not packed in prepared holes or depressions. Since no suitable vehicle had been found to bond the getters, and since dry getters would not adhere sufficiently, the powdered getters were moistened with distilled water to form a slurry, which was then applied to the specimen surface with a small brush. The specimens were then placed on a 250°F hot plate and heated until all visible traces of moisture were gone. The dried, getter-coated specimens were stored in a dessicator while awaiting the welding operation. On the day of the welding run, these specimens were placed in an oven at 400°F and allowed to remain heated for at least one hour before the first specimen was removed for welding.

Photographs of cross sections of the welds are shown in Figure 15, and the results of the porosity measurements are shown in Table VIII.[8] There were two ungettered welds, No. 133 and 134. The ungettered weld made with dry helium (No. 133) contained very little porosity. The ungettered weld made with moist helium (No. 134) was porous, and all of the gettered welds contained porosity. Each of three additional getters (No. 139, 140 and 141) produced greater porosity than the original four, although Ca (applied as lime) had

SHIELDING GAS		GETTER USED
DRY HELIUM	133	NONE
MOIST HELIUM	134	NONE
MOIST HELIUM	135	TITANIUM
MOIST HELIUM	136	ZIRCONIUM
MOIST HELIUM	137	CERIUM
MOIST HELIUM	138	LIME
MOIST HELIUM	139	SULPHUR
MOIST HELIUM	140	SODIUM BORATE
MOIST HELIUM	141	SODIUM NITRATE

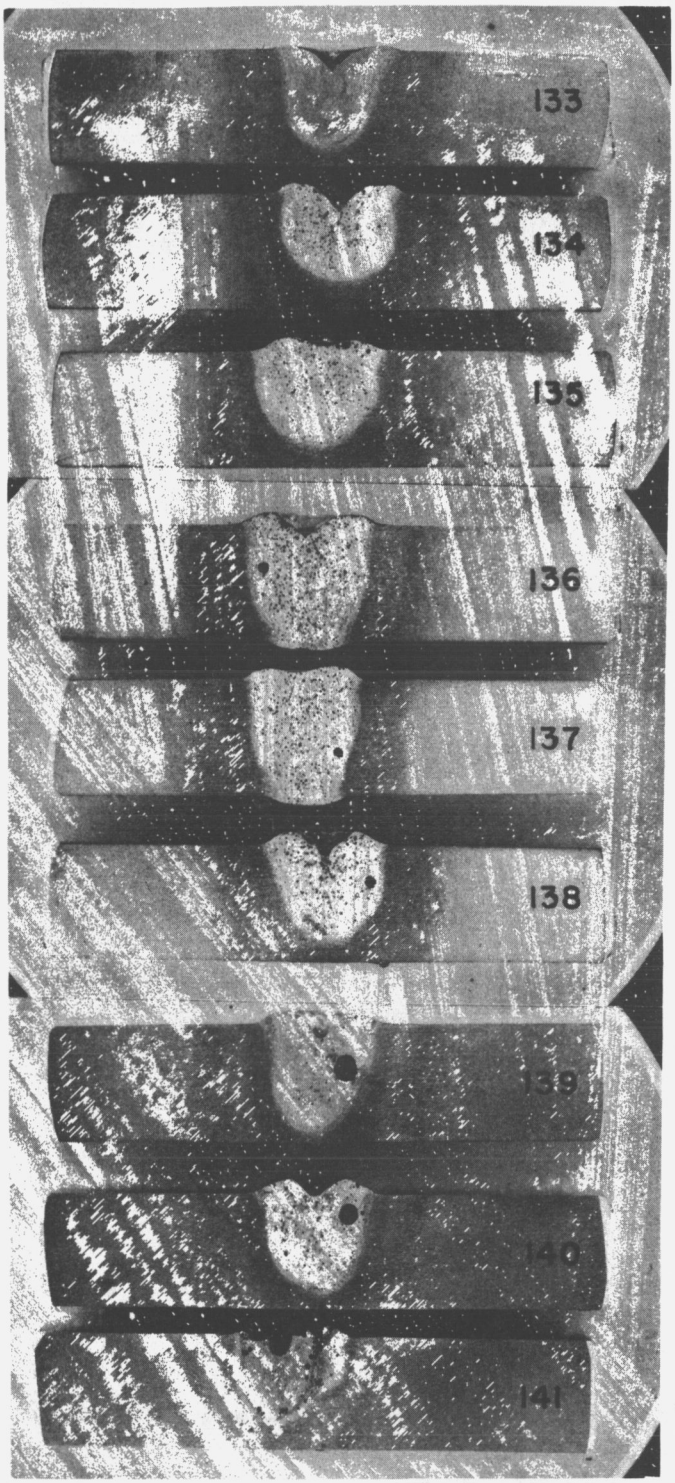

(Black and white spots both indicate pores within the weld nugget; etched with 10% NaOH and Keller's concentrated etch.)

FIGURE 15. POROUS CONDITIONS OF FIRST SLURRY SERIES

TABLE VIII. RESULTS FROM FIRST SLURRY SERIES

Spec No.*	Getters**	Porosity (%)	Largest Pore Dia (in.)	Joint † Temperature (°F)
133	None (dry gas)	3.2	0.00275	869 ††
134	None	39.8	0.0159	791
135	Titanium	35.4	0.0205	851
136	Zirconium	33.4	0.0291	890
137	Cerium	29.4	0.0370	874
138	Lime	43.8	0.0376	812
139	Sulphur	45.5	0.0615	789
140	Sodium borate	45.0	0.0511	827
141	Sodium nitrate	50.0***	0.0199	715

*All welds made with 14 v and 150 amp for 7 sec.

**All welds made with +50°F dewpoint helium except No. 133 and with -35°F dewpoint. Gas flow was 53 CFH for all welds.

***Average of one reading of 25.6% porosity at centerline vertical traverse, and one reading of 74.3% porosity with vertical traverse made at the area of maximum porosity.

† Average temperatures from two thermocouples on bottom of nugget 1/4 in. from centerline.

†† Reading from one thermocouple only. Other thermocouple become detached during welding.

nearly as much porosity. Although the relationship was not visually evident in Figure 15, the quantitative measurements showed the welds made with Ti, Zr, and Ce (No. 135, 136, and 137) to have less porosity than the ungettered specimen welded with moist gas (No. 134), as shown in Table VIII. These results indicated that some benefit was derived from Ti, Zr, and Ce, but porosity was only slightly reduced not eliminated.

Second Slurry Series. The second slurry series was performed to check the previous results with Ti, Zr, and Ce, and to investigate a large number of other elements and compounds for their capabilities as getters. This series was performed in the same manner as the first slurry series, except that equal volumes of the getter materials were used in making the slurries, and the slurries were applied to the electrodes as well as to the specimens.

The percent porosity in welds made with Ti, Zr, Ce, and Ca as getters was approximately the same as in the first slurry series. However, because there was less porosity in the ungettered specimen than in the first series, none of the gettered specimens appeared to have reduced porosity. Several of the elements and compounds used resulted in welds with porosity present in the same range as the Ti, Zr, and Ce specimens. These materials included Fe, Mn, $CuCl_2$, LiCl, NaCl, $AlF_3 \cdot 3NaF$, MnO, NiO, TiO_2, and $CaSi_2$. All of the other getters produced greater porosity, and two of them, Al and KCl, produced extremely high porosity.

c. Analysis and Evaluation of the SRI Study on Hydrogen Getters

The conclusions drawn by the Southern Research Institute investigations are summarized in the Appendix. The integrator's discussion follows.

Experiments were made to determine whether porosity could be reduced by applying hydrogen getters in areas near a GTA arc spot weld. The getters were prepared in powder form and applied to specimens by various techniques as outlined in the preceding discussion. None of the techniques proved to be effective for reducing porosity.

Fine powders have large surfaces compared to their volumes and are easily contaminated. Air is always present around powders, even when they are packed. As demonstrated by other investigators in the NASA program, porosity in aluminum welds can result from very slight shielding-gas impurities and very minimum contamination of the electrode or workpiece surface. Findings obtained at Boeing indicate that the existence of only 250 ppm of gas impurity, or of a single fingerprint on the metal surface, will cause porosity. At SRI, no measurement was made of the impurities around the hydrogen getters applied to specimens.

It is the integrator's opinion that SRI work has neither proved nor disproved whether porosity can be reduced by using hydrogen getters. Therefore, it may be worthwhile to try a different approach to the problem. Perhaps an approach would be the use of experimental filler wires containing hydrogen getters.

6. Effects of Porosity on Weld-Joint Performance

Effects of porosity on weld-joint performance were studied by The Martin Company under Contract NAS8-11335. The work done at Boeing also

includes data on the effects of porosity on mechanical properties of welds. These programs are discussed in this section following a brief general discussion on the effects of weld defects on the performance of welded structures.

a. General Discussion on the Effects of Weld Defects on the Performance of Welded Structures

Weld defects such as porosity, slag inclusions, incomplete penetration, and cracks cause reduction in mechanical properties of welded joints for two reasons. First, the presence of the defects causes decreases in sectional areas. Second, stress concentrations take place around the defects. The extent to which weld defects affect the strength of structures depends upon the following factors:

1) Nature and extent of defects. Sharp cracks that cause severe stress concentrations have more significant effects than do porosity or slag inclusions which cause rather minor stress concentrations. The effect of the defects on the strength becomes more severe as the size and number of defects increase.

2) Properties of the material. The properties of a material are significant factors that determine the effects of weld defects on the strength of welded structures. When a material is ductile, the reduction of strength is approximately proportional to the reduction of cross-sectional area, as described later. For less ductile materials, the effects of defects become more serious.

3) Type of loading. When the structure is subjected to impact or repeated loading, the effects of defects on the strength become more serious than when the structure is subjected to static loading.

Stress Concentrations Around Defects. The shape of a defect and its orientation to the direction of loading significantly effect stress concentrations around the defect.[30, 31]

Figure 16a, b, and c show stress distributions around a general triaxial, ellipsoidal cavity in a homogeneous, isotropic, elastic body of infinite length which is under a uniform tensile stress, σ, at infinity. It is assumed that the stress at infinity is acting parallel to one of the major axes of the cavity (z-axis), as shown in Figure 16a. The important stress concentrations occur along the "equator" ABA'B'A. The curves in Figure 16a show how rapidly the tensile stresses drop to the average value σ within the material.

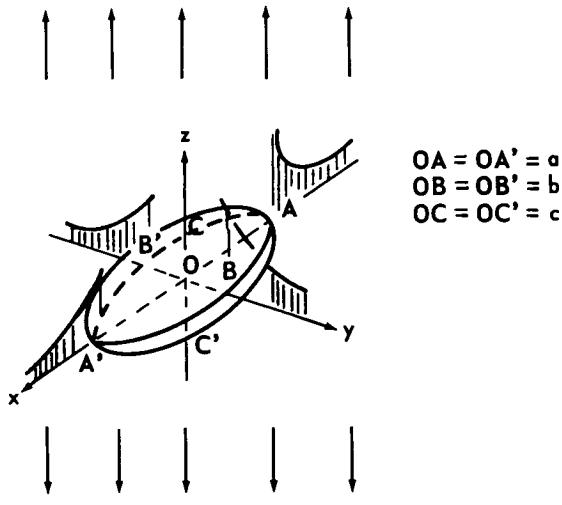

$\sigma_z = \sigma$ AT INFINITY

a. ELLIPSOIDAL CAVITY IN AN INFINITE BODY UNDER UNIAXIAL TENSILE STRESS

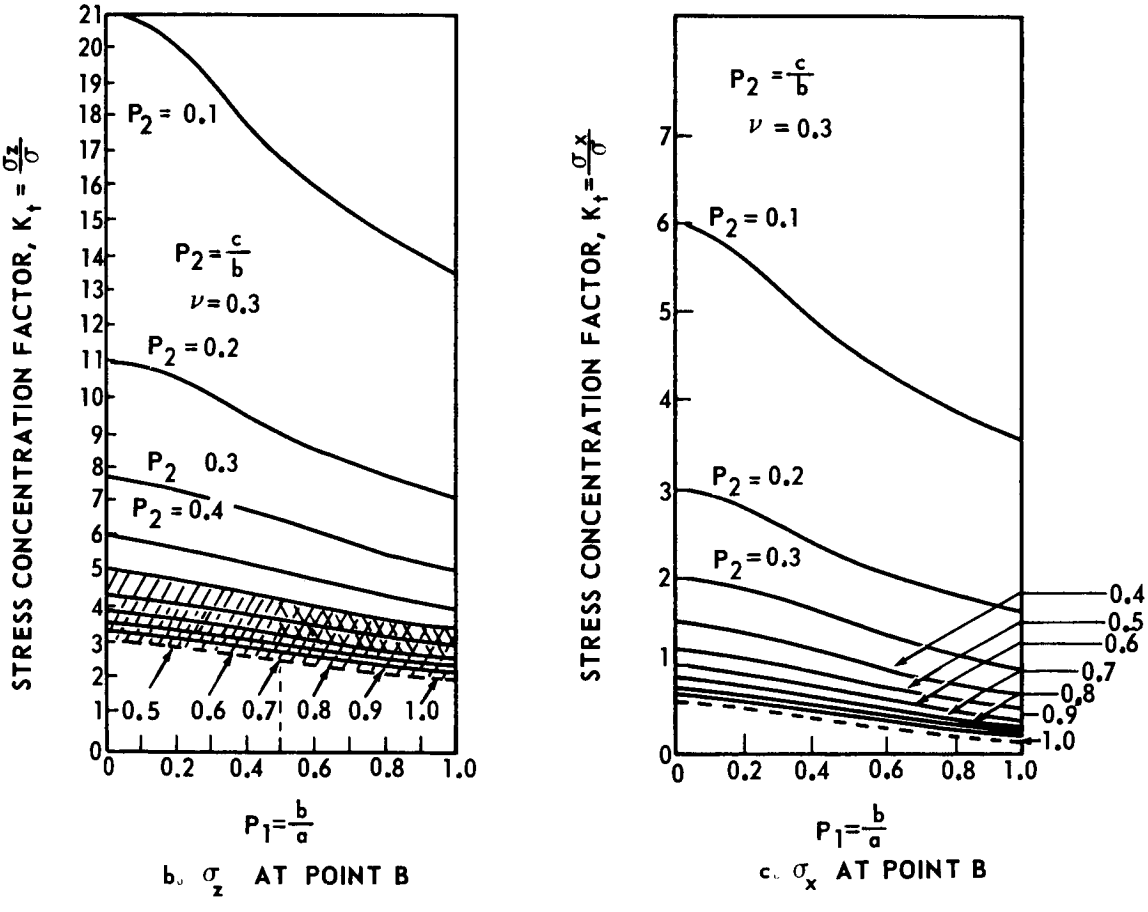

FIGURE 16. STRESS CONCENTRATIONS AROUND AN ELLIPSOIDAL CAVITY IN AN INFINITE BODY UNDER UNIAXIAL TENSILE STRESS

The severity of stress concentration is expressed frequently in terms of the stress-concentration factor, K_t, which is defined as the ratio of the stress at a point concerned and the stress at infinity, σ. Figures 16b and c show values of $\frac{\sigma_z}{\sigma}$ and $\frac{\sigma_x}{\sigma}$ ($\sigma_y = 0$ at Point B) as a function of the shape ratios $\rho_1 = b/a$ and $\rho_2 = c/b$.[32] The value of Poisson's ratio is assumed to be 0.3.

The curves for $\rho_2 = 1$ apply to a cavity in the shape of a prolate spheriod (cigar-shaped cavity). The limiting case of $\rho_1 = 0$, $\rho_2 = 1$ can be interpreted geometrically in two ways. If b is fixed and approaches infinity, the shape of the cavity approaches that of a circular cylinder of infinite length; if a is fixed and b and c approach zero, the cavity approaches a line crack. The curves for $\rho_1 = 1$ apply to a cavity in the shape of an oblate spheroid (button-shaped cavity). The case of $\rho_1 = \rho_2 = 1$ applies to a spherical cavity. As shown in Figures 16b and c, the stress concentrations are mild for cigar-shaped cavities, the value of $\frac{\sigma_z}{\sigma}$ ranging between 2.05 (for a spherical cavity) and 3 (for a long cylindrical cavity). On the other hand, high stress concentrations occur around a thin, button-shaped cavity having its surfaces perpendicular to the direction of loading.

Porosity in weld metals in aluminum alloys is spherical in many cases, as shown in Figures 9 and 10. The porosity may be worm shaped; elongated in the direction of weld metal solidification. Weld porosity with the shape of an oblate spheroid is rarely found; porosity rarely contains sharp notches. Consequently, stress concentrations around weld porosity usually are not very severe. The values of stress-concentration factors around porosity appear to be in the cross-hatched areas in Figure 16b--either in the single cross-hatched areas ($\rho_2 > 0.5$) or more often in the double cross-hatched areas ($\rho_1 > 0.5$, $\rho_2 > 0.5$).

Ductile Fracture. Let us consider a case in which a flat plate (width, B, and thickness, t) containing a circular hole of diameter, d, is under a tensile load, P, as shown in Figure 17. The average stress, $\bar{\sigma}$, and the net stress, σ_{net}, are defined as follows:

$$\bar{\sigma} = \frac{P}{A_0}, \quad \sigma_{net} = \frac{P}{A_{net}} = \frac{A_0}{A_{net}} \bar{\sigma}, \tag{10}$$

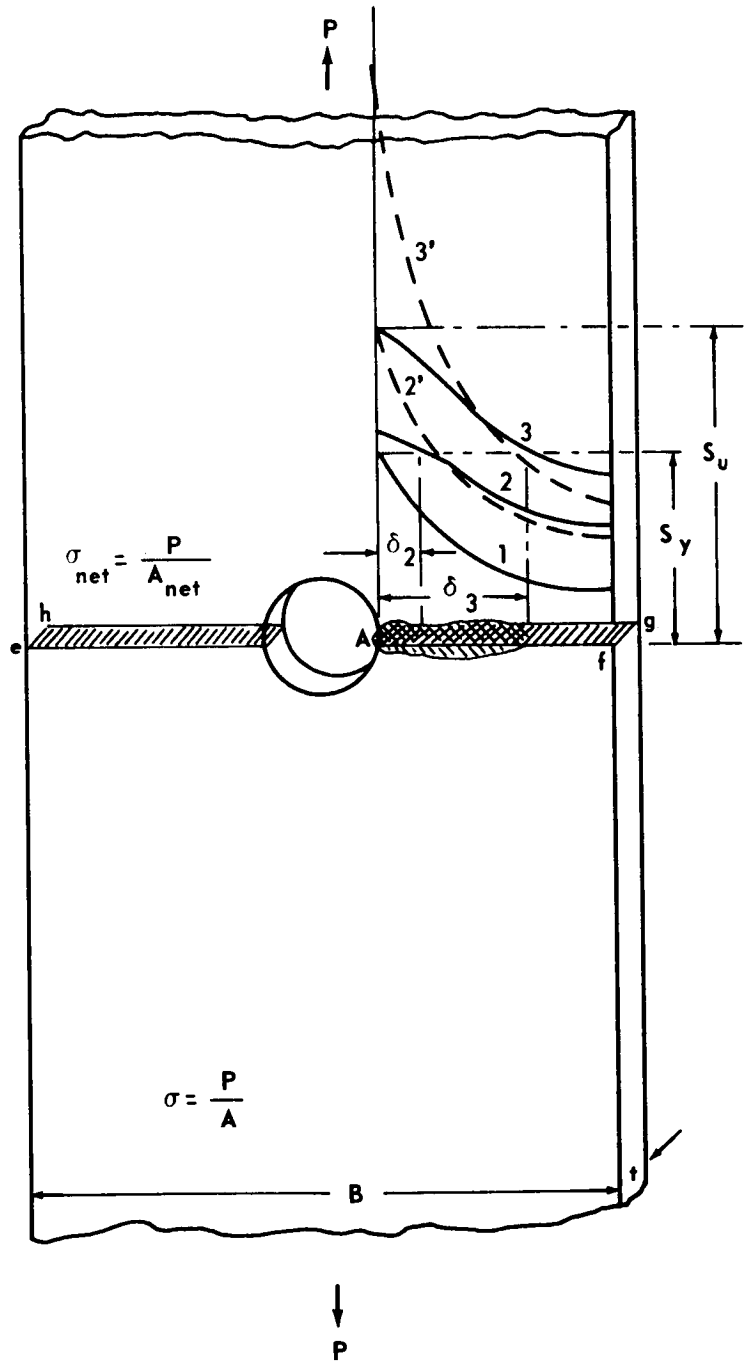

FIGURE 17. EFFECT OF DEFECT ON BEHAVIOR OF DUCTILE MATERIAL UNDER TENSILE LOADING

where

A_0 = Bt is the original section area

A_{net} = (B - d)t is the net section area.

When B/d is sufficiently large, the leastic stress-concentration factor, K_t, is close to 3. S_y and S_u are the yield strength and the ultimate tensile strength of the materials, respectively.

Curve 1 shows the distribution along line Af at the stress level $\overline{\sigma} = \frac{S_y}{K_t}$. The magnitude of stress at Point A reaches the yield strength of the material. If the magnitude of applied stress exceeds $\frac{S_y}{K_t}$, plastic deformation takes place in the highly stressed regions as shown by the cross-hatched areas in Figure 17, and finally fracture occurs.[33]

It would be quite unrealistic to assume that fracture occurs at an average stress of $\frac{S_u}{K_t}$. When the average stress is $\frac{S_u}{K_t}$, the stress distribution would be as shown by Curve 2 instead of being shown by Curve 2', elastic stress distribution.[34] The stresses in the plastic region (depth, δ_2) are in the neighborhood of the yield stress, S_y, and considerably lower than S_u.

The stress distribution at fracture would be as shown by Curve 3, average stress at fracture being $\overline{\sigma}_f$. The plastic region extends to a depth of δ_3. Curve 3' is the imaginary elastic stress distribution at the average stress of $\overline{\sigma}_f$. The maximum stress at Point A, K_t, $\overline{\sigma}_f$, is much higher than S_u. If the material is ductile (undergoes large plastic deformation before fracture occurs), the plastic regions extend and the stress concentrations around the defect are reduced.

However, since the section area along Plane efgh is less than the original section area, fracture usually occurs when the net stress approaches S_u. In other words, the average fracture stress $\overline{\sigma}_f$ is:

$$\bar{\sigma}_f = \frac{A_{net}}{A_0} S_u \,. \qquad (11)$$

The fracture is a shear fracture and propagates relatively slowly.

A number of research programs have been carried out to determine experimentally the effects of defects on the strength of weldments in various materials. For example, Kihara, et al.[35] have summarized experimental results obtained from a large number of specimens to show the general tendency of the effects of weld defects on the static tensile strength of aluminum welds (Figure 18). The ultimate strength did not decrease appreciably when the reduction of sectional area due to defects was less than about 10 percent. From that point the strength decreased gradually as the reduction of sectional area increased. For example, a 40 percent decrease in sectional area caused between about 20 and 40 percent decrease in the ultimate tensile strength.

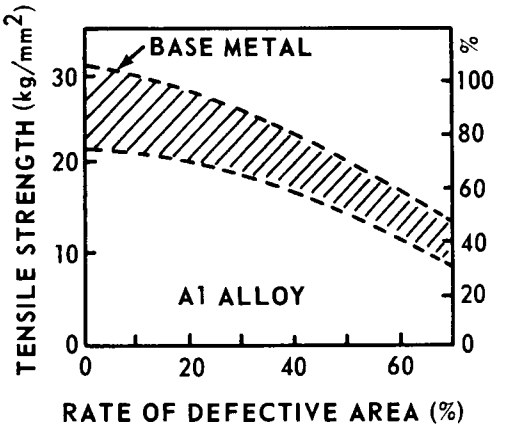

FIGURE 18. RELATIONSHIP BETWEEN RATE OF DEFECTIVE AREA AND ULTIMATE TENSILE STRENGTH BUTT WELDS IN ALUMINUM ALLOY

Chemical Composition of the Aluminum Alloy

	Chemical Composition (%)								
Specification	Cu	Fe	Si	Mn	Mg	Zu	Cr	Ti	Al
ANP-O	0.03	0.16	0.09	0.56	4.3	0.02	0.19	Nil.	Bal.

Unstable Brittle Fracture. Unstable rapid propagation of fracture has been experienced in a number of welded structures.[36,37] The fracture mechanics theory developed by Griffith,[38] Irwin,[39,40] and other investigators has been applied to the study of unstable fractures, especially of those in high-strength materials for aerospace applications. Figure 19 illustrates typical behavior

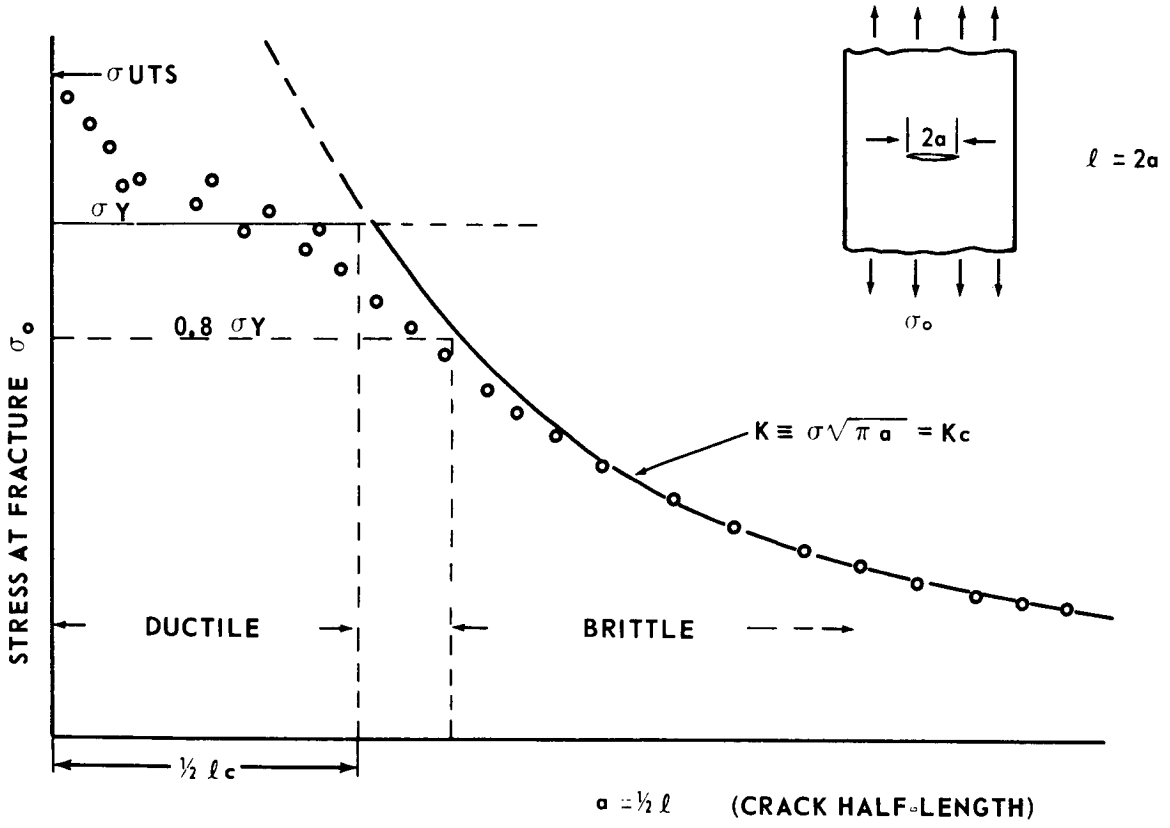

FIGURE 19. UNSTABLE FRACTURE, HIGH-STRENGTH MATERIALS CONTAINING A CENTRAL CRACK--EFFECT OF CRACK LENGTH ON STRESS AT FRACTURE

when a sheet containing a transverse central crack is subjected to uniform tensile loading. For small cracks, fracture strength exceeds yield strength. Gross yielding is observed in the load-deflection diagram, and extensive plastic deformation is observed in the fracture surface. However, fracture from long cracks occurs abruptly with negligible plastic deformation. The observed fracture stress decreases with increasing crack length. Unstable fracture occurs when the stress-intensity factor, K, reaches a value, K_c, which is characteristic for the material.

$$K \equiv \sigma \cdot \sqrt{\pi a} = K_c, \tag{12}$$

where

σ = average fracture stress

a = half crack length.

K_c is called the critical stress intensity factor or fracture toughness of the material. The critical crack length, ℓ_c, also may be used to characterize the brittle behavior of the material; when the preexisting crack is shorter than ℓ_c, fracture stress, σ, exceeds the yield stress and fracture is ductile. The ASTM Committee on Fracture Testing of High-Strength Sheet Materials[41] has described methods of measuring fracture toughness of high-strength sheet metals (ferrous and nonferrous materials having a strength-to-density ratio of more than 700,000 psi/lb/in.^{3}). K_c can be determined by fracture tests of notched specimens.

An important consideration in unstable fracture is that the absolute size of a flaw is the controlling factor. If the material contains a crack larger than the critical size, the crack can grow under low applied stress even though the loss of sectional area due to the crack is minor.

It is known that metals with a body-centered cubic lattice, such as steels and titanium alloys, are sensitive to unstable fracture, while metals with a face-centered cubic lattice, such as aluminum alloys and austenitic stainless steels, are not. Unstable fracture is not a major problem for structures made in 2014-T6 and 2219-T87 alloys unless they are subjected to cryogenic temperatures.

b. Research Procedures Under Contract NAS8-11335

Production of Defective Welds. Welds were made in two materials (2219-T87 and 2014-T6), two thicknesses (1/4 and 3/4 in.), and three welding positions (flat, horizontal, and vertical). Filler wire used was 2319 with the 2219-T87 material, and 4043 with the 2014-T6 material. Arc welding was GTA, D-C, straight polarity with helium shielding. Welds had to be intentionally contaminated to produce porosity. This was done by metering additions of hydrogen and/or moisture to the shielding gas in the tungsten torch. However, extensive additions of hydrogen tended to form a large number of

very fine pores, relative to typical porosity size-frequency distribution in production welding. In some instances, the porosity was so fine that the X-rays would have been acceptable by most current standards; and yet the strength of these welds was appreciably reduced.

Another difficulty was changes in the electrical characteristics of the arc which were induced by contamination of the arc atmosphere. Specimens welded with heavy contamination had poor or nontypical bead geometry.

Defect Classification System. Classification of defects was performed both before and after destructive testing of the specimen. Nonspecific and arbitrary levels of porosity were assigned by comparison with an adopted series of standards. Five levels, 0 through 4, from water clear to quite bad, were adopted as target porosity levels for specimen production purposes.

Mechanical Property Evaluation. The defective welds were evaluated by longitudinal and transverse tensile testing and by transverse fatigue testing. The specimen width of the transverse tensile test was the standard 1-in. wide specimen for the 1/4-in. stock, and 1-1/2-in. wide for the 3/4-in. stock. The dimensions for the longitudinal specimen were chosen to insure that weld metal, heat-affected zone, and parent metal were included in the load-carrying cross section of the specimen. The objective was to simulate the stress picture which a weld sees in the girth orientation of a pressure vessel. In this orientation, the base plate adjacent to the weld is capable of carrying the larger part of the load, as long as the (possibly defective) weld metal is able to elongate and transfer this load to the adjacent base metal. Fatigue specimens were chosen according to a Martin Company standard (0.3 in. wide in the weld).

c. Results Obtained at Martin Under Contract NAS8-11335

Static Tensile Tests on Transverse Welds. Figure 20 shows relationships between the porosity level and mechanical properties of transverse-weld specimens.[9] Shown in the ordinate are the high, medium, and low values for each porosity level, and the "2σ minimum" values of the following:

1) Ultimate tensile strength

2) Yield strength

3) Elongation for 0.4-, 1-, and 2-in. gage length.

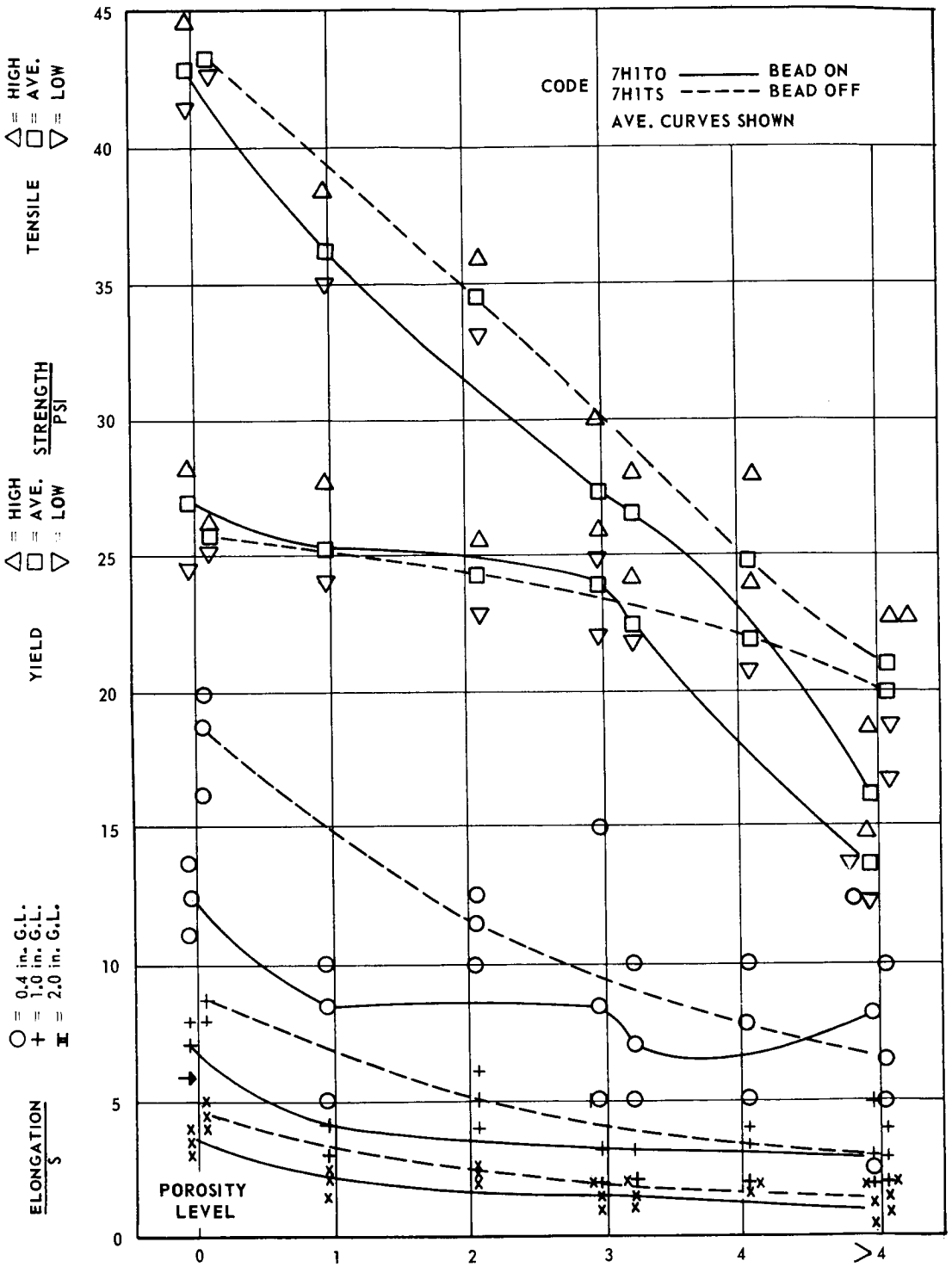

FIGURE 20. MECHANICAL PROPERTIES OF 2219-T87, 1/4-IN. ALUMINUM ALLOY CONTAINING INCREASING LEVELS OF POROSITY, TRANSVERSE HORIZONTAL POSITION, D-C GTA WELD 2319 FILLER METAL

Different curves are shown for data obtained with specimens with and without weld reinforcement.

Figure 21 shows that the ultimate strength decreased markedly as porosity increased.[9] Elongation, especially with a short gage length, also was affected by the porosity level. The porosity level had the least effect on the yield strength.

Attempts were then made to determine quantitative relationships between the porosity level and the ultimate strength. After specimens were fractured, fracture surfaces were examined to determine the loss of sectional area due to porosity. All pores larger than 1/64 in. in diameter were counted to determine the loss of sectional area.

Figure 21 shows data for 1/4-in. thick transverse welds in 2219-T87 (horizontal position). Data for specimens with and without weld reinforcement are shown. Shown in the abscissa are the total pore areas in terms of equivalent numbers of 1/64-in. diameter pores and the reduction of sectional area in percent.* Good correlations were obtained between the reduction of sectional area and the loss of strength. Marked decreases in the strength were observed on specimens with small loss of cross-sectional area. The Martin investigators stated that most specimens that showed significant loss of strength had many fine pores but pores smaller than 1/64 in. in diameter were not counted.

A study also was made of how existing aerospace industry specifications rate as instruments for predicting mechanical properties. Figure 22 illustrates ranges of ultimate strength found within welds of given classification levels according to the ABMA-PD-R-27A, in 2219 and 2014 weldments, respectively.[9] A large amount of scatter in data is noticed. The very low values under Class I were all taken from samples which contained large numbers of very fine pores.

Longitudinal Welds. The tensile strength of longitudinal specimens decreased as loss in cross-sectional areas due to increased porosity. Since a specimen contained the weld metal and the base plate, the porosity caused rather minor reduction in sectional area. Even specimens containing extensive porosity maintained strength over 40,000 psi. The effects of porosity on elongation and yield strength were minor.

*For example, one pore with 1/32-in. diameter and one with 1/16-in. diameter are considered to be equivalent to 4 and 16, respectively, of 1/64-in.-diameter pores.

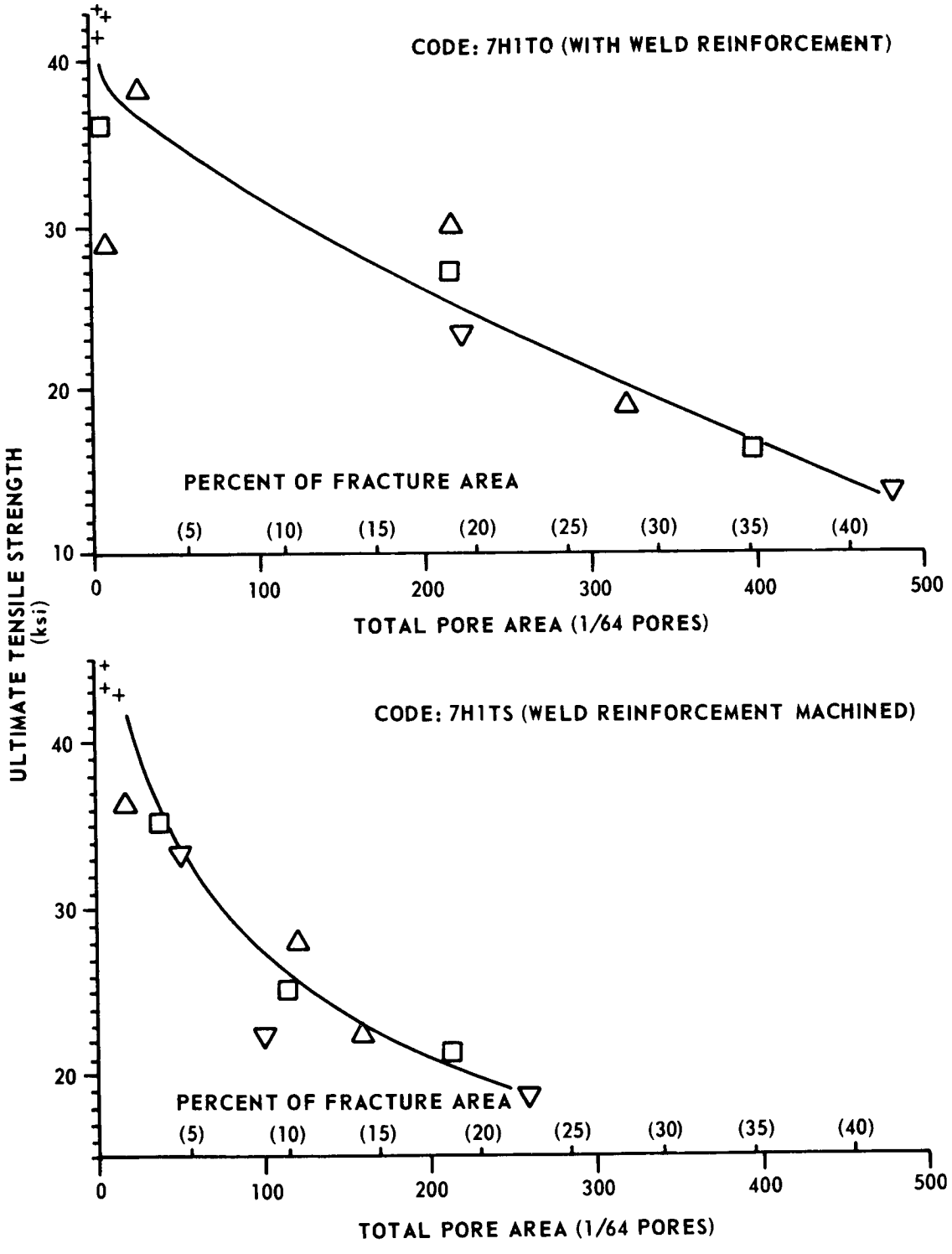

FIGURE 21. STRENGTH VERSUS PORE AREA, 2219-T87, HORIZONTAL WELD, 1/4 IN. TRANSVERSE TEST

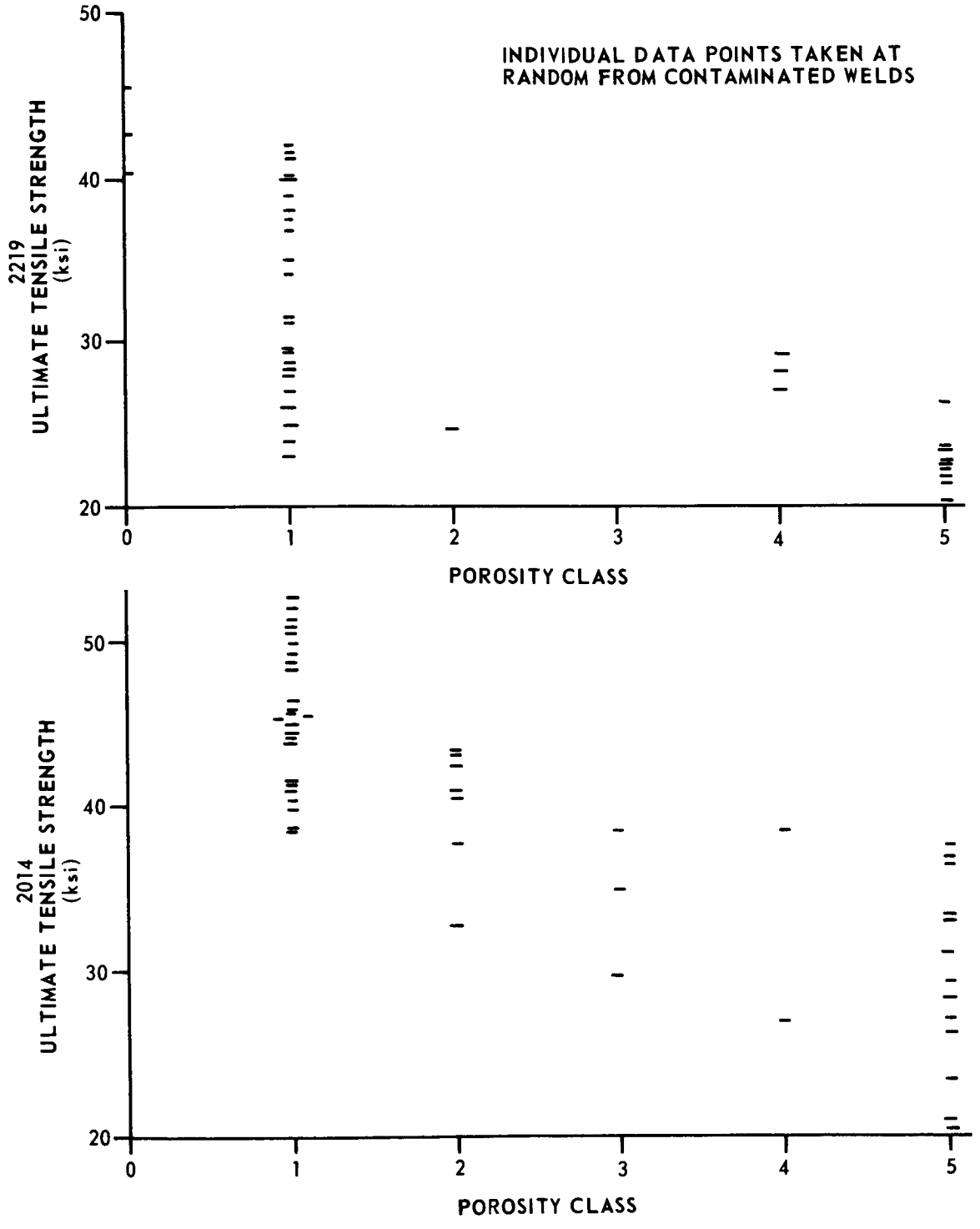

FIGURE 22. TRANSVERSE TENSILE STRENGTH VERSUS ABMA SCATTERED POROSITY CLASSIFICATION, 1/4 IN., BEAD ON AND BEAD OFF, MIXED TOGETHER

Fatigue Results. The results of the reversed-tension fatigue tests* were evaluated in terms of radiographic porosity counts; this showed that fatigue life decreased as porosity increased. Figure 23 summarizes results obtained on all 1/4-in. welds made in different alloys and welding positions. Shown in the figure are relationships between the pore count and the number of cycles to fatigue under various stress levels. On the basis of experimental data, lines indicating the minimum expected life are drawn for three stress levels, 10, 15, and 20 ksi. For example, a weldment containing twenty 1/64-in. pores per 1/4-in. length may have a life of over 100,000 cycles at 10 ksi, over 10,000 cycles at 15 ksi, over 1000 cycles at 20 ksi, but less than 1000 cycles at 25 ksi. The reduction of sectional area due to twenty 1/64-in. diameter pores per 1/4-in. weld is about 6 percent.

The 3/4-in. thick welds showed similar general trends.

d. Analysis and Evaluation of the Martin Study on Porosity and Mechanical Properties

The conclusions drawn by the Martin investigators are summarized in the Appendix. The integrator's discussion of significant findings follow.

An important finding obtained at Martin is the significance of small pores. If the reduction of strength due to a pore is determined by its cross-sectional area, a pore size which gives the least ratio of cross-sectional area to volume is to be desired. For a spherical void, the ratio of cross-sectional area to volume, α, is

$$\alpha = \frac{\pi R^2}{\frac{4}{3}\pi R^3} = \frac{3}{4}\frac{1}{R} . \qquad (13)$$

The value of α increases when R decreases. Thus, a given volume of contaminant gas in a freezing puddle can cause more damage in the form of small pores than large pores. Experimental results showed that small pores did cause significant reduction in strength.

However, the reduction of strength due to a small amount of pores observed during this study was very great, as shown in Figure 21. The author's interpretation of the experimental results is described briefly in the following paragraphs.

*The loading cycle went from a minimum of 10 percent of the nominal stress to a maximum 100 percent.

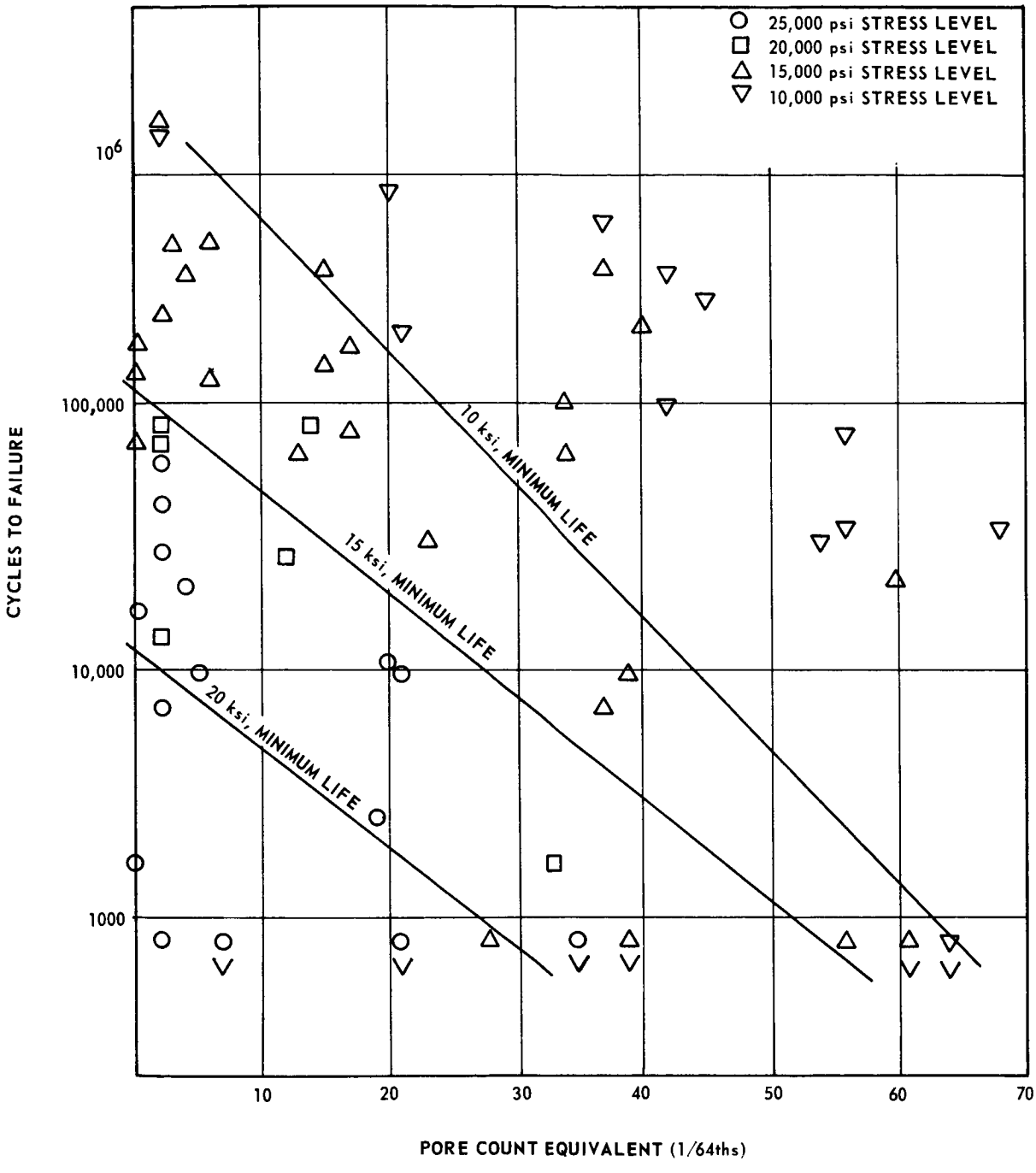

FIGURE 23. FATIGUE LIFE VERSUS FRACTURE PORE COUNT, 1/4 IN., ALLOYS AND POSITIONS MIXED

Figure 24 illustrates the relationship between the reduction of sectional area due to porosity, X percent, and the loss of ultimate tensile strength, Y percent. Obviously, Y = 100 at X = 0 (full strength at no defect, point A), and Y = 0 at X = 100 (no strength at 100 percent defect, point P).

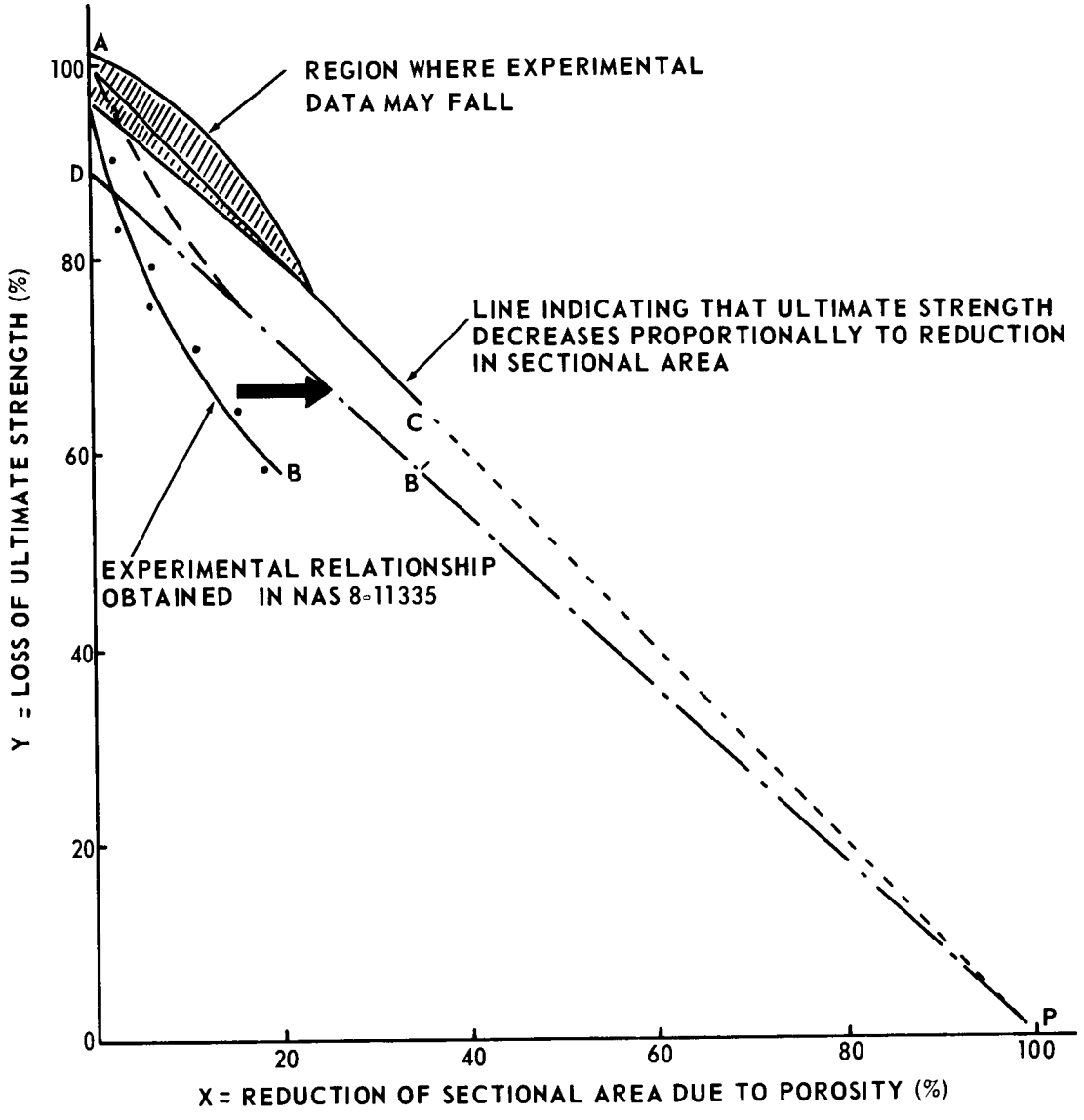

FIGURE 24. EFFECTS OF POROSITY ON ULTIMATE TENSILE STRENGTH OF A TRANSVERSE WELD

Curve AB shows a typical result obtained under Contract NAS8-11335. A small loss of sectional area caused considerable loss of strength; for example, 5 percent reduction of sectional area caused about 30 percent loss of

strength. The results obtained are different from those which can be expected from the theoretical consideration and experimental finding obtained by other investigators as follows:

1) If the net stress at fracture remains constant, the loss of strength is proportional to the reduction of area, as shown by line AC.

2) Very small amounts of porosity may have little effect on the strength. Consequently experimental data may be scattered in the hatched band on both sides of line AC.

As the Martin investigators stated, a large number of fine pores existing in the specimens are believed to be primarily responsible for the marked decrease in strength. If the loss of sectional area due to these fine pores were added, curve AB would move to the right as indicated by the arrow.* The modified curve, however, may be as shown by curve AB', and it may not match line AC. In other words, the inclusion of the fine pores may not be the only factor that caused the great reduction in strength. Since the welds were made using highly contaminated shielding gas, some material degradation may take place; then the curve would follow line DB'P rather than ACP. It is recommended that additional studies be made on the following subjects:

1) Recount the loss of sectional area by including fine pores

2) Conduct a metallographic study of fractured surfaces to determine whether welds made with highly contaminated shielding gas contain unusual structures which may cause further reduction in strength.

e. Results Obtained at Boeing Under Contract NAS8-20168

The major part of Boeing's work under Contract NAS8-20168 has been discussed in Section V-2. However, in Phase II of the program, a study was made of the effects of gas contamination on mechanical properties of weldments. The following tests were made:

1) Static tensile tests of transverse-weld specimens

2) Static tensile tests of longitudinal-weld specimens

*Additional analysis by the investigators supports this conclusion.

3) Fatigue tests of transverse-weld specimens

A statistical analysis was made of the effects of shielding-gas contamination levels on mechanical properties of welds. The stepwise regression analysis [Eq. (2)] was used to determine the relationships between the levels of the four gases (oxygen, X_1; hydrogen, X_2; nitrogen, X_3; and water vapor, X_4) and several variables indicating mechanical properties. The results of the stepwise regression analysis relating weld quality (Y_i) to the contamination levels (X_i) are shown in Table V. Values of coefficient of determination, R^2, are as follows:

1) Transverse-weld ultimate tensile strength: 0.770

2) Transverse-weld elongation: 0.684

3) Longitudinal-weld elongation: 0.670

4) Transverse-weld fatigue cycles: 0.515

5) Longitudinal-weld ultimate tensile strength: 0.502

6) Longitudinal-weld yield strength: 0.249

7) Transverse-weld yield strength: 0.161

Among the seven properties, the ultimate strength of transverse welds had the most significant correlation with the contamination level, while the cycles to failure in fatigue test and the yield strengths of longitudinal and transverse welds had low correlations with the contamination level.

Static Tensile Test Results. Static tensile test data were statistically analyzed. When holding other gases at a 5-ppm level, the addition of any gas, except oxygen, caused decreases in the longitudinal and transverse strengths; approximately 2 percent at the 500-ppm level. The addition of oxygen had no significant effect. Individual gases were also added while keeping the level of other gases at 250 and 500 ppm, respectively. The analyses of tensile tests in these cases basically indicated decreased strength with increased contamination. Hydrogen and water vapor combinations were generally most detrimental, causing 20 percent decrease in strength in some instances. In contrast, oxygen and nitrogen additions increased strength about 1 percent above the base gas reference under some contamination conditions.

Fatigue Test Results. Five fatigue specimens prepared from a joint welded with pure shielding gas were used to establish an S/N (stress/cycles to failure) curve. On the basis of the S/N curve, 26,000 psi was chosen for testing fatigue properties of other welds. Above 26,000 psi, excessive necking down was experienced in the weld bead region, indicating that the elastic limit had been exceeded. Below 26,000 psi, the cycles to failure were in excess of 1,000,000 and were unrealistic from the standpoint of time required to test the samples.

There was extreme variation in the number of cycles between specimens from the same weldment of specimens with similar contamination treatment. Statistical analyses were conducted on the correlation between shielding-gas contamination and fatigue life. As shown in Table III (Section VI-1), the correlation was not very significant; the coefficient of determination was 51.5 percent.

The general trend was for fatigue life to decrease as the shielding-gas contamination level increased; however, in some cases further increase in contamination resulted in an increase of fatigue life.

f. Analysis and Evaluation of the Boeing Study on Porosity and Mechanical Properties

The conclusions drawn by the Boeing investigators are summarized in the Appendix. The trends observed at Boeing generally agree with the trends observed at Martin. The integrator's discussion of important findings follows.

The Boeing investigators made statistical analyses on correlations between

1) The shielding-gas contamination level and porosity level

2) The shielding-gas contamination level and mechanical properties.

No statistical analysis was made between the porosity level and mechanical properties. Let us consider why mechanical properties of a weld decrease as the shielding-gas contamination level increases. An increase in shielding-gas contamination causes more pores in the weld, more loss of sectional area which results in loss of strength. The correlations between the shielding-gas contamination level and mechanical properties are indirect. This indirectness is indicated in the results of the regression analysis. Values of coefficient of

determination between the shielding-gas contamination level and porosity level are about 80 percent, much higher than those between the shielding-gas contamination level and mechanical properties. These results can be explained in the following way. If the correlation between the shielding-gas contamination level and porosity is 0.80 and that between porosity and mechanical properties is 0.75, for example, it could be assumed that the correlation between the shielding-gas contamination level and mechanical properties is about 0.60. It would be worthwhile to investigate the correlation between the porosity level and mechanical properties.

However, the pore-counting technique such as the one used at Martin will be more useful than the above-mentioned statistical analysis, because the reduction of strength is controlled by the reduction of sectional area due to porosity. Further study needs to be made of the relationship between the loss of sectional area measured on fracture surfaces and the reduction of strength. In this study, attention should be directed to whether a small amount of porosity causes a sudden decrease in strength as observed at Martin.

7. Effects of Time-Temperature Characteristics on Mechanical Properties of Welds

Effects of time-temperature characteristics on mechanical properties of welds in high-strength, heat-treated aluminum alloys were studied at Harvey Aluminum under Contract NAS8-11930.

a. Background and Technical Approach

Jackson[42] has proposed the time-temperature concept to study the effects of heat input on the strength of aluminum welds. Figure 25 shows the temperature change during welding of a point in a weldment. Maximum temperature is defined as the peak temperature which the material being joined experiences during the welding heat cycle. Time at temperature is defined as the time that the material being joined is above the temperature that adversely affects strength properties of the base metal being joined. According to Jackson, the strength properties of 2219-T87 aluminum alloy are found to be adversely affected above 450°F.

An investigation was made to develop relationships between weld heat input and strength characteristics of 2219 aluminum welds. By the use of multivariate regression analysis of experimental data, the relationship among maximum temperature, time at temperature, and mechanical property

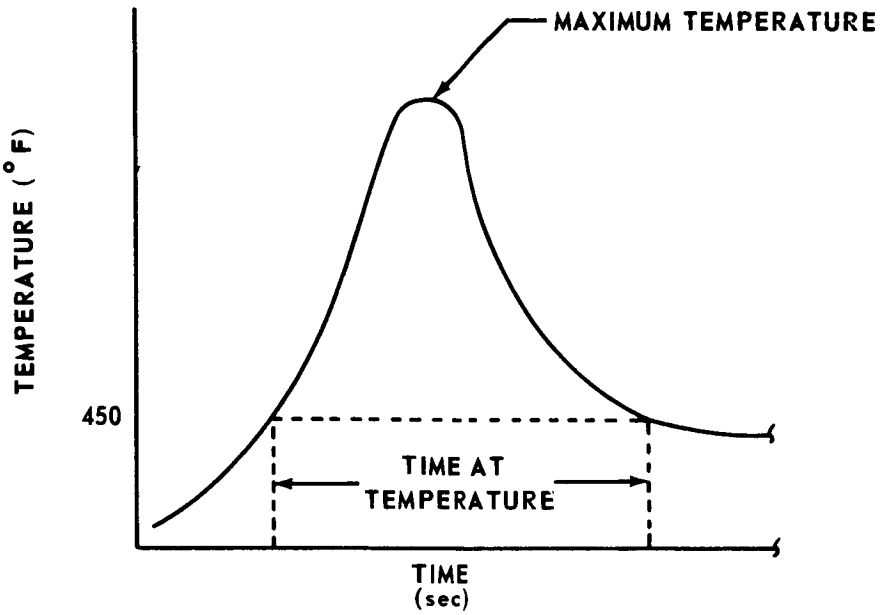

FIGURE 25. TIME-TEMPERATURE CHARACTERISTICS CURVE

characteristics including yield strength, ultimate tensile strength, and elongation were determined. The results indicated that shortening the time-temperature cycle through the critical ranges (solidification and overaging) improves mechanical properties of weldments in 2219 aluminum alloy. Attempts were being made under Contract NAS8-11930 to improve weld properties by shortening the time at temperature by impingement of a cryogenic liquid on the weldment during welding.

b. Survey of Literature and Industry

A literature and industry survey was made to determine the state of the art, to avoid duplication of effort, and to obtain any information that might be useful in this program. It was determined that this program did not duplicate any previous work, and that the approach of supercooling had merit. Some theoretical background in heat transfer applicable to welding (unsteady state with a moving, single-point heat source) was obtained.

c. Experimental Procedures

Materials selected for the experimental work were aluminum alloys 2219-T87 and 2014-T6 in plate thickness of 5/16 and 1/2 in. The

welding process selected was gas tungsten-arc welding, D-C, straight polarity with helium shielding gas welding done from one side in the horizontal position using 2319 filler wire for both alloys. One pass was prescribed for the 5/16-in. material and two passes for the 1/2-in. material.

Experimental equipment and procedures were developed for welding 12- by 48-in. panels with sufficient instrumentation to monitor pertinent heat input and extraction variables. Weldment temperatures were measured by thermocouples embedded in the plate. Limited investigations were conducted for measuring weld temperatures by means of infrared radiometers.

Two series of welded panels were fabricated. They were bead-on plate and square-butt welds. Table IX shows typical welding parameters. Half of each series was welded without chilling and half with liquid CO_2 chilling,

TABLE IX. TYPICAL WELDING PARAMETERS USED IN THE HARVEY ALUMINUM STUDY

Plate Thickness (in.)	Penetration Pass				Filler Pass			
	Arc Current (amp)	Voltage (v)	Travel Speed (ipm)	Wire Speed	Arc Current (amp)	Voltage (v)	Travel Speed (ipm)	Wire Speed
5/16	215-220	11	7-10	80	--	--	--	--
1/2	320-325	11	7	None	300	11	18	120

attempting to maintain comparable weld-bead dimensions. In the first series, chilling was effected from the back side of the weldment using a double layer of glass tape to prevent deformation and contamination of the underbead by the liquid CO_2. In the second series, weldments were chilled from the front (torch) side using a shield to prevent leakage of CO_2 into the arc area. Several systems of jet orifice sizes and arrangements were used for each series.

Comparable unchilled and chilled weldments for both series were examined by X-ray, fracturing, and macrosectioning. Tensile tests were performed after natural aging, artificial aging, and after reheat treating to the T-6 condition.

d. Experimental Results

Thermal Cycle Curves. Figure 26 shows examples of thermal cycle curves for points at 3/8 and 3/4 in., respectively, from the weld centerline on 12-by 48-in. butt welds in 1/2-in. thick 2219-T87 plates.[10] Data are compared for the unchilled weld and the weld chilled with the Jet System No. 14.* The chilling resulted in rapid cooling of the weldment.

Macrosections. In most cases, the macrosections showed that chilling reduced the extent of the heat-affected zone, and reduced the grain size of the cast structure. For example, Figure 27 shows comparisons of macrosections of the unchilled and the chilled weld in 1/2-in. thick 2219-T87 plate.[10]

Tensile Properties. Specimens were selected from chilled and unchilled weld panels of each alloy and each thickness for room-temperature tensile tests. The selection was made on the basis of X-rays which indicated less than 1 percent porosity. All specimens were cut to 3/4-in. wide straight-sided bars with the weld transverse and weld bead intact. One group of specimens from each panel was artifically aged to the -T6 condition after welding. All tests were performed at room temperature.

Table X summarizes average tensile values obtained for artifically aged specimens, and Table XI shows such values for naturally aged specimens.[10]

Yield strengths are substantially increased by chilling from the front side. The greatest increase in average values was 17.8 percent for artifically aged welds in 1/2-in. 2014-T6 plate. The greatest increase in average yield strength for welds in 2219-T87 plate was 8.8 percent (for welds in 5/16-in. artifically aged specimens).

Efforts were made to correlate strength with effective heat input by calculating a theoretical effective heat-input value for the chilled welds using a formula based on a ratio of the cooling rates affected for each weldment. While a relationship between heat input and tensile strength appeared to follow a somewhat consistent pattern for unchilled welds, no such correlation could be obtained for chilled welds. Undoubtedly some pattern exists, but sufficient testing has not been accomplished in this project to determine the relationship.

*Jet System No. 14 was designed for front-side chilling, using a cryogenic liquid. It utilized a traveling shield with a spring-loaded, metallic wool-and-wire brush seal and a metallic-shirt, 7-jet manifold for helium purging.

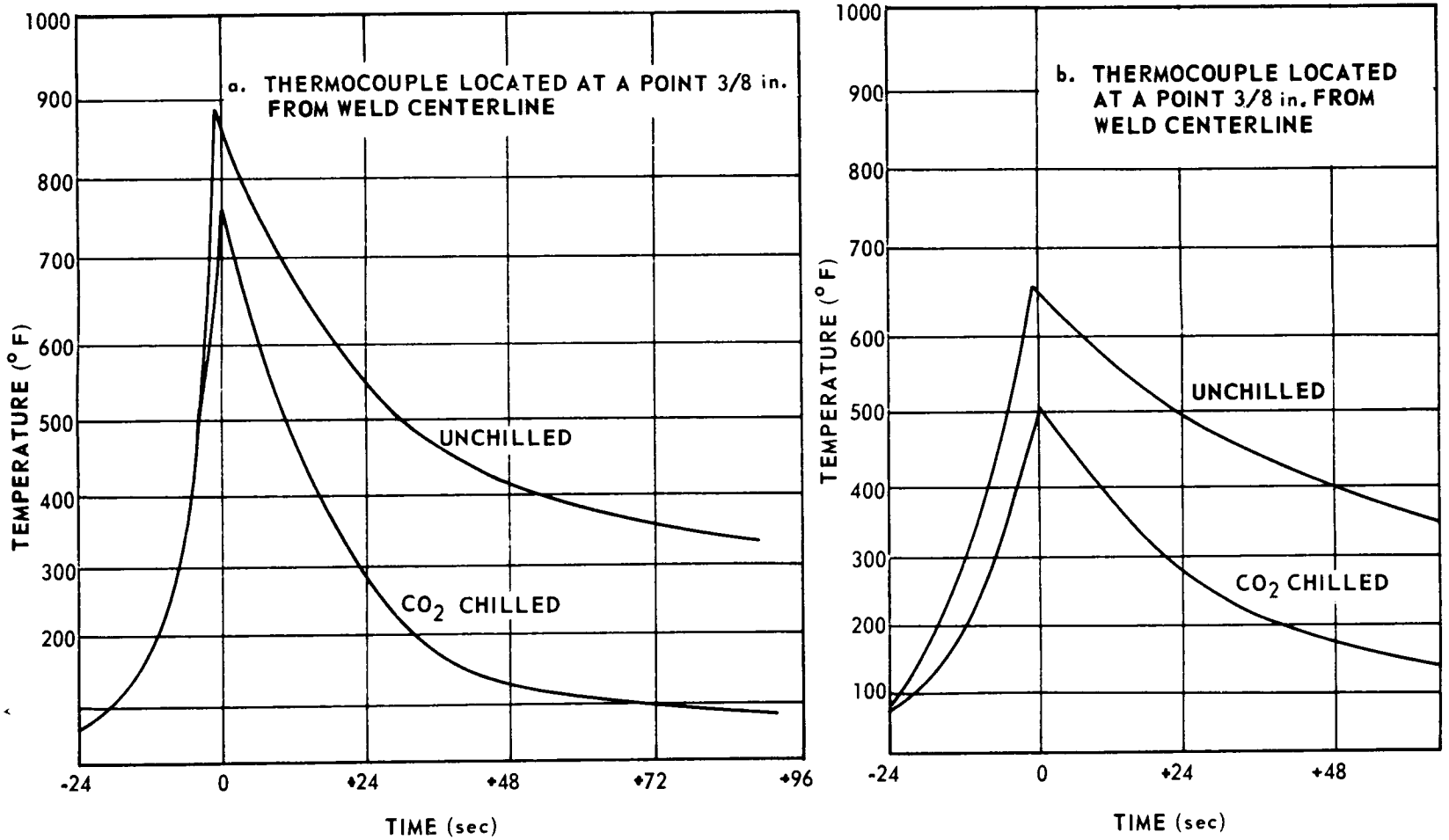

FIGURE 26. EFFECT OF FRONT-SIDE CHILLING ON THERMAL-CYCLE CURVES

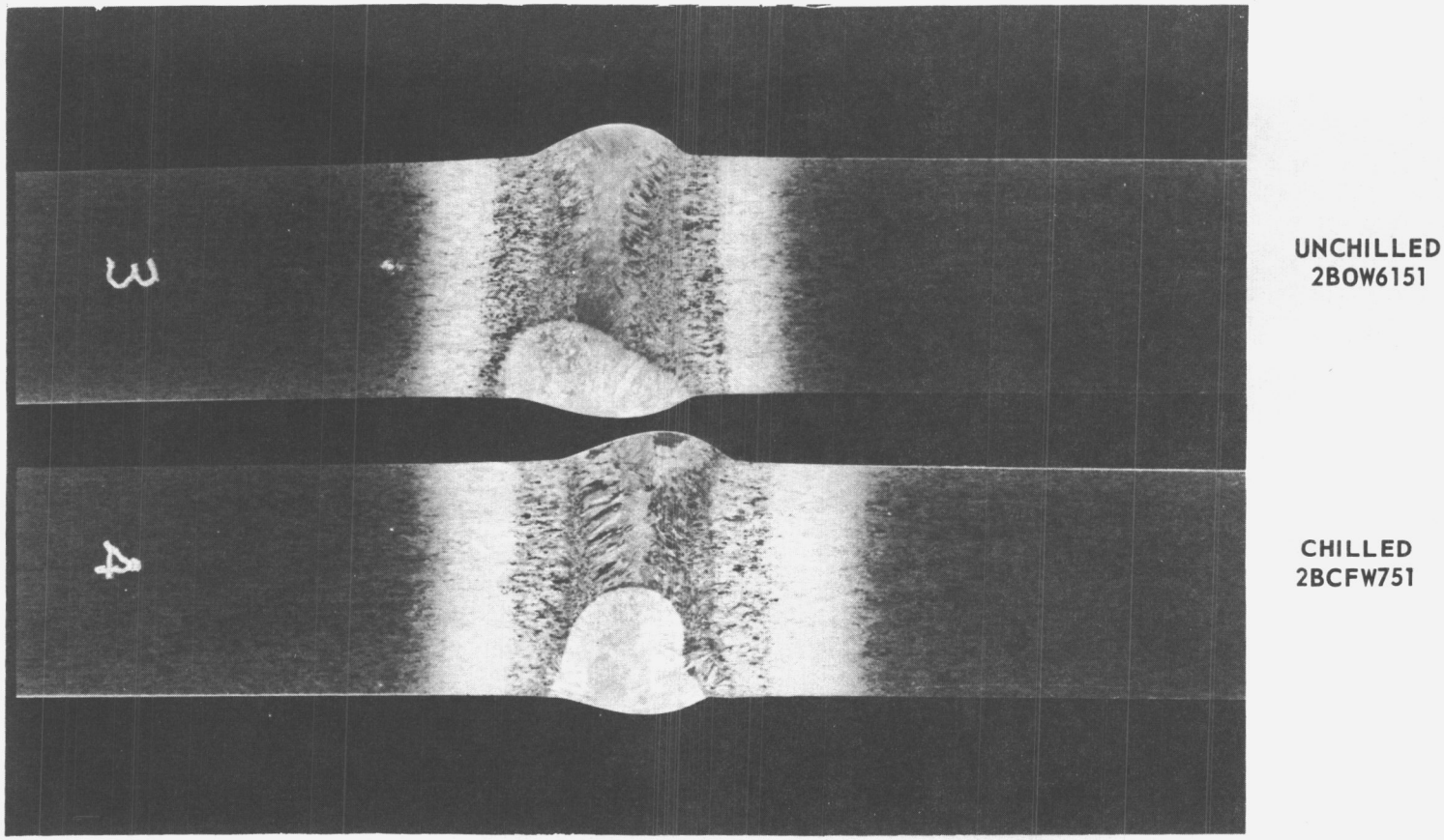

FIGURE 27. MACROSECTIONS SHOWING EFFECT OF FRONT-SIDE CHILLING OF WELDS

TABLE X. EFFECT OF FRONT-SIDE CHILLING ON TENSILE PROPERTIES OF WELDMENTS, ARTIFICIAL AGING

Weldment Material	Chill System (No.)	Average Tensile Strengths (ksi)					
		Yield			Ultimate		
		Unchilled	Chilled	Change (%)	Unchilled	Chilled	Change (%)
5/16-in. 2014-T6	18	33.9	36.9	+ 7.7	45.9	41.3	-10.0
	18	37.1	39.9	+ 7.6	49.0	48.3	- 1.4
	19	32.5	34.7	+ 6.8	44.8	42.3	- 5.6
	23	36.3	39.0	+ 7.5	48.5	47.5	+ 2.0
1/2-in. 2014-T6	18	30.9	36.4	+17.8	47.0	47.3	+ 0.6
	19	34.4	38.9	+14.4	47.2	47.6	+ 0.1
	19	34.0	38.7	+13.8	47.2	48.7	+ 3.2
5/16-in. 2219-T87	19	31.9	33.2	+ 4.2	38.4	39.0	+ 1.6
	19	35.4	38.5	+ 8.8	40.4	44.7	+10.7
	23	35.1	36.0	+ 2.6	42.5	40.7	- 4.2
1/2-in. 2219-T87	18	35.1	36.7	+ 4.6	46.8	48.1	+ 3.4
	19	34.2	36.0	+ 6.4	43.7	45.6	+ 4.3
	23	35.1	36.6	+ 4.3	45.0	46.8	+ 4.0

TABLE XI. EFFECT OF FRONT-SIDE CHILLING ON TENSILE PROPERTIES OF WELDMENTS, NATURAL AGING

Weldment Material	Chill System (No.)	Average Tensile Strengths (ksi)					
		Yield			Ultimate		
		Unchilled	Chilled	Change (%)	Unchilled	Chilled	Change (%)
5/16-in. 2014-T6	18	32.7	34.5	+ 5.6	45.5	45.2	-0.6
	19	33.5	36.6	+ 9.3	40.2	40.4	+0.5
	23	33.0	35.5	+ 7.6	49.7	45.5	-8.5
1/2-in. 2014-T6	19	28.8	32.1	+11.5	47.4	48.3	+1.9
	19	28.8	33.2	+15.5	47.4	49.0	+3.4
5/16-in. 2219-T87	23	24.2	26.8	+ 2.6	37.8	40.5	+2.5
	19	25.5	25.7	+ 0.8	36.1	37.3	+3.3
1/2-in. 2219-T87	18	20.9	22.5	+ 7.7	40.4	41.5	+2.7
	19	19.7	20.2	+ 2.5	38.8	40.1	+3.8
	23	21.7	21.6	- 0.5	39.4	40.8	+3.6

Porosity. Comparison of X-rays of the initial series of welds chilled from the front side with unchilled welds indicated some decrease in porosity for the chilled welds. Approximately 60 percent of the unchilled weld samples contained porosity ranging from 1/2 to 20 percent of the cross-sectional area, while more than 90 percent of the chilled welds were free of porosity.

Distortion. Several panels fabricated by chilling from the front side remained essentially flat after welding, exhibiting almost no longitudinal bow or peaking. Unchilled weld panels have contained a longitudinal bow up to 1-1/2 in. and peaking to 10 deg, depending upon the amount of heat input.

e. Analysis and Evaluation of the Harvey Aluminum Study on on Time-Temperature Control

The conclusions reached by the Harvey Aluminum investigators are included in the Appendix of this report. The integrator's discussion and analysis of the program follows.

The results and conclusions obtained by Harvey appear valid. The integrator would agree with these conclusions up to the point that they recommend that chilling should have application in production welding and should be investigated further. This conclusion is based on the improvements in yield strength and porosity level brought about by chilling. There is no question that these improvements exist, but there are definite reservations as to their significance. The strength increases shown generally range from 5 to 10 percent. These increases are not considered significant unless they occur in a very critical range.

On the basis of data shown in Figure 2, the increase in strength due to cryogenic chilling would be more significant when welds are made with lower heat input. From the practical viewpoint, attempts should first be made to improve weld strength by decreasing weld-heat input. Further increase of strength due to cryogenic chilling would become worthwhile when adequate means for reducing heat input cannot be found.

The cryogenic chilling may prove to be an effective way for reducing distortion. Further studies are needed on this effect.

Regardless of their significance, these improvements due to cryogenic chilling will be accomplished at the risk of (1) contamination of the weld by the cooling jet and (2) contamination of the weld by water condensation on the surface. It has been shown in the Boeing report that even the contamination from a single fingerprint can cause a significant increase in porosity.

Certainly, any steps that risk weld contamination should be carefully considered. And, it should be noted, that although these welds were apparently well shielded, they were bead-on plate and square-butt welds. Production welds will be much more difficult to shield in any practical manner.

8. Transferability of Setup Parameters

Transferability of setup parameters was studied by Lockheed-Georgia under Contract NAS8-11435. Analysis was made of GTA and GMA welds made in the horizontal position. The work was thermally insulated from the holding fixture to simulate the minimum tooling, tack-up welding technique very often used in the aerospace industry. No hard tooling or inert gas back-up was used. Welds were made in 1/4- and 3/4-in. thick, 2219-T87 aluminum alloy. All joints were prepared with square-butt edges. The shielding gas was helium.

a. Phases and Experimental Design

The welding test program included two phases. In Phase I, GTA welding parameters and their effect on the response variables were evaluated. The welding setup parameters investigated were current, voltage, weld travel speed, wire deposit, gas purity, gas flow, temperature of the weldment, joint design, and electrode tip diameter. These setup parameters were referred to as the independent variables for the GTA welding process. Table XII lists symbols and units used for independent and dependent variables by the Lockheed investigators.[12] Figure 28 defines by illustration those variables related to weld cross section and penetration.

A complete factorial for these nine independent variables at two levels requires $2^9 = 512$ test conditions. In this study, a 1/16-fractional factorial requiring 32 test conditions was used. Four additional test conditions were used to improve the accuracy of statistical analysis. The effects of the independent variables on various weld characteristics were studied by statistical analysis using regression equations. Phase II of the project dealt with the GMA welding process. The design principles were the same as for GTA, except that fewer setup parameters were required. There were only five basic parameters investigated for the GMA process, current, voltage, weld travel speed, angle of the torch, and the distance from the contact tube to the work. A one-half replication of the five variables with all two-variable interaction being measurable was used for the GMA study.

TABLE XII. SYMBOLS AND UNITS FOR VARIABLES USED BY THE LOCKHEED INVESTIGATORS

Symbols	Description and Units for Computer Use	
C	Welding arc current	(amp/100)
V	Welding arc voltage	(v)
T	Travel speed of the arc	(ipm)
Wd	Volume of filler wire deposited per inch of weld	($in.^3 \times 100/in.$)
Gp	Gas purity - total ppm contamination	(ppm/100)
Gf	Gas flow - cubic feet per hour	(cfh/100)
°F	Work temperature before welding	(°F/100)
J	Joint gap	(in.)
D	Diameter of electrode at the tip	(in.)
M	Cross section area total of melt zone	($in.^2$)
Mc	Cross section area of crown	($in.^2$)
Mf	Cross section area of fall through	($in.^2$)
H	Cross section area of heat-affected zone	($in.^2$)
P	Penetration of melt zone from part surface	(in.)
B	Height of the crown	(in.)
Ep	Electrode position from part surface	(in.)
X	Percent of porosity reading	(%)
Mt	Maximum temperature reading	(°F/100)

TABLE XII. (Concluded)

Symbols	Description and Units for Computer Use	
Tt	Time temperature exceeded 450°F	(sec)
At	Area under temperature curve above 450°F	($in.^2$)
Ftu	Ultimate tensile strength	(ksi)
Fty	Yield tensile strength	(ksi)
E	Elongation	(%)
Q	Overlap of welds from both sides	(in.)
A	Angle of GMA torch	(deg)
CP	Distance from contact tube to work	(in.)

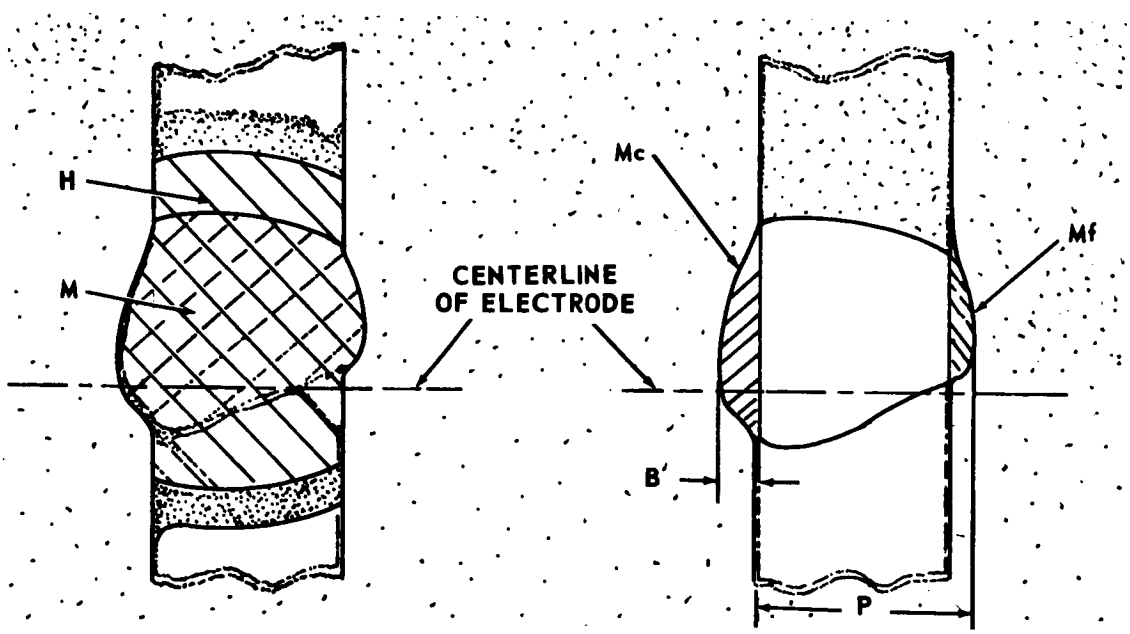

FIGURE 28. ILLUSTRATED DEFINITIONS OF VARIABLES RELATED TO WELD CROSS SECTION AND PENETRATION

b. Welding Test Procedure

Facilities and Equipment. The following two welding units were used in the program:

1) Welding Unit No. 1

Power:	Sciaky Model S-6, functional control, D-C welding power source
Head:	Airco Model HME-E, automatic head
Carriage:	Lockheed-developed carriage controlled by a Servo-Tech techometer feedback governor
Wire feed:	Airco Model AHF-B feedrolls with Airco Model AHC-B feedback type governor control
Instrumentation:	Texas Instrument "Servo/riter" 4 channel potentiometric recorder

2) Welding Unit No. 2

Power:	Sciaky Model S-6, functional control, D-C welding power source
Head:	Precision Sciaky (GTA-GMA) welding head with proximity head control
Carriage:	Servo-Tech control system to operate a Lockheed designed carriage
Wire feed:	Airco AHC-B wire feed control with tachometer feedback governor
Instrumentation:	Minneapolis-Honeywell "Electronic 17" four-channel potentiometric recorder

Electrode Proximity Recording System. It was necessary to better understand the relationship between the welding voltage or arc-length control of the GTA process and the proximity of the torch to the work. A new system developed by Lockheed was used to continuously monitor the electrode proximity. This system operated independently of the arc voltage. The electrode position

was measured by the potentiometric recorder, and charted with the welding voltage.

c. Welding Parameter Control Development

Welding Control Studies. During many tests, the electrode position was held constant. With this condition, both the voltage and depth of penetration were erratic. However, when the voltage was held constant with an automatic voltage-control head, the electrode position was erratic and equally erratic penetration measurements resulted. It was concluded that neither present automatic voltage control nor constant electrode-position control by themselves maintain adequate process control of the welding arc and molten puddle. Another control system had to be applied to hold a constant electrode position (Ep) in addition to a constant current (C), constant voltage (V), constant carriage travel speed (T), and constant filler-wire deposit rate (Wd). The wire-feed system used was reasonably accurate and reliabile; therefore, no attempt was made to couple this system to the other systems influencing the welding arc process. All of the systems used, in various ways, incorporated the other four welding variables. All of the systems were designed to be regulated by equipment settings and still maintain process control of the welding arc and the molten puddle. Cross-coupled feedback controls were defined as controls used for measuring the response of one variable and to simultaneously change the settings of another variable. For example, a change in Ep causes a change in C. Self-coupled feedback controls were defined as controls used to measure the response of a variable and to adjust the controls of that same variable until the response agrees with the desired set point. For example, if Ep deviated from the set point, the error was measured on the recorder, amplified, and used to operate a servo system bringing Ep back to the set point. The basic difference in these two feedback systems was the source of the feedback information. The cross-coupled system depended upon the response of another variable caused by a change in the welding process, while the self-coupled system was a direct measure of the response, independent of all other variables necessary to make up the welding process.

The following six welding control systems were examined:

1) Automatic voltage control

2) Automatic electrode-position control

3) Carriage control coupled to electrode position

4) Current control coupled to electrode position

5) Current control coupled to voltage

6) Self-coupled feedback.

The first three systems were evaluated and considered inadequate for accurate control of the welding process. Tests with the last three systems indicated that they might be capable of maintaining process control of the arc and the molten puddle.

Electrode Position Alignment and Distance From Work. During the first 1/4-in. test series of horizontal welds, the electrode was centered over the joint; however, in the welded cross section the melt zone was not symmetrical about the centerline of the electrode. In fact, the point of maximum penetration was approximately 0.075 in. above the electrode centerline, as shown in Figure 29.[12] Although Figure 29 shows cross sections of welds 3/4 in. thick, similar phenomena were observed in welds 1/4 in. thick. In several specimens, although penetration was complete, the melt zone did not cover the entire joint. New specimens were welded to replace these joints. During all further welding of 1/4-in. thick material the electrode was centered 0.075 in. below the joint. Additional tests were conducted to further evaluate this phenomenon.

Welds in the 3/4-in. thick plate were made from both sides. As in the 1/4-in. welds, a nonsymmetrical melt zone often caused lack of penetration. For example, Weld No. U154 ST, shown in Figure 29a, had sufficient penetration to indicate overlap, but again the melt zone did not cover the joint. This condition could not be detected in X-ray inspection, nor was it observed during fixed 3X photographic examination of the cross section. It became apparent in the fracture surface of the tensile-test specimen for which tensile strength was very low.

Another phenomenon observed during the experiments that will require additional investigation is the relationship of electrode position and depth of penetration. Some specimens had considerably deeper penetration on one side than on the other side, as shown in Figure 29b and c. The welds on each side of the plate were set up with identical weld parameters and examination of recordings confirmed that these setups were actually established. In some cases the second weld had less penetration than the first weld, while the reverse was indicated in other tests. It was found that in almost all cases with less penetration, the electrode position was deeper. The electrode position for these welds was controlled by the automatic head to maintain a

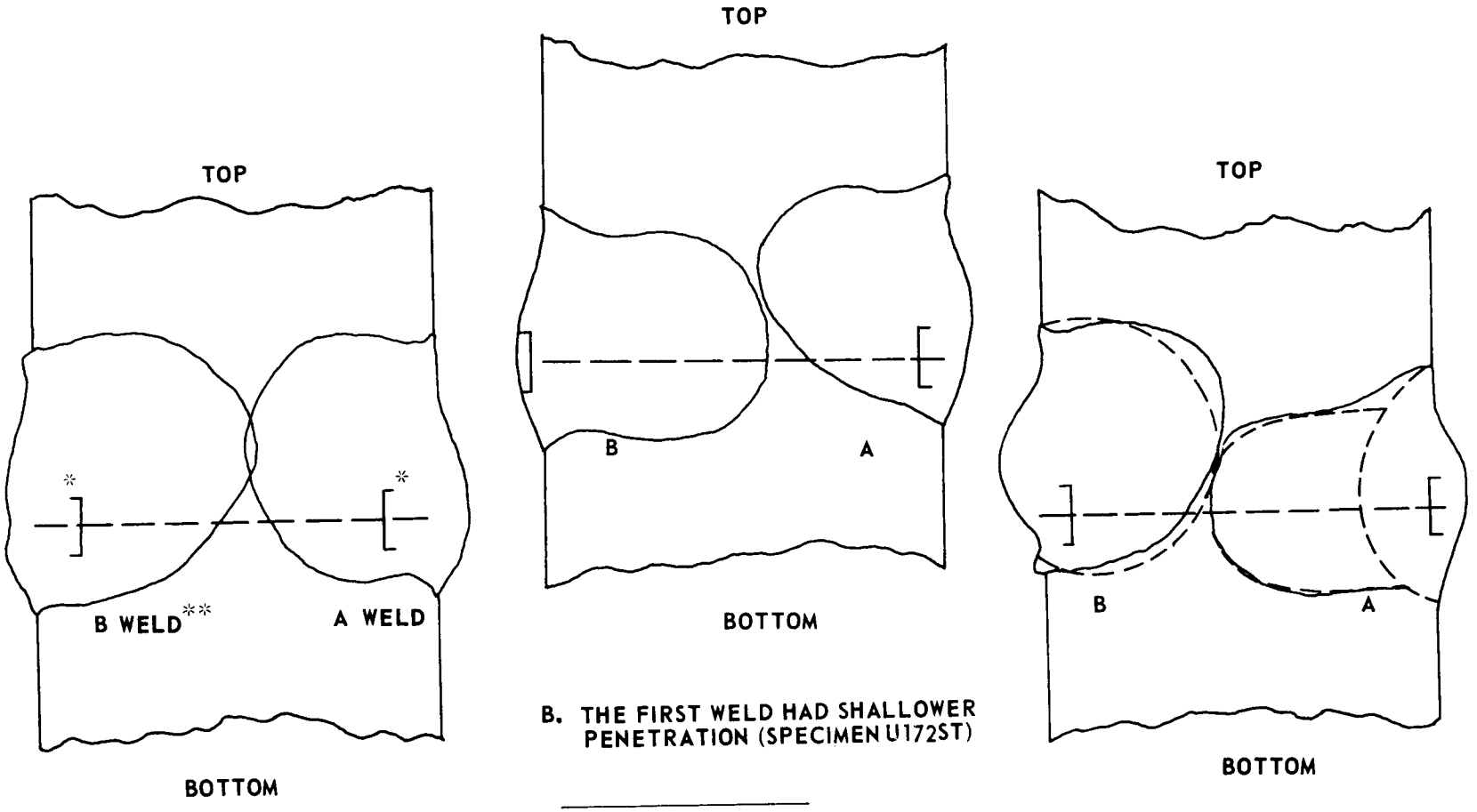

A. INCOMPLETE FUSION DUE TO NON SYMMETRICAL MOLTEN ZONES (SPECIMEN U154ST)

B. THE FIRST WELD HAD SHALLOWER PENETRATION (SPECIMEN U172ST)

C. THE SECOND WELD HAD SHALLOWER PENETRATION (SPECIMEN U182ST)

*Electrode penetration and tip diameter

**Joint location

FIGURE 29. EXAMPLES OF WELDS HAVING INCOMPLETE FUSION AND IRREGULAR NUGGET SHAPES

constant arc voltage. In every case, the arc voltage readings were stable and accurately controlled at the correct settings. However, the electrode position recording was erratic in most cases.

The Lockheed investigators concluded that (1) with a given welding setup and with automatic voltage control, the deeper electrode position indicates that a hemispherical arc cavity has developed that will result in a reduction of penetration and (2) variation in penetration due to changes in electrode position is as great as that due to changes resulting from the classic parameters.

Other Problems. Investigations also were made of various other problems including:

1) Accuracy of inert-gas flowmeter

2) Variation in tungsten-electrode resistance

3) Variation in torch resistance

4) Shielding gas contamination

5) Effect of tungsten electrode on welding parameters.

d. Statistical Analyses of the Effects on Welding Parameters on Weld Qualities

Procedures. Table XIII shows three values for each of nine independent parameters used for GTA welds in 1/4- and 3/4-in. plate. A constant-current, voltage-control GTA system was used. Table XIV shows how the nine parameters were changed in the experimental design for each of 36 specimens. The letters H (high), M (medium), and L (low) are used to represent the value for each parameter as shown in Table XIII.

Table XV shows values of parameters used for GMA welds in 1/4-in. plate. The variables were changed in the three levels shown so that welds were made under 21 different conditions.

Figure 30 shows how specimens were prepared from both GTA and GMA welds.[11] Three tensile-test specimens, one cross-section specimen, and one longitudinal-section specimen, were prepared from each weld. On all weldments the following 14 responses were measured: ultimate tensile strength (FTV), yield strength (FTY), elongation (E), melt area (M), melt crown

TABLE XIII. PARAMETERS FOR GTA WELDING 2219-T87 ALLOY PLATES 1/4 AND 3/4 IN. THICK

	Code Letter	1/4-in. Thick Welds*			3/4-in. Thick Welds**		
		High	Medium	Low	High	Medium	Low
Arc current	C	2.85	2.73	2.60	4.40	4.20	4.00
Arc voltage	V	12.75	12.5	12.25	11.5	11.35	11.2
Travel speed	T	23	21	19	10	9	8
Wire deposite per inch of weld	Wd	1.228	0.955	0.682	0.3835	0.1817	0
Shielding-gas purity	Gp	1.50	0.90	0.30	1.50	0.90	0.30
Shielding-gas flow	Gf	1.25	1.00	0.75	1.25	1.00	0.75
Work temperature	°F	1.50	1.13	0.75	1.50	1.13	0.75
Joint gap	J	0.020	0.010	0	0.020	0.010	0
Electrode tip diameter	D	0.125	0.108	0.090	0.135	0.122	0.108

*One-pass weld

**Two-pass weld (one pass from both surfaces)

TABLE XIV. EXPERIMENTAL DESIGNS FOR GTA WELDS 1/4 AND 3/4 IN. THICK

Weld Sequences	C	V	T	Wd	GP	Gf	°F	J	D
1	L	L	L	H	L	H	L	L	H
2	H	L	L	H	L	H	H	H	L
3	M	M	M	M	M	M	M	M	M
4	L	L	L	L	H	H	L	H	L
5	L	H	L	L	H	L	L	L	H
6	L	L	H	H	H	L	L	H	H
7	H	L	L	L	H	H	H	L	H
8	L	H	H	L	L	H	L	H	H
9	H	H	L	H	L	L	H	L	H
10	M	M	M	M	M	M	M	M	M
11	L	H	L	H	H	H	H	H	H
12	L	H	H	L	H	L	H	H	L
13	H	L	L	L	L	L	L	L	L
14	L	L	L	H	H	L	H	L	L
15	L	H	L	L	L	H	H	L	L
16	H	H	H	H	L	L	L	H	L
17	L	H	H	H	L	L	H	L	H
18	L	L	L	L	L	L	L	L	L
19	L	L	H	L	H	H	H	L	H
20	M	M	M	M	M	M	M	M	M
21	H	H	H	L	L	H	H	L	L
22	H	H	L	H	H	H	L	L	L
23	L	H	H	H	H	H	L	L	L
24	H	L	H	L	L	L	H	H	H
25	L	L	H	H	L	H	H	H	L
26	M	M	M	M	M	M	M	M	M
27	L	L	H	L	L	L	L	L	L
28	H	H	H	L	H	L	L	L	H
29	H	L	H	H	L	H	L	L	H
30	H	L	H	H	H	L	H	L	L

TABLE XIV. (Concluded)

Weld Sequences	C	V	T	Wd	GP	Gf	°F	J	D
31	L	L	L	L	L	L	H	H	H
32	H	L	L	H	H	L	L	H	H
33	H	L	L	H	H	L	H	H	L
34	H	L	H	L	H	H	L	H	L
35	L	L	L	H	H	L	L	H	L
36	H	H	L	L	L	H	L	H	H

TABLE XV. PARAMETERS FOR GMA WELDING 2219-T87 ALLOY 1/4 IN. THICK

	Code Letter	High	Medium	Low
Arc current	C	210	200	190
Arc voltage	V	24.5	23.5	22.5
Travel speed	T	26	24	22
Torch angle	A	20	10	0
Distance from contact tube to work	CP	0.500	0.450	0.400

area (Mc), melt fall-through area (Mf), heat-affected area (H), penetration (P), build up (B), electrode position (Ep), porosity (X), maximum temperature of back bead (Mt), time above 450°F (Tt), and area under temperature curve above 450°F (At).

A multiple stepwise regressive analysis was made, using an IBM 7094 computer to determine the correlation between the independent variables and each of the responses.

Results of Statistical Analyses. Table XVI summarizes results of the regression analyses. Regression equations and the coefficient of determination, which is the square of the multiple coefficient, are shown. For example, the ultimate tensile strength, Ftu, of the 1/4-in. welds is

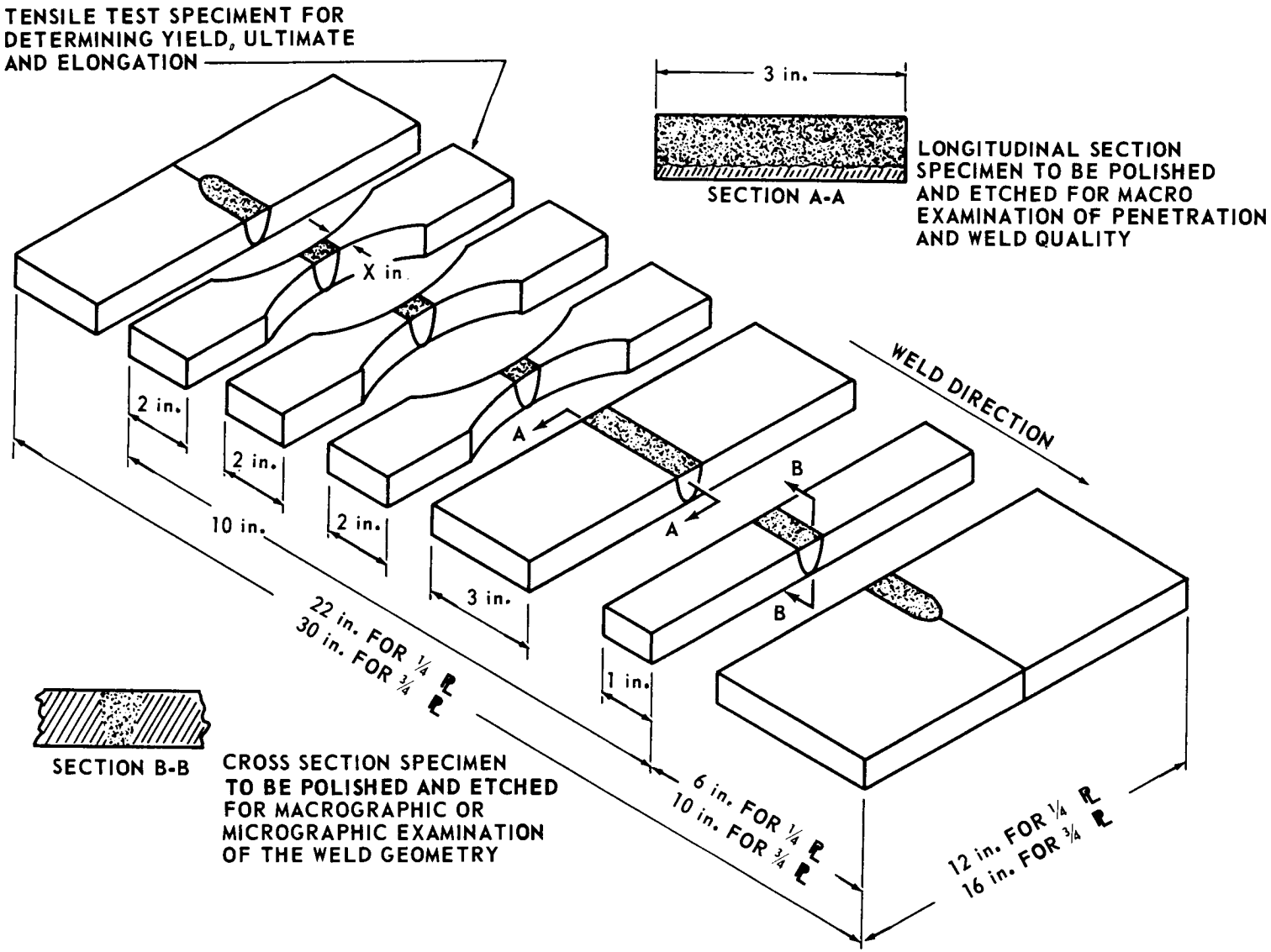

FIGURE 30. WELD TEST SPECIMEN OF 1/4- AND 3/4-IN. THICK 2219-T87 ALUMINUM ALLOY

TABLE XVI. RESULTS OF STATISTICAL ANALYSES OF THE EFFECTS OF WELDING PARAMETERS ON WELD QUALITIES

Regression Equations Determined	Coefficient of Determination, percent
1) 1/4-in. GTA weld	
Ftu = 446.13854 - 21.61667 (T) + 9.24738 (C · T) - 172.85070 (C) - 60.01508 (T · D) + 1138.0066 (D) - 0.22755 (T · Wd)	86
Fty = 29.75927 - 10.05339 (T · D) + 62.75876 (C · D) + 0.68234 (T · Gp) - 4.74571 (C · Gp) - 2.89151 (Gf)	55
M = 0.05805 - 0.00597 (T) + 0.00480 (C · D) + 0.00040 (T · °F) - 0.00060 (T · Wd) - 0.00047 (T · Gf)	86
H = 0.07413 - 0.00495 (T) + 0.00526 (C · V)	57
P = 3.94197 - 0.19187 (T) + 0.07597 (C · T) - 1.25753 (C)	61
B = 0.09253 + 0.00138 (T · Wd) - 0.00309 (C · V) + 0.01063 (T · D)	54

TABLE XVI. (Continued)

Regression Equations Determined	Coefficient of Determination, percent
2) 3/4-in. GTA weld	
Ftu = 173.89012 - 4.53235 (T) + 78.89110 (Ep) - 8.37078 (V) - 2.18180 (Gp)	74
Fty = 118.32079 + 68.89160 (Ep) - 2.47662 (T) - 5.53961 (V)	56
E = 17.68104 - 0.68521 (T) + 16.18741 (Ep) - 1.08126 (V) + 1.53388 (C)	64
M = 0.11159 - 0.01110 (T) + 0.06422 (C) + 0.30611 (Ep) - 0.38142 (D) + 0.00959 (°F) + 0.01059 (V)	82
Q = 0.75779 - 0.07020 (T) + 0.03589 (Gp) + 1.37834 (Ep) + 0.17712 (C) - 0.05904 (V) - 1.32220 (D)	87
H = - 0.63726 - 0.02646 (T) + 0.16348 (C) + 0.66632 (Ep) + 0.94564 (V) - 0.87501 (D) + 0.02070 (°F)	85
P = 0.28945 - 0.03090 (T) + 1.19985 (Ep) + 0.13459 (C) - 1.48151 (D) + 0.01139 (Gp)	82
B = - 0.03320 + 0.02956 (Wd) + 0.02293 (C) - 0.00375 (T) + 0.00446 (Gp) + 0.00570 (°F)	65

TABLE XVI. (Concluded)

Regression Equations Determined	Coefficient of Determination, percent
3) 1/4-in. GMA weld	
$Fty = 49.18872 - 3.42473\,(A \cdot Cp) + 0.02603\,(A^2) + 0.16532\,(V \cdot A) - 0.03485\,(V^2) - 2.39324\,(A) - 0.01963\,(T \cdot A)$	71
$M = -0.06014 + 0.08260\,(C) - 0.00006\,(T^2)$	53
$Q = -0.83123 + 0.40188\,(C) - 0.00021\,(V \cdot T) + 0.07513\,(A) - 0.00034\,(A^2) - 0.00115\,(V \cdot A) + 0.35249\,(Cp) - 0.1747\,(A \cdot Cp) - 0.00032\,(T \cdot A)$	88
$P = -0.28764 + 0.25248\,(C) - 0.00038\,(V \cdot T) + 0.03060\,(A) - 0.00020\,(A^2) - 0.00917\,(C \cdot A) + 0.01113\,(T \cdot Cp) - 0.01714\,(A \cdot Cp)$	70

$$Ftu = 446.1 - 21.62\,(T) + 9.247\,(C{:}T) - 172.9\,(C) - 60.02\,(T \cdot D) + 1138\,(D) - 0.2276\,(T \cdot Wd) \quad (14)$$

where,

Ftu = Ultimate tensile strength, ksi

T = Travel speed, ipm

C = Arc current, amp/100

D = Electrode tip diameter, in.

Wd = Volume of filler wire deposited per inch of weld, $in.^3 \times 100/in.$

The coefficient of determination in this case was 86 percent; i.e., the variables expressed in the regression equation accounted for 86 percent of the variation observed in Ftu. Regression equations are not given in Table XVI for those items with less than 50 percent coefficient of determination.

In reviewing the regression equations, it was noticed that travel speed (T) is a significant parameter for many responses, especially for GTA welds. Table XVII shows the most significant parameter for each response and the percentage of response explained by that parameter. Travel speed was the most significant parameter for 5 of the 6 responses listed for 1/4-in. thick welds and 6 of the 8 responses listed for 3/4-in. thick welds. For example, Ftu decreased as T increased, and the change in T was responsible for over 40 percent of the changes in Ftu.

On GMA welds, the coefficient of determination was more than 50 percent for only 4 responses, as shown in Table XVI. The accuracy of the three equations which had coefficients of determination better than 70 percent, Fty, Q, and P, are questionable because many terms are involved. For this reason, the regression analysis for GMA welds are not considered reliable, as pointed out by the Lockheed investigations.

TABLE XVII. PERCENTAGE OF VARIATION IN RESPONSE EXPLAINED BY THE INDICATED PARAMETER IN REGRESSION ANALYSIS FOR WELDS 1/4 AND 3/4 IN. THICK

Responses	1/4-in. Thick Welds		3/4-in. Thick Welds	
	Parameter	Percentage of Response Explained	Parameter	Percentage of Response Explained
Ftu	T	43	T	44
Fty	T	14	Ep	41
E	-	-	T	43
M	T	53	T	51
Q	-	-	T	58
H	T	29	T	48
P	T	30	T	47
B	Wd	25	Wd	30
Linear effects only are included.				

e. Analysis and Evaluation of the Lockheed Study on Transferability of Setup Parameters

The conclusions drawn by the Lockheed investigators are summarized in the Appendix. The integrator's discussion of important findings follows.

It has been found that in order to transfer weld quality in the GTA process good instrumentation must be provided for the six basic GTA welding variables, travel speed, electrode position, current, voltage, gas purity, and electrode tip diameter, listed in their order of importance. The instrumentation should have high resolution, with trace-type potentiometric recorders preferred. Where the conditions above are met, along with duplicate conditions of weld-joint preparation, tooling, and welding position, duplicate trace recordings indicate duplicate welds.

No definite conclusions have been drawn by the Lockheed investigators regarding parameters which need to be duplicate for a successful transfer of GMA welds.

Integrator's Comments on the Statistical Analysis. Welding engineers have always needed a reliable, rational means of selecting proper welding parameters. There are many variables such as welding current, arc voltage, travel speed, etc., and there are many factors to be considered including penetration, weld shape, mechanical properties of the joint, etc. So far, the selection of proper parameters has been made primarily on the basis of past experience and empirical data. It is very important to develop a scientific technique for this selection.

There is no doubt that statistical analysis would be useful for analyzing experimental data. The attempts in this direction by Lockheed investigations are worthwhile. However, their results are not completely satisfactory.

First of all, results of the statistical analysis are not consistent. This is shown in the regression equations in Table XV. For example, the ultimate tensile strength, Ftu, was a function of T, C × T (interaction between C and T), C, T × D, D, and T × Wd for 1/4-in. GTA welds; while it was a function of T, Ep, V, and Gp for 3/4-in. GTA welds. No significant correlation existed between Ftu and independent variables for 1/4-in. thick GMA welds. The yield strengths of welds were functions of the following parameters:

1/4-in. GTA Welds	3/4-in. GTA Welds	1/4-in. GMA Welds
T × D	Ep	A × Cp
C × D	T	A^2
T × Gp	V	V × A
C × Gp		V^2
Gt		A
		T × A

A second shortcoming in the statistical analysis is the fact that little attention was paid to the physics of the problems studied. As an example, let us discuss problems related to the ultimate tensile strength of a weld. In the Lockheed study, tensile tests were made on transverse specimens, as shown in Figure 31. Many welds contained various degrees of incomplete fusion, as shown in Figure 30. Mechanical properties of such welds should be determined by the amount of incomplete fusion, which is a mechanical factor, as well as by properties of the weld metal, heat-affected zone, and the bare metal, which are material or metallurgical factors. The ultimate tensile

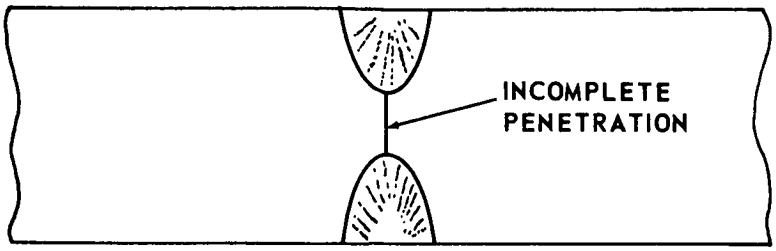

a. WELD WITH LARGE AMOUNT OF INCOMPLETE FUSION, VERY LOW STRENGTH

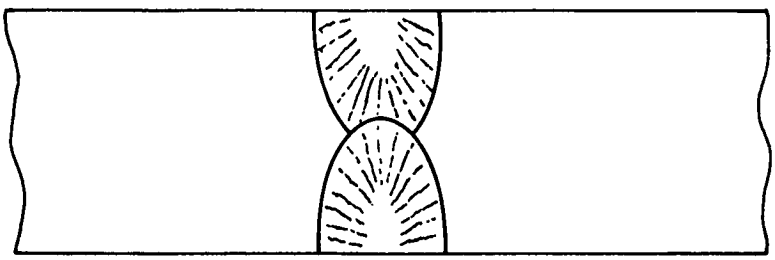

b. WELD WITH COMPLETE PENETRATION, HIGH STRENGTH

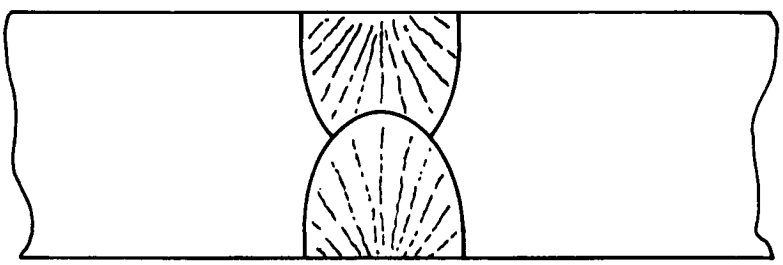

c. WELD WITH EXCESSIVE HEAT INPUT, NOT VERY HIGH STRENGTH

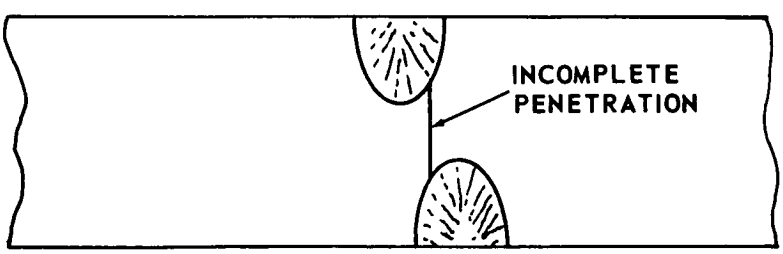

d. WELD WITH MISMATCH, VERY LOW STRENGTH

FIGURE 31. EFFECTS OF WELDING PARAMETERS ON CROSS SECTION AND STRENGTH OF WELDMENTS

strength of the well will decrease as the amount of incomplete fusion increases. It is also known that weld strength in 2219-T87 aluminum alloy decreases as the weld heat input increases, as shown in Figure 2. These mechanical and metallurgical factors affect the strength of welds prepared under various conditions.

Figure 31 shows schematically how welding conditions could affect the strength of a weldment. When a square butt joint is welded with very low heat input, low arc current and high travel speed, the penetration is shallow, as shown in Figure 31a and weld strength would be very low. When a joint is welded with medium heat input to obtain complete penetration, as shown in Figure 33b, weld strength would be high. When a joint is welded with high heat input, excessive penetration results, as shown in Figure 31c, and weld strength would not be very high, because of metallurgical damages due to the excessive heat. When welds made from either side are mismatched, as shown in Figure 31d, weld strength would be very low.

In analyzing effects of welding parameters on the strength of welds, it is important to separate the mechanical effect and the metallurgical effect. Since the strength of welds with incomplete penetration has, in this case, no practical meaning, the analysis should be limited to welds with complete penetration. However, many welds included in the Lockheed study contained various amounts of incomplete penetration. Consequently, the usefulness of the regression equations, shown in Table XVI, on mechanical properties is questionable. For example, consider the regression analysis of ultimate tensile strength. The equation indicates that travel speed had the greatest effect on ultimate strength and that strength decreased as travel speed increased. The results might actually be due primarily to the fact that the sectional area of the specimen decreased as the travel speed increased. Further studies need to be made of physical meanings of regression equations for this and other responses.

9. Magnetic Arc Shaper and Molten-Puddle Stirrer

The use of a magnetic arc shaper and a molten-puddle stirrer for improving properties of GTA welds was studied by Air Reduction Company under Contract NAS8-11954.

The work was conducted in four phases as follows:

Phase I. Design and development of equipment

Phase II. Fabrication and testing

Phase III. Weld evaluation

Phase IV. Equipment refinement.

As of 15 February 1967 Phases I, II, and III had been completed. This report covers information presented in the Thirteenth Monthly Report prepared under Contract NAS8-11954 which summarizes the work conducted in Phase III.

a. Technical Approach and Equipment Development

The object of this phase of the program was to apply various magnetic field configurations to a welding arc and study their effect on weld bead shape, grain structure, porosity, and mechanical strength, in an effort to determine if higher quality welds could be obtained. Three modes of operation were employed.

1) Molten-puddle stirring,

2) Plasma oscillation

   a) Transverse

   b) Longitudinal

3) Plasma shaping

Figure 32 illustrates the three magnetic field arrangements and the respective forces that were produced. For the puddle stirrer (Figure 32a) vertical components of the field interacted with radial components of current flowing in the puddle to produce a rotational force acting on the molten weld.[13] Reversal of the field reversed the force, resulting in a rotational oscillating action in the weld puddle.

In the plasma oscillation mode, two directions of plasma motion were employed, one in the direction of the weld and one at right angles to the weld direction (Figure 32b). The fields were directed perpendicularly toward the plasma current, resulting in forces tending to displace the plasma. An oscillating motion was obtained by using an A-C field.

Plasma shaping was obtained by applying a four pole D-C field to the plasma (Figure 32c). This field (250 gauss maximum at pole face), combined with the field due to the arc current, produced compression forces inward and perpendicular elongation forces in the direction of the weld, resulting in a narrower and longer plasma cross section.

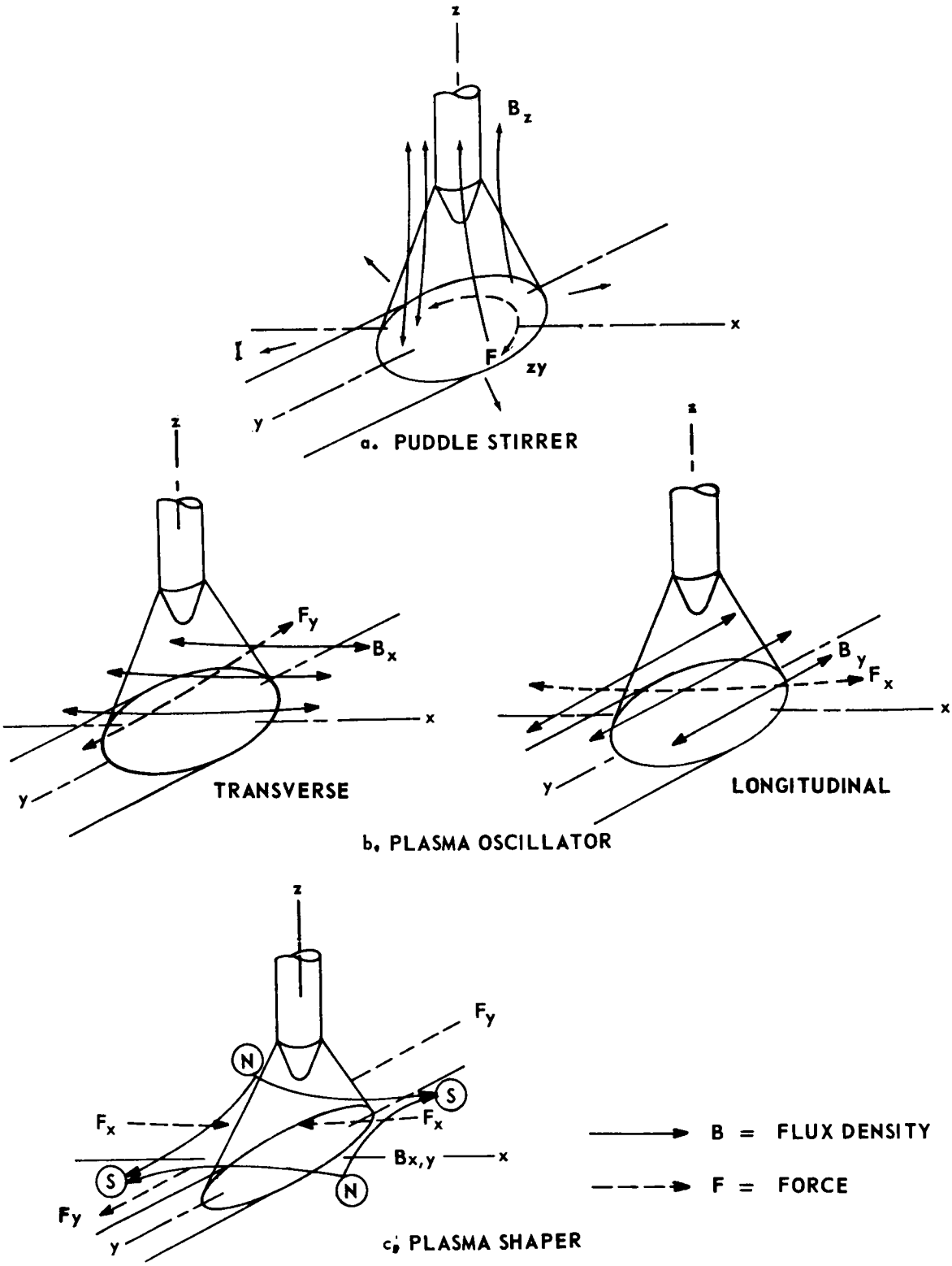

FIGURE 32. MAGNETIC FIELD CONFIGURATIONS

Physical details of the shaper and stirrer coils can be seen in Figure 33.[13] The shaper coil is basically a four pole electromagnet and performs either the shaping or oscillating function by appropriate connection of the coils. The stirrer coil is essentially a solenoid of water-cooled aluminum tubing.

b. Test Conditions

The materials evaluated during this phase were 2014-T6 and 2219-T87 aluminum alloys. Bead-on plate tests were made throughout using 1/2-in. thick plate, 6 in. wide by 18 in. long, unless otherwise noted. The plates were prepared by degreasing and alkaline cleaning, after which they were stored in special plastic bags.

A proximity control was added to welding equipment to maintain constant separation between the head and workpiece. This was chosen over arc-voltage control since the application of magnetic fields modifies the arc voltage and results in arc-length changes.

Unless otherwise stated, the range of the main welding variables was arc current from 240-270 amp and travel speed from 10-11 ipm. The arc length was held at 0.1 in., and helium shield gas was used at a flow rate of 100 cfh. It should be noted that porosity was not introduced by any of the modes of operation. As a result it was necessary to conduct separate tests with induced porosity. This was done by using a premixed tank of shielding gas consisting of 5.5 percent hydrogen in helium.

c. Molten-Puddle Stirring

The general effect of stirring on bead shape was to reduce the depth-to-width ratio of the bead. This was particularly noticeable at low frequencies (10-30 cps) where a severe stirring effect can be obtained. In an extreme case, a depth-to-width ratio of 0.25 was obtained as compared to 0.57 for an unstirred bead. It is believed that under these conditions the molten puddle, due to its fluidity, is being excited into a resonant condition by the stirring action of the magnetic field. As the frequency is increased and the coil current (flux density) is reduced, the bead width decreases and penetration increases toward the dimensions of the unstirred bead. Associated with the bead effect at low frequencies is larger columnar grain growth, viewed in the transverse plane (x-z plane of Figure 32), as compared to corresponding unstirred samples. This implies a possible difference in cooling rate due to

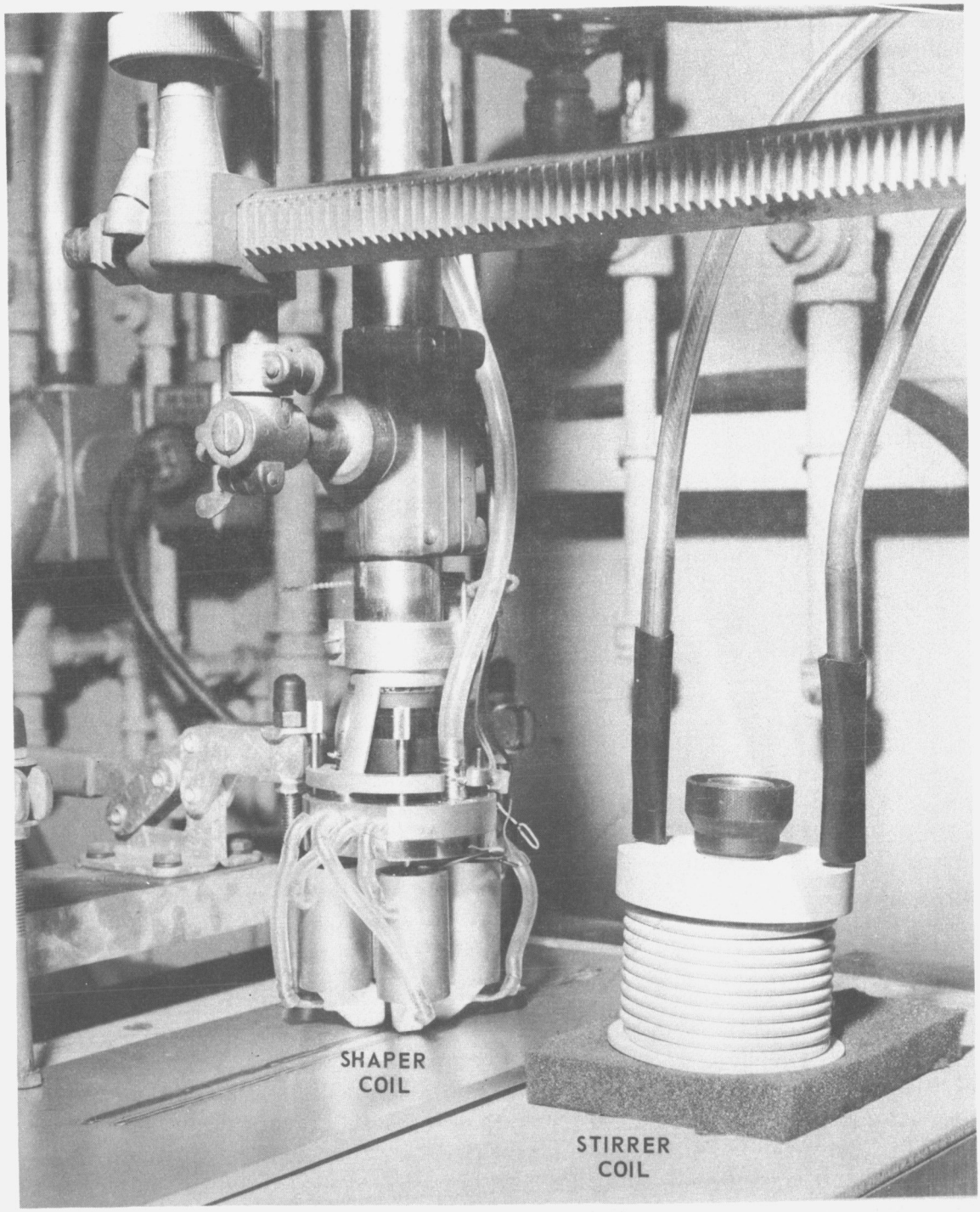

FIGURE 33. COIL DETAILS

the change in bead geometry caused by stirring. One result of this is an effect on porosity as observed in tests where hydrogen was purposely introduced. An increase in porosity level was found at lower frequencies under these conditions. Under normal welding tests, stirring did not introduce porosity.

Increases in mechanical strength properties have been found as a function of stirrer coil current. The most consistent trend occurred in the high frequency range (60-300 cps) with statistically significant increases in ultimate tensile strength near 5 percent. Attempts to relate this to grain structure have not been successful. Subtle differences exist when viewing the macrostructure in various planes but the relationship to strength is not obvious.

The general results indicate that a significant advantage that can be obtained as a result of stirring under certain conditions is an increase in ultimate tensile strength and yield strength. This has been found in the 60-300 cps frequency. An additional advantage of this frequency range is that the depth-to-width ratio of the bead is least affected and also porosity, if present, is not increased due to stirring.

d. Plasma Oscillation

Of the two methods of operation, the longitudinal mode has least effect on bead shape over the frequency range of 10-30 cps. In the transverse mode, the major effect on bead contour is an increase in bead width with increasing flux density. In both modes, increases in ultimate tensile strength were found under certain conditions as compared to welds made with no plasma oscillation. The greatest increases, 4 to 8 percent, were found for the longitudinal mode. Here again, the correlation of grain structure to strength was not obvious. The general trend was toward large columnar grains in the central portion of the bead (transverse section) for the welds subjected to plasma oscillation. Induced porosity was also affected by plasma oscillation, although only in the longitudinal mode. Under these conditions a reduction of gross porosity was found, particularly at the low level of frequency, 10 cps.

Longitudinal plasma oscillation appears to offer the best advantage of these two modes of operation. Improved mechanical properties have been observed with no change in the bead depth-to-width ratio over the range of variables tested. In addition, gross porosity is reduced when operating at the low level of frequency, 10 cps. An observed surface characteristic in this mode of operation is bead undercut, which has been reached at the high level of flux density, frequency, and maximum energy input for the range of variables covered in this test.

e. Plasma Shaping

Plasma shaping had significant effects on weld bead contour. Bead width was found to decrease with increasing flux density under all combinations of the variables tested. The effect of shaping on penetration, however, is dependent on energy input conditions. Initial tests on 1/2-in. aluminum (using helium) showed no significant changes in penetration. However, additional tests on 1/4-in. aluminum (using argon) showed that at high speeds and low energy input, an increase in penetration resulted with the application of a shaping field. This trend reversed with lower speeds and near full penetration welds. Possible explanations may lie in the modified surface-to-volume ratio of the molten puddle and the mode of heat transfer in the plate, which may be two- or three-dimensional flow. Another factor is plasma force, which is related to current density. The plasma cross section is modified due to shaping, resulting in a redistribution of these forces.

A potential benefit of plasma shaping is the increased penetration that may be obtained over an appropriate range of energy input to the weld. Within this range, it is possible to maintain a given bead penetration at a higher speed. This implies lower energy input to the weld and the possibility of higher strength welds. Since penetration effect shows a variance with welding conditions, the specific conditions for obtaining the above advantages require further delineation.

Some mechanical strength tests were performed; however, the conditions were such that the shaping effect was not great and significant differences in penetration did not exist. These results are not considered conclusive, and additional tests would be required to obtain more complete information on the mechanical strength response.

The amount of plasma shaping that can be obtained is limited to that level of flux density that will cause arc "blowout" (e.g., in the longitudinal direction). This is observed using helium gas and relatively long arc lengths, about 0.25 in. Stable operation is possible at a 0.1-in. arc length but with reduced shaping effect. Operation with argon shield gas and a 0.25-in. arc length is possible; tests were made under these conditions. Although poor bead surface and excessive undercut resulted, this was not considered pertinent to determining the major effects of shaping on bead width and penetration.

f. Analysis and Evaluation of the AIRCO Study on Magnetic Arc Shaper and Molten-Puddle Stirrer

Conclusions reached by the AIRCO investigators may be found in the Appendix of this report. The integrator's discussion and evaluation follows.

The work performed at AIRCO is interesting, and the results appear to be valid and well supported. However, judging from these results, the study appears to be of little importance in its application to actual structures. Although increased strengths were obtained by puddle stirring and plasma oscillation, the percentage increases appear to be too small to be of any real significance in any but the most critical ranges. A strength increase of 5, or even 8, percent does not seem worth the addition and complication of special devices near the torch. Such an increase would be significant only if it brought the weld quality from an unacceptable to an acceptable level.

10. Material Preparation

The problem of base-metal surface preparation and contamination was studied at Illinois Institute of Technology Research Institute, under Contract NAS8-20363. The program was divided into three phases. Phase I was concerned with the determination of deleterious surface conditions. As of 15 February 1967, this was the only phase completed. Therefore, this report covers briefly the work accomplished in Phase I. Only 2014-T650 aluminum alloy plate 1/4-in. thick was used in Phase I evaluation. Phase II will involve the development and standardization of analytical methods and measurements of harmful surface conditions. Phase III will apply the results of Phases I and II to produce surface treatments providing high weld quality.

a. Surface Preparations

There are currently an overwhelming number of accepted methods of preparing aluminum surfaces for aerospace welding applications. A systematic study of each particular one would be impractical. Therefore, treatments representative of solvent degreasing, chemical cleaning, and mechanical cleaning were employed in this investigation.

As-Fabricated Specimens. Surfaces of as-fabricated specimens were heavily contaminated with oils, greases, ink, and foreign particles picked up in fabrication, handling, and storage. Small blanks, approximately 1 by 1-1/2 by 1/4 in. were saw cut from the sheets and individually stored in tightly capped jars for subsequent treatment. All further handling of specimens was by Teflon-lined tongs, disposable tissue, or plastic gloves.

Degreasing was performed by a detergent and/or solvent soak. The solvent was a reagent grade of benzene. Samples were immersed for a period of 1 min, followed by a vigorous tissue wipe or warm air dry using a hair dryer.

The original oxide film was removed by chemical cleaning (a 1-min immersion in a 5 w/o NaOH solution at 180 to 190°F). The dark film that formed was removed (desmutted) by a short dip in 50 v/o HNO_3. Agitated rinsing in water and warm air drying followed.

A number of additional treatments were included to produce surfaces having a range of weld-defect potential. These were boiling in water, storage over water, coating with silicone grease, anodizing, and certain combinations of these. Anodizing was done in an electrolyte of 15 w/o H_2SO_4 at 72°F and a current density of 12 amp/ft^2 for periods ranging from 1 sec to 60 min. Water rinsing and warm air drying followed.

Machined Specimens. Numerically programmed machining was done with a Sundstrand 2-axis, Om-3 Omnimil to obtain a reproducible strating surface. The specimen chamber enabled the maintenance of a controllable environment during machining. A dry air (20 percent relative humidity) or a moist air (90 percent RH) atmosphere was used.

The master-specimen configuration for all machining is illustrated in Figure 34.[14] The five surfaces of each arm of the cross were face-milled to remove about 0.015 in. of material. Subsequent treatments were a trichlorethylene degrease, water soak, chemical cleaning in NaOH and HNO_3, or anodize, as before.

b. Weld Tests

In order to determine the weld-defect potential of several surface preparations, a simple weld test, highly sensitive to surface properties, was used in conjunction with selected surface analysis methods.

Samples of a particular preparation were placed together on their 1- by 1-1/2-in. faces and spot welded at the midpoint along the interface. The spot welds were made with the DCSP/GTA process, using the following settings: arc current, 320 amp; arc voltage, 18 v; arc length, 1/16 in., gas, high-purity helium (less than 10 ppm H_2O); arc duration, 2 sec; gas preflow, 1 min; and gas flow, 100 cfh. The resulting welds represented the crater region of a horizontal weld. Depth of penetration was about 1/4 in.

This type of test is extremely sensitive to the properties of the butting surfaces. The gases liberated from the surfaces by the heat of the arc are trapped by solid contact along the fusion line. The pressure of gases generated at the melting front is a function of the amount of surface contamination. At

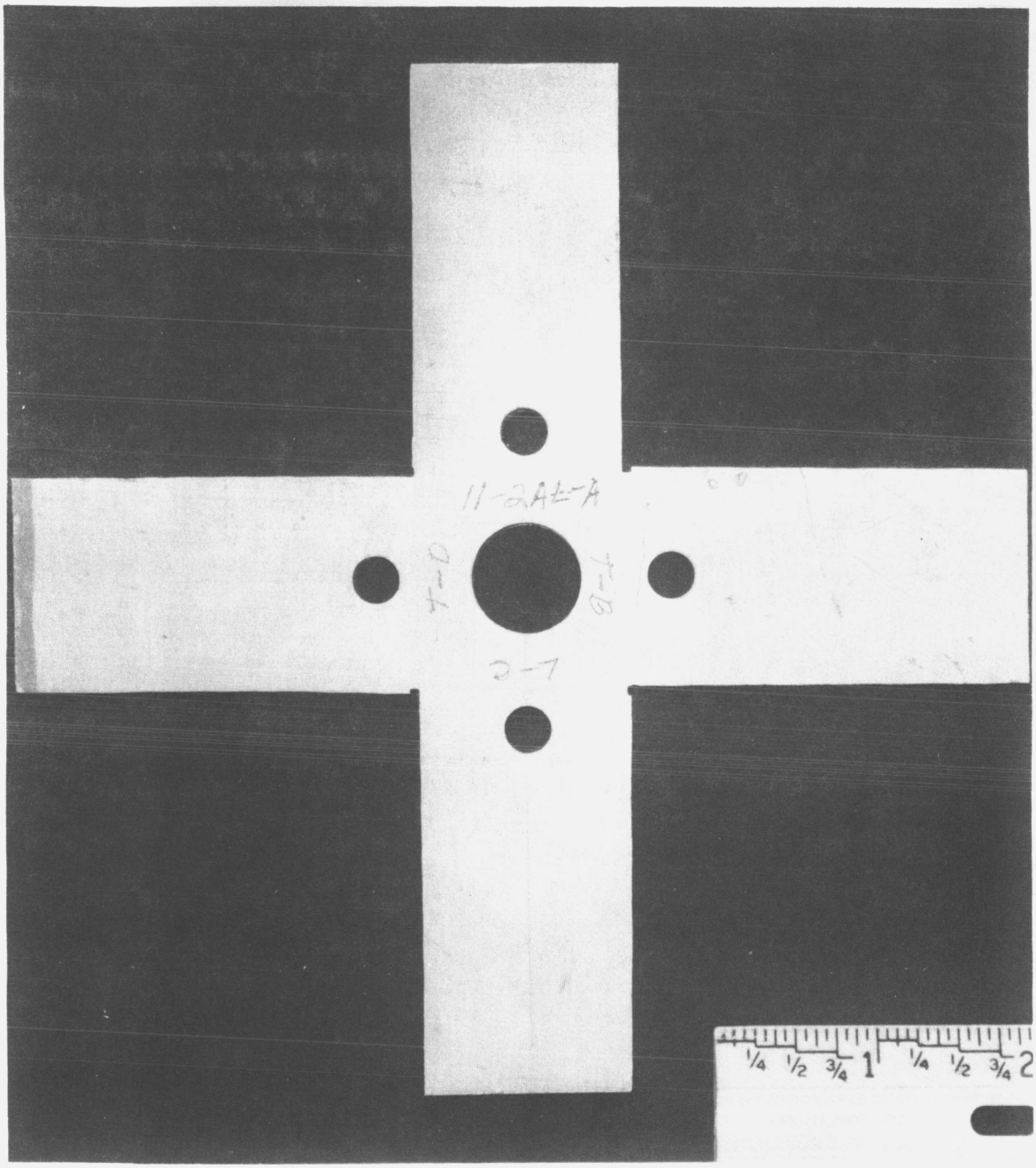

FIGURE 34. MASTER SPECIMEN FOR MACHINING COUPONS

some level of contamination there is sufficient pressure built up to cause the gases to "escape" into the weld pool. Porosity is formed by the rejection of the dissolved gases during solidification and cooling. Heavily contaminated surfaces exhibit porosity throughout the fusion zone, whereas cleaner surfaces are characterized by porosity along the fusion line or complete absence of porosity. The amount of oxide film present on the surfaces regulates the fusibility and depth of penetration along the interface.

In the tests at IITRI porosity was evaluated by separating the pieces, exposing the interface, and inspecting at 30X magnification. The results of these preliminary weld tests are given in Figure 6, as a weld-defect potential scale.

Weld-Defect Potential of Metal Surfaces. The most significant result of this study was that, of the surface preparations examined, only the as-machined surfaces had a zero weld-defect potential as shown in Figure 6. All of the machined-only surfaces exhibited this characteristic. Surface roughness and ambient moisture had no adverse effect within the limits of 50- and 200-μin. finishes and 20 to 90 percent relative humidity.

Surfaces prepared in a moist environment should represent the greatest defect potential of the as-machined specimens. The specimens that were prepared in a 90 percent relative humidity had freshly machined surfaces exposed to this moisture for a period of at least 5 min during machining. Without drying, these specimens were placed in tightly capped jars at about 60 percent relative humidity and stored for 10 to 20 days before welding. This extended exposure to moist air did not result in porosity formation on welding. Similar results were reproduced in two sets of the four as-machined conditions.

Any subsequent treatment of machined surfaces, and all surface preparations used on nonmachined material, produced some degree of porosity. Degreasing alone produced a rather harmful level of porosity, trichlorethylene on machined surfaces being worse than benzene on as-fabricated material. This was apparently due to residual solvent since the porosity was discolored, with an oily or sooty appearance, and the surface water contents were very low.

Chemical cleaning and water rinsing produced a defect potential slightly less than that of water rinsing alone on a fresh surface. Chemical cleaning may reduce the number of adsorption sites and passivate the surface to a degree. Prolonged storage over water (10 days or more) after chemical cleaning had a negligible effect on welding.

Anodizing treatments or silicone coatings on chemically or mechanically cleaned surfaces resulted in a further degradation of weld soundness. Surfaces

anodized for up to 15 sec have a defect potential slightly greater than those chemically cleaned. Longer anodizing treatments (1, 5, and 60 min), or a silicone coating on surfaces, promoted cavernous porosity throughout the weld bead. Fusion was inhibited across and along the interface. Such welds often fell apart on removal from the vise.

It is not possible to make direct comparisons between machined and nonmachined surfaces at this stage. There was no common baseline from which to evaluate the absolute weld-defect potential of the subsequent treatments of each group. The differences in defect potential of a particular treatment from one group to the other may be due to surface finish, surface activity, or contamination burnished in the surface layers of as-received material which can only be completely removed by machining.

c. Surface Analysis Methods

Several methods of surface analysis were selected to obtain a comprehensive characterization of the surfaces. These were radioactive evaporation (Meseran), spectral reflectance, mass spectrometry, gas chromatography, and spark emission spectroscopy. Many of the procedures and results presented for each technique by IITRI are still preliminary rather than proven and accepted. Each will require a great deal more experimentation and refinement in Phase II of this program. In addition, still other methods of analysis are being investigated during Phase II. For these reasons, any present evaluation of these techniques may change and therefore they are not discussed individually in this report. The IITRI report may be consulted for detailed discussion of work to date on each technique. The data that are presented in the Phase I report indicate that gas chromatography and mass spectrometry offer the most promise for reliable analysis.

d. Analysis and Evaluation of the IITRI Study on Surface Preparations

The conclusions reached by the investigator in Phase I of the study are included in the Appendix of this report. The integrator's discussion and analysis of the program follows.

The work conducted thus far has resulted in interesting and important findings. The most important conclusion is that simple machining is the best surface preparation to avoid porosity in aluminum weldments. An extended exposure of a machined surface to moist air did result in porosity formation

on welding. Any subsequent treatment of machined surfaces, and surfaces prepared on nonmachined material, produced some degree of porosity.

At this time, it is the integrator's opinion that future work should be based on these results. This opinion, which could change as work at IITRI develops, has the following basis. Although work on surface analysis techniques is still preliminary, and some of these techniques show promise, none is yet satisfactory or reliable. Each of them is highly sophisticated and will require very closely controlled conditions and highly trained personnel. It would appear that any of these techniques would create both economy and personnel problems if used in a manufacturing process. In addition, their development will run into considerable cost. In light of the conclusion that machining is a satisfactory surface preparation, the question arises as to whether such development is worthwhile. The integrator feels that it might be better to expend funds on developing a method for machining just before welding. This might be accomplished through some device which could precede the welding torch during the welding operation.

LITERATURE CITED

1. J. Sessler and V. Weiss, eds., ALUMINUM ALLOY 2014, Materials Data Handbook, Syracuse University Research Institute, April 1966.

2. J. Sessler and V. Weiss, eds., ALUMINUM ALLOY 2219, Materials Data Handbook, Syracuse University Research Institute, April 1966.

3. W. E. Strobelt, INERT GAS WELDMENT EFFECTS STUDY, Phase I Report (July, 1965-November, 1965), Phase II Report (January, 1966-June, 1966), and Final Report (January, 1966-June, 1966) on Contract NAS8-20168 from Aerospace Group, Quality Control Research Section, The Boeing Company, Boeing Reports Nos. D2-23647-4, D2-23647-5, and D2-23647-6.

4. D. L. Cheever, P. A. Kammer, R. E. Monroe, and D. C. Martin, WELD-BASE METAL INVESTIGATION, Final Report on Contract NAS8-11445 from Battelle Memorial Institute-Columbus Laboratories, July 1965.

5. D. L. Cheever, H. W. Mishler, R. E. Monroe, and D. C. Martin, WELDING COMMERCIAL BASE-PLATE INVESTIGATION, Final Report on Contract NAS8-20303 from Battelle Memorial Institute-Columbus Laboratories, September 1966.

6. D. D. Pollock, W. V. Mixon, and W. W. Reinhardt, MECHANISMS OF POROSITY FORMATION IN ALUMINUM WELDS, Final Report on Contract NAS8-11332 from Douglas Missile and Space Systems Divisions, Douglas Aircraft Company, Inc., Douglas Report SM-52039, June 1966.

7. A letter dated September 9, 1966 from S. F. Frederick, Section Chief, Research Projects, MR & PM, Douglas Missile and Space Systems Division, Douglas Aircraft Company, Inc. to Earl Hasemeyer, Marshall Space Flight Center, NASA.

8. A. C. Willhelm, STUDY ON DEVELOPMENT OF SATURN MANUFACTURING TECHNOLOGY FOR WELDING METHODS AND TECHNIQUES TO REDUCE HYDROGEN POROSITY, Final Report on Contract NAS8-20307 from Southern Research Institute, October 1966.

LITERATURE CITED (Continued)

9. E. J. Rupert and J. F. Rudy, ANALYTICAL AND STATISTICAL STUDY ON THE EFFECTS OF POROSITY LEVEL ON WELD JOINT PERFORMANCE, Technical Summary Report on Contract NAS8-11335 from Martin Marietta Corporation, Martin Company, March 1966.

10. D. Q. Cole, L. W. Davis, and P. E. Anderson, DEVELOPMENT OF CONTROLS FOR TIME-TEMPERATURE CHARACTERISTICS IN ALUMINUM WELDMENTS, Final Report on Contract NAS8-11930 from Harvey Engineering Laboratories, Harvey Aluminum, Inc., October 1966.

11. E. R. Seay and R. H. Kilpatrick, A STUDY OF INERT-GAS WELDING PROCESS TRANSFERABILITY OF SET-UP PARAMETERS, Interim Report on Contract NAS8-11435 from Lockheed-Georgia Company, November 1965.

12. P. A. Gillespie, R. H. Kilpatrick, and R. C. Stewart, A STUDY OF INERT-GAS WELDING PROCESS TRANSFERABILITY OF SET-UP PARAMETERS, Final Report on Contract NAS8-11435 from Lockheed-Georgia Company, January 1967.

13. P. Beischer, MAGNETIC ARC SHAPER AND MOLTEN PUDDLE STIRRER, PHASE III. WELD EVALUATION, Thirteenth Monthly Report on Contract NAS8-11954 from Air Reduction Company, Inc., January 1967.

14. D. E. Kizer, Z. P. Saperstein, and H. Schwartzbart, PREPARATION AND INSTRUMENTATION FOR WELDING S-1C COMPONENTS, Phase I Report on Contract NAS8-20363 from Illinois Institute of Technology Research Institute, November 1966.

15. R. V. Hoppes, WELDING STUDY ON 2219-T87 ALUMINUM ALLOY, Technical Information Report No. TIR-15-64, R-ME MW, Manufacturing Engineering Laboratory, Marshall Space Flight Center, NASA, April 27, 1964, plus additional informal communication.

16. J. D. Dowd, INERT SHIELDING GASES FOR WELDING ALUMINUM, The Welding Journal, 35, No. 4, Welding Research Supplement, 1956, pp. 207s-210s.

17. W. I. Pumphrey and E. W. West, THE METALLURGY OF WELDING ALUMINUM AND ITS ALLOYS, British Welding Journal, 4, No. 7, 1957, pp. 297-306.

LITERATURE CITED (Continued)

18. M. B. Kassen and A. R. Pfluger, CHLORINE ADDITIONS FOR HIGH-QUALITY METAL WELDING OF ALUMINUM ALLOYS, The Welding Journal, 37, No. 6, Welding Research Supplement, 1958, pp. 269s-276s.

19. J. C. Bailey and G. W. Eldridge,. FACTORS INFLUENCING THE PROPERTIES OF WELDS IN ALUMINUM, British Welding Journal, 8, No. 5, 1961, pp. 227-236.

20. G. Westendorp, SOME REMARKS ON THE WELDABILITY OF ALUMINUM, British Welding Journal, 8, No. 6, 1961, pp. 310-315.

21. Z. P. Saperstein, G. R. Prescott, and E. W. Monroe, POROSITY IN ALUMINUM WELDS, The Welding Journal, 43, No. 10, Welding Research Supplement, 1964, pp. 443s-453s.

22. P. J. Rieppel, WELD DEFECTS IN ALUMINUM VERSUS BASE-PLATE AND FILLER-WIRE COMPOSITION, Aluminum Welding Symposium held July 7, 8, and 9, 1964, at G. C. Marshall Space Flight Center, National Aeronautics and Space Administration.

23. F. R. Baysinger, SOME OBSERVATIONS ON POROSITY IN ALUMINUM WELDMENTS, Aluminum Welding Symposium held July 7, 8, and 9, 1964, at G. C. Marshall Space Flight Center, National Aeronautics and Space Administration.

24. D. Rosenthal and R. Schmerber, THERMAL STUDY OF ARC WELDING--EXPERIMENTAL VERIFICATION OF THEORETICAL FORMULAS, The Welding Journal, 17, No. 1, Welding Research Supplement, 1938, pp. 2s to 8s.

25. C. M. Adams, Jr., COOLING RATES AND PEAK TEMPERATURES IN FUSION WELDING, The Welding Journal, 37, No. 5, Welding Research Supplement, 1958, pp. 210s to 215s.

26. T. R. P. Gibb, Jr., J. Electrochemical Society, 93, No. 5, 1948, pp. 198-211.

27. H. J. Emeleus and J. S. Anderson, MODERN ASPECTS OF INORGANIC CHEMISTRY, Van Nostrand, New York, 1944, pp. 231-262.

LITERATURE CITED (Continued)

28. D. T. Hurd, AN INTRODUCTION TO THE CHEMISTRY OF THE HYDRIDES, Wiley, New York, 1952.

29. G. G. Libowitz, Advances in Chemistry Series, 39, 1963, pp. 74-86.

30. E. Sternberg, THREE-DIMENSIONAL STRESS CONCENTRATIONS IN THE THEORY OF ELASTICITY, Applied Mechanics Review, 11, No. 1, 1958, pp. 1-4.

31. J. N. Doodier, CONCENTRATION OF STRESS AROUND SPHERICAL AND CYLINDRICAL INCLUSIONS AND FLAWS, Transactions ASME, 55, No. 7, 1933, pp. 39-44.

32. M. A. Sadowsky and E. Sternberg, STRESS CONCENTRATION AROUND A TRIAXIAL ELLIPSOIDAL CAVITY, Journal of Applied Mechanics, 16, No. 2, pp. 148-157.

33. G. N. Savin, STRESS CONCENTRATION AROUND HOLES, Pergamon Press, New York, 1961.

34. I. I. Faerberg, TENSION APPLIED TO A PLATE WITH A CIRCULAR HOLE WITH STRESSES EXCEEDING THE LIMIT OF ELASTICITY, Trudy, Tsentr. Aerogidr. Inst., No. 615, 1947.

35. H. Kihara, Y. Tada, M. Watanabe, and Y. Ishii, NONDESTRUCTIVE TESTING OF WELDS AND THEIR STRENGTH, 60th Anniversary Series, 7, The Society of Naval Architects of Japan, Tokyo, 1960.

36. E. R. Parker, BRITTLE BEHAVIOR OF ENGINEERING STRUCTURES, John Wiley and Sons, Inc., New York, 1957.

37. FRACTURE TOUGHNESS TESTING AND ITS APPLICATIONS, ASTM Special Technical Publication, No. 381, 1965.

38. A. A. Griffith, THE PHENOMENA OF RUPTURE AND FLOW IN SOLIDS, Phil. Trans. Roy. Soc., 221, 1921, pp. 163-198, and THE THEORY OF RUPTURE, Proc. First International Cong. Appl. Mech., 1924, pp. 55-63.

LITERATURE CITED (Concluded)

39. G. R. Irwin and J. A. Kies, FRACTURING AND FRACTURE DYNAMICS, The Welding Journal, 31, No. 2, Welding Research Supplement, 1952, pp. 95s-100s.

40. G. R. Irwin, FRACTURE, Encyclopedia of Physics, Vol. VI, Elasticity and Plasticity, Springer-Verlag, Berlin, Goettingen, Heidelberg, 1958, pp. 551-590.

41. FRACTURE TESTING OF HIGH STRENGTH SHEET MATERIALS: A REPORT OF A SPECIAL ASTM COMMITTEE, ASTM Bulletin, No. 243, June 1960, pp. 29-40; No. 244, February 1960, pp. 18-28; and Materials Research and Standards, 1, No. 11, November 1961, pp. 877-885.

42. F. L. Jackson, ANALYSIS OF TIME-TEMPERATURE EFFECTS IN 2219 ALUMINUM WELDING, The Welding Journal, 45, No. 8, Welding Research Supplement, 1966, pp. 189s-192s.

APPENDIX

CONCLUSIONS DRAWN BY INVESTIGATORS WORKING ON THE NINE PROGRAMS COVERED IN THIS REPORT

This appendix summarizes conclusions given in the final reports and the interim report on the nine NASA sponsored programs that are covered in this report.

The conclusions given in this summary are essentially those of the investigators on the programs, although they may not be presented exactly as in the original documents.

Research Study for Alternate Development of Saturn Manufacturing Technology for Welding Methods, Contract NAS8-20168, at Aero-Space Division, The Boeing Company, Seattle, Washington

Objective

The major objective of the program was to establish a quantitative relationship between atmospheric contaminants in the arc-shielding medium and the magnitude, frequency, and level of porosity in 2219-T87 aluminum GTA weldments.

Conclusions

Definition of Control Limits. Weld shielding-gas contamination is directly related to the weld quality requirements of a particular production part. As a potential guide for generating control parameters, some of the significant contamination effects have been combined in chart form (Figure 3). The concentration points, relative to a contamination effect, indicate where occurrence of a weld quality change is initially observed. In using this chart, shielding-gas flow rate must be considered in setting weld contamination limits. This is because changes in flow at a given contamination level cause variation in the quantity of contamination introduced to the welding arc per unit length.

Source of Contamination. The determination of the quantitative effects of gases on weldment quality provides an insight into the sources of contamination. High-quality weldments would generally be expected with the present shielding gas purity level if commercially purchased gas were the only consideration. However, contamination originates from many sources, such as residual impurities in the shielding gas; dirty or old connecting lines from the cylinder to the torch; atmosphere influx; airborne particles; oil, water or atmospheric leaks; and surface contamination, and the combination of these determines the absolute level of the impurities introduced to a weldment. As demonstrated in the program, it took 250 ppm of any of the contaminants studied to cause significant quality changes. Should a 250-ppm limit be required for a production process, exceptionally tight control would be necessary on the various sources of contamination. Less than 1 mg/in. would be necessary to continuously generate 250-ppm hydrogen in the shielding envelope. It is estimated that a single fingerprint would result in a 750-ppm hydrogen increase in the area contaminated and a significant increase in porosity. These estimates have been based on the assumption that hydrocarbons on the surface of the weld joint would

have the same effect as an equivalent amount of hydrogen being introduced as a contaminant in the shielding gas. However, hydrocarbons on the surface are expected to be more detrimental because they enter directly into the arc area without dilution, while only a portion of the shielding gas comes in contact with the molten puddle, permitting absorption into the weld metal.

Water vapor or hydrocarbons from atmosphere influx appear to be an unlikely major source of hydrogen contamination.

Individual-and Mixed-Gas Effects. This study showed that for highest weldment quality, impurities in the arc should be maintained below the levels achieved with a 250-ppm addition to shielding gas. A definition of the actual production contamination levels would establish the feasibility of maintaining such a low maximum limit.

In the case of porosity, addition of a contaminant, such as oxygen, could improve weldment quality under certain conditions. It should be emphasized that improved characteristics could be obtained only in isolated circumstances and that the quality would generally be lower than the optimum low-contamination condition.

The addition of hydrogen decreases the tendency for formation of undercut due to weld-bead sag. Undercut is essentially eliminated at 250-ppm hydrogen in the shielding gas without any perceptible change in mechanical properties or porosity levels. The necessity to conduct a second pass weld, which causes a significant decrease in weld strength, might feasibly be eliminated by hydrogen addition if environmental conditions could be sufficiently controlled. It is highly questionable at this time whether the high degree of control necessary for hydrogen addition could be accomplished in a production application.

The program will be of significant value in arriving at shielding gas control levels required for various production situations. In Saturn V welding it would be desirable to establish the optimum control limit below 250 ppm. However, for welding under field conditions, where contamination cannot be carefully controlled, additions of specific contaminants might be used to improve general quality. The data accumulated would be of value in identifying the particular addition and control limits necessary to improve a weld characteristic.

Statistical Treatment of Data. The statistical evaluation was a key factor for the successful correlation and definition of quantitative contamination effects on weldment quality. Mathematical relationships were established for calculation of a specific quality effect when contamination levels are known. The

mathematical formula is limited in that the equation does not provide a universal fit for all points within the ranges studied. More effort is necessary to improve the mathematical expressions.

Methods of Evaluation. The radiographic and density analyses proved most sensitive to determination of porosity change, while the metallographic analyses provided a visual indication of the porosity levels. The fatigue analyses showed a great deal of variation between specimens of the same general quality. This indicates that future evaluation of fatigue like should be based on more samples than were used for this study. The tensile analyses did not show any appreciable change until large amounts of porosity occurred.

Welding-Base Metal Investigation, Contracts NAS8-11445 and NAS8-20303 at Battelle Memorial Institute, Columbus Laboratories

Objectives

The objective of the final phase of this program under Contract NAS8-11445 was to determine the contribution of several specially defined factors, alloying content, hydrogen content, metallic impurities, and shielding gas moisture content, to the weld defect potential of two experimental base plate alloys, 2219 and 2014, and two experimental filler-metal alloys, 2319 and 4043.

The second phase of this program, under Contract NAS8-20303, was to determine specifications for welding materials that would take into account a factor called defect potential. Defect potential indicates the relative possibility of weld defects occurring in a weld made in a base metal of specific composition.

Conclusions

The conclusions reached during the first phase of this program, under contract NAS8-11445, were as follows:

Effect of Four Factors. The relative strength of the relationship between weld porosity (the only weld defect observed) and each of four factors was determined primarily by statistical analyses. The factors are listed below in decreasing order of their significance to porosity level.

1) Shielding-gas moisture content

2) Alloy content

3) Metallic impurities

4) Hydrogen content

An interaction existed between the factors of alloying content and metallic impurities such that the relationship of weld porosity to the level of one factor was dependent upon the level of the other factor. Increasing weld-porosity levels were related to increasing base-plate hydrogen content, but an

interaction between the material composition and hydrogen content prevented any conclusions regarding a definite cause and effect relationship. For X2014 base plate, however, a hydrogen content of 1.8 ppm, by weight, was sufficient to overshadow the strength of the alloying content and metallic impurities to cause a high porosity level. For the filler wires studied, changes in the porosity level were not significant for changes in the hydrogen gas content of up to 1.9 ppm, by weight, except in one anomalous result where an increasing porosity level was related to a decreased hydrogen content. The weld-defect potential for welds made with the materials studied would generally be lowest when all four factors were low.

Pore Occurrence and Weld Composition. The composition of the weld metal was related to the pore size and the pore distribution within the welds. Segregation layers of alternately enriched and impoverished weld metal occurred regularly within the weld in groupings that depended upon the weld composition. Pores within the welds grouped themselves preferentially in the impoverished segregation layers.

Hydrogen Content and Base-Plate Composition. The hydrogen content of the experimental X2219-T87 and X2014-T6 base plate was quite independent of the chlorination times and melting atmosphere. The hydrogen content of the experimental base plate significantly increased as the plate composition was increased from low alloying content and low metallic impurities to high alloy content and high metallic impurities. The filler-wire hydrogen content was controlled by the casting methods used.

Hydrogen Content and Porosity Level. As the hydrogen content of the experimental base plate increased, the weld-porosity level of welds on the base plate also increased. This was probably partly due to the interaction of the material composition and hydrogen content. For 1/4-in. thick X2014* plate, hydrogen content of 1.9 ppm appeared to cause a high porosity level. Increasing hydrogen content of the filler metals for the levels studied was not related to increasing weld-porosity levels.

Arc Waveforms and Shielding Gas. The arc voltage and arc amperage waveforms changed from smooth waveforms when the weld shielding gas contained essentially no moisture to irregular waveforms with large numbers of inflections when the arc shielding gas contained water vapor. The arc voltage waveform also changed shape when contaminants were present in the shielding gas.

---

*The prefix "X" denoted experimentally prepared alloys to distinguish them from commercial alloys.

The results of the second phase, under Contract NAS8-20303, indicated that base-metal composition of commercial 2014 and 2219 alloys was no more than a secondary factor in the formation of weld porosity for the conditions studied. The following significant conclusions were reached:

1) No single element, or combination of elements, was identified as causing weld porosity. The composition of the 2014 and 2219 base plate was related to the amount and size of weld porosity when the arc shielding gas was contaminated with water vapor.

2) The composition variables studied which had a significant relationship to weld porosity for welds in 2014-T651 base plate were, in order of decreasing significance, an interaction of magnesium and manganese and titanium, iron, and internal hydrogen content. Increasing amounts of all of the elements except iron were related to decreased weld porosity.

3) The composition variables studied which had a significant relationship to weld porosity for welds in 2219-T81 base plate were, in order of decreasing significance, zinc, magnesium, a manganese-iron interaction, zirconium, internal hydrogen, and a manganese-iron interaction. Increasing amounts of all of the elements except the manganese-iron interaction were related to decreasing weld porosity.

4) The use of radioactive hydrogen isotopes to study the occurrence of hydrogen in the macrostructure and microstructure of aluminum welds was feasible and can yield definitive results.

5) The hydrogen content of 2014 base plate was strongly related to iron and zinc content. The hydrogen content of 2219 base plate was strongly related to magnesium content. For both alloys, increasing amounts of these elements were related to increased hydrogen content.

6) The presence of increased intermetallics did not seem to have any effect on weld porosity.

7) Pores occurred preferentially within the welds at solute-depleted regions. Nucleation and growth of pores was not uniform across the weld. There was evidence that volatilization of elements such as magnesium formed pores or pore nuclei.

8) Welds in 2014 aluminum tended to fracture inside the weld along the fusion-zone boundary where intermetallics were concentrated and where small epitaxial grains change to large grains. The 2219 aluminum alloy welds fractured diagonally across the weld.

9) Base-metal porosity occurs when gradual thermal gradients exist in the base metal adjacent to the weld. These pores may be associated with the $CuAl_2$ plus aluminum eutectic.

10) The parameters of arc voltage, arc current, and arc travel speed do not completely define the actual welding conditions.

Study of Mechanisms of Porosity Formation in Aluminum Welds, Contract NAS8-11332, at Missile and Space Division, Douglas Aircraft Company

Objective

The objective of this program was to study the mechanisms causing porosity in aluminum welds in terms of metallurgical phenomena as well as welding parameters. Hydrogen is considered to be largely responsible for this problem. The kinetics of this behavior are not well known. Thus, the major emphasis was directed toward an attempt to determine the way in which porosity forms and grows.

Conclusions

The following conclusions were reached:

1) Porosity formation in welds in 2219-T87 and 2014-T6 aluminum alloys results from the absorption of hydrogen by the molten alloys followed by the nucleation and growth of pores during solidification.

2) The porosity nucleation rate is a function of the inverse square of the time required for the melt to reach the eutectic temperature.

3) The porosity growth rate is a direct function of the square of the time required for the melt to reach the eutectic temperature.

4) The percent porosity, time to reach the eutectic temperature, and number of pores in static welds are functions of the water vapor content in the arc atmosphere.

5) The hydrogen content of the static welds is a function of water vapor in the shielding gas, arc current and voltage, arc-exposure time, and thickness of the plate.

6) The percent porosity, time to reach eutectic temperature, hydrogen content, dendrite cell size, and number of pores in bead-on plate welds are a complex function of water vapor in the shielding gas, arc current and voltage, travel speed, and thickness of the plate used in the bead-on plate welds.

7) Free hydrogen in the arc atmosphere in equivalent amounts slightly greater than the highest water-vapor contamination level employed in this study did not produce porosity in the static welds.

8) Free hydrogen in amounts greater than 1475 ppm was required to produce radiographically visible porosity in the bead-on plate welds in 2219-T87 and 2014-T6 aluminum alloys.

9) Statistical analyses of the welding conditions and results of tests on 2219-T87 and 2014-T6 showed no difference in porosity within the limits of experimental error.

Study of Development of Saturn Manufacturing Technology for Welding Methods and Techniques to Reduce Hydrogen Porosity, Contract NAS8-20307, at Southern Research Institute

Objective

The objective of this program was to investigate the feasibility of using scavenging elements for eliminating hydrogen porosity in aluminum welds. The program was designed to determine if these elements would attract hydrogen and remove it from the vicinity of the weld or combine with it to form a harmless inclusion in the weld. The latter phenomenon would be analogous to the role of manganese in combining with harmful sulfur to form relatively harmless manganese-sulfide inclusions in steel.

Conclusions

Under conventional inert-gas arc-welding conditions for aluminum alloys, hydrogen porosity was not eliminated or significantly reduced by the getter materials, which had been chosen as most promising on the basis of literature describing hydride formation. Although the best of the getters did not appear to be primary sources for porosity, they frequently increased the severity of porosity arising from other sources of contamination, such as moisture in the inert gas. With the exception of Ca, which was difficult to apply in its elemental form, the four most promising getters on the basis of the literature study (Ti, Zr, Ce, and Ca) were among the most effective getters in the experimental work. However, other transition elements (such as Fe and Mn) and some compounds were equally as effective in the one group of experiments in which they were included.

It was recommended that fundamental studies of the comparative hydrogen-attracting propensities of molten aluminum and other materials be performed prior to further welding experiments. These studies should include considerations of the form of the materials (finely divided powders, "atomized" liquids, ionized compounds, etc.) as well as the elemental content.

Analytical and Statistical Study of the Effects of Porosity Level on Weld-Joint Performance, Contract NAS8-11335, at Martin Marietta Corporation, Martin Company

Objective

The objective of this program was to enable an inspector to describe pertinent characteristics of a defect in a manner that allows precise prediction of the expected mechanical properties of the weld joint. This information could then be assimilated by a designer, and an intelligent decision could be made regarding expected hardware performance.

Conclusions

The following conclusions were reached:

1) Weld behavior under transverse load is best predicted as a function of the total cross-sectional area of the defects in the expected plane of fracture.

2) For transverse tension testing, the decrease in strength from a constant value (not necessarily the zero defect strength) is approximately proportional to the increase in cross-section area of the defects.

3) A contaminated weld suffers a given reduction in transverse strength, even though the contamination was insufficient to introduce a measurable amount of porosity. This contamination effect may not be contamination in the physical metallurgy sense, but shows itself in fine porosity which is difficult to detect or evaluate by X-ray.

4) This reduced weld strength, caused by "contamination," is the point from which strength varies as porosity increases.

5) Existing weld acceptance criteria do not emphasize enough the effect of very fine pores (less than 1/64 in.) on mechanical properties. Predicting behavior without considering such flaws can lead to erroneous conclusions.

6) The techniques used for obtaining porous welds in this investigation appear to cause a greater incidence of very fine pores than would be expected in normal production welding. This may have biased these conclusions toward an overemphasis of importance of small flaws.

7) Improved nondestructive techniques are required for determining the total cross-section area of flaws in the expected fracture plane. Multiple X-ray shots appear to offer the best promise, but can become difficult or unsolvable if the porosity pattern becomes too complex.

8) Transverse tension fatigue testing is very sensitive to spherical porosity. Fatigue life of a sample with any defect is lower than fatigue life without defect, and continues to fall as the defect increases in total area.

9) Welds which are loaded or stretched parallel to the welding direction are not particularly sensitive, in their mechanical behavior, to defects. Quite respectable strengths and elongations were obtained with this mode of loading with defects which would ordinarily not be accepted in a structure.

10) Sharp defects such as lack of penetration or lack of fusion exert a marked influence on transverse mechanical properties, but a negligible influence on longitudinal mechanical properties. These defects were always found in the plane which is normal to the transverse load.

11) Positions or patterns of multiple porosity arrays are influential to mechanical behavior only to the extent that these patterns place a greater number of flaws in a single plane which is normal to the expected load.

Development of Methods, Tooling Concepts, and Processes to Control the Time-Temperature Characteristics in the Weld and Heat-Affected Zone to Improve Tensile Properties and Reduce Porosity in Aluminum Weldments, Contract NAS8-11930, at Harvey Aluminum, Inc.

Objectives

The objectives of this program were to develop methods, tooling concepts, and processes to control the time-temperature characteristics in the weld and heat-affected zone, in order to improve tensile properties and reduce porosity in aluminum weldments.

Shortening the time-temperature cycle through the critical range (solidification and overaging) improves the properties of aluminum alloys in general and copper-bearing aluminum alloys in particular, and can be extended to apply to weldments in this material. The concept employed in this program for accomplishing the shortened cycle consisted of impingement of a cryogenic liquid on the weldment during welding, and balancing heat input and heat extraction to produce thermal patterns which will result in improved weld properties.

Conclusions

Tensile properties can be improved and porosity can be reduced by properly controlling time-temperature relationships during the welding process.

Use of cryogenic liquid jets as a means of accomplishing the required control is feasible. Limited experimental development performed in this program resulted in improvements in yield strength up to 20 percent for welds chilled by liquid carbon dioxide, with reductions in porosity over 100 percent and drastically reduced warpage. Further work is warranted to obtain statistical data and to refine the concept preparatory to its application to production welding.

It was recommended that such work be performed to establish the limits of the concepts for improvement in properties of welds on a statistical basis and to provide sufficient information for development of criteria for equipment, instrumentation, and procedures to be used in application of the concept of welding of production parts.

A Study of Inert-Gas Tungsten-Arc Welding Process Transferability of Setup Parameters, Contract NAS8-11435, at Lockheed-Georgia Company

Objectives

The major objectives of this research program were (1) to determine and quantize the significance of welding variables in the inert-gas welding process, and (2) to analyze the factors necessary for the successful transfer of weld settings which produce welds with similar characteristics.

Conclusions

Data Analysis. With statistically designed experiments, computer reduction, and analysis of data, it is possible to quickly solve problems and explore the relationships of the variables far beyond our capability using "conventional" techniques. One set of raw welding data may be used in different combinations with computer analysis to simulate many additional welding experiments and equipment modifications.

GTA Penetration. Within the range of the data, the variables that account for a majority of the variation in weld penetration are travel speed, electrode position, current, tungsten tip diameter, and gas purity.

GTA Ultimate Strength. The variables that account for a majority of the variation in ultimate strength are travel speed, electrode position, voltage, and gas purity.

GTA Porosity. Within the range of the data, the variables that account for variations in porosity are inert-gas purity and time-temperature function. Although these variables are the only ones entering the regression equation at the 90 percent confidence level, they account for only a small percentage of the variation in porosity. The predominant porosity variables are not identified.

Transferability, GTA. In order to transfer the following conditions must be met:

1) Accurate instrumentation must be provided for the six basic GTA welding variables of travel speed, electrode position, current, voltage, gas purity, and electrode tip diameter, in order of importance. The instrumentation should have high resolution and, preferably, trace-type potentiometric recorders.

2) The static variables, gas purity, and tungsten-tip diameter must be accurately maintained to set up standards.

Where the conditions above are met, along with duplicate conditions of weld-joint preparation, tooling, and welding position, duplicate trace recordings indicate duplicate welds.

A change of the welding control system from one system to another may preclude the ability to successfully transfer a weld setting. For example, settings that are stable and satisfactory when welding with the conventional automatic "voltage" control system can be transferred to the "Voltage-Proximity-Current" system but the opposite is not always possible. However, duplicate trace recordings of the four dynamic variables indicates duplicate welds regardless of system change.

An accumulation of variation in the minor static variables such as wire-deposit rate, gas flow, gas purity, etc., will cause significant variation in the resulting welds. Wire-deposit volume normally is not a critical variable; however, the angle and position of entry into the weld puddle is extremely sensitive. The filler-wire angle and position of entry must be duplicated in order to duplicate welds.

Design, Develop, and Fabricate a Magnetic Arc Shaper and Molten Puddle Stirrer, Contract NAS8-11954 at Air Reduction Company, Incorporated

Objectives

The objectives of this program were to (1) develop a magnetic arc shaping device and a magnetic molten-puddle stirrer and (2) evaluate the usefulness of these devices for improving properties of GTA welds in aluminum alloy. The program was conducted in four phases:

Phase I. Design and development of equipment

Phase II. Fabrication and Testing

Phase III. Weld Evaluation

Phase IV. Equipment refinement.

Conclusions

This report covers information presented in the Thirteenth Monthly Report which summarizes the work conducted in Phase III. Conclusions presented in the report are described below.

Through the use of the various magnetic field configurations, it was possible to produce effects on weld bead shape, porosity, mechanical strength, and grain structure. It was not within the scope of the program to determine the exact mechanism of these effects, but it was concluded that a primary effect of the magnetic fields is to change the bead geometry either by forces acting on the puddle or by agitation of the puddle. This in turn modifies the cooling rate and produces changes in grain structure, mechanical strength, and porosity. The addition of puddle agitation also introduces a factor in determining resultant porosity level.

Over the range of variables tested, some improvements can be obtained from each of these modes of operation as summarized below.

1) By molten puddle stirring, higher strength welds can be obtained for some optimum value of flux density. In addition, operation of the frequency range of 60 to 300 cps has the least effect on bead penetration, and porosity, if present, is not increased due to stirring.

2) Of most interest in the plasma oscillating configurations is the longitudinal mode of operation. For the conditions tested, increased strength can be obtained, and also a reduction in induced porosity, with no significant effect (i.e., no deterioration) on the bead depth-to-width ratio.

3) Use of the plasma shaper can produce an increase in bead depth-to-width ratio over an appropriate range of energy input to the weld. A given penetration can thus be maintained at higher speed resulting in the possibility of increased strength welds.

Material Preparation and Instrumentation for Welding S-1C Components, Contract DCN6-30-32061 Illinois Institute of Technology Research Institute

Objective

The ultimate objective of this research program, which is still in progress, is to establish standardized methods of assuring high-quality surface preparation for the welding of aluminum alloy S-1C components. To achieve this objective, attempts were made to undertake a logically phased program which includes the following phases of investigation:

Phase I. Identification and classification of deleterious surface conditions

Phase II. Standardization of surface condition measurements

Phase III. Correlation of surface condition and weld quality

Conclusions

This report covers only Phase I of the program. Conclusions reached during this phase are described below.

As-machined surfaces are characterized by a zero weld-defect potential. Conventional surface treatments such as solvent degreasing, chemical cleaning, and water rinsing promote the formation of porosity during welding. The porosity-forming agents are adsorbed solvent, hydrogen, and water. Anodizing and silicone coating produce extremely detrimental conditions for welding. Prolonged storage in moist environments has a negligible effect on welding.

It is not possible to make direct comparisons between machined and nonmachined surfaces at this stage. There is no common baseline from which to evaluate the absolute weld-defect potential of the subsequent treatments of each group. The differences in defect potential of a particular treatment from one group to the other may be due to surface finish, surface activity, or contamination burnished in the surface layers of as-received material which can only be completely removed by machining.

Several measuring techniques show promise for quantitative analysis of surface properties affecting weld quality.

The mass spectrometer method of analysis is attractive in that it permits an identification of all elements and compounds, up to atomic mass 300, released from the surface. All surfaces examined were found to contain trace amounts of C, CO, CO_2, and O_2, along with hydrogen and water.

The data obtained with gas-chromatographic analysis are more reliable and quantitative than others. The total vapors are removed from the specimen so that equilibrium need not be achieved and maintained between the sampling chamber and measuring apparatus during a test. Calibration of the system is simpler and more reproducible than others. Known amounts of water are flashed into the column material, and corresponding peak areas are determined. Unknown quantities are determined by comparison with a plot of standardized peak areas. The calibration of other techniques involves the introduction of vapors into the sampling chamber.

The spark emission analysis technique has the greatest potential since sampling is done under conditions related to the action of a welding arc on a surface. On sparking, the adsorbed layers and oxide film are dissociated from the surface thus permitting a sampling of the total surface. The other techniques rely on much less energetic desorption and probably only measure a portion of the contamination.

(U) DISTRIBUTION

EXTERNAL

	No. of Copies
Air University Library ATTN: AUL3T Maxwell Air Force Base, Alabama 36112	1
U. S. Army Electronics Proving Ground ATTN: Technical Library Fort Huachuca, Arizona 85613	1
U. S. Naval Ordnance Test Station ATTN: Technical Library, Code 753 China Lake, California 93555	1
U. S. Naval Ordnance Laboratory ATTN: Library Corona, California 91720	1
Lawrence Radiation Laboratory ATTN: Technical Information Division P. O. Box 808 Livermore, California 94550	1
Sandia Corporation ATTN: Technical Library P. O. Box 969 Livermore, California 94551	1
U. S. Naval Postgraduate School ATTN: Library Monterey, California 93940	1
Electronic Warfare Laboratory, USAECOM Post Office Box 205 Mountain View, California 94042	1
Jet Propulsion Laboratory ATTN: Library (TDS) 4800 Oak Grove Drive Pasadena, California 91103	2
U. S. Naval Missile Center ATTN: Technical Library, Code N3022 Point Mugu, California 93041	1
U. S. Army Air Defense Command ATTN: ADSX Ent Air Force Base, Colorado 80912	1
Central Intelligence Agency ATTN: OCR/DD-Standard Distribution Washington, D. C. 20505	4
Harry Diamond Laboratories ATTN: Library Washington, D. C. 20438	1
Scientific & Tech. Information Div., NASA ATTN: ATS Washington, D. C. 20546	1
U. S. Atomic Energy Commission ATTN: Reports Library, Room G-017 Washington, D. C. 20545	1
U. S. Naval Research Laboratory ATTN: Code 2027 Washington, D. C. 20390	1
Weapons Systems Evaluation Group Washington, D. C. 20305	1
John F. Kennedy Space Center, NASA ATTN: KSC Library, Documents Section Kennedy Space Center, Florida 32899	2
APGC (PGBPS-12) Eglin Air Force Base, Florida 32542	1
U. S. Army CDC Infantry Agency Fort Benning, Georgia 31905	1
Argonne National Laboratory ATTN: Report Section 9700 South Cass Avenue Argonne, Illinois 60440	1
U. S. Army Weapons Command ATTN: AMSWE-RDR Rock Island, Illinois 61201	1
Rock Island Arsenal ATTN: SWERI-RDI Rock Island, Illinois 61201	1
U. S. Army Cmd. & General Staff College ATTN: Acquisitions, Library Division Fort Leavenworth, Kansas 66027	1
Combined Arms Group, USACDC ATTN: Op. Res., P and P Div. Fort Leavenworth, Kansas 66027	1
U. S. Army CDC Armor Agency Fort Knox, Kentucky 40121	1
Michoud Assembly Facility, NASA ATTN: Library, I-MICH-OSD P. O. Box 29300 New Orleans, Louisiana 70129	1
Aberdeen Proving Ground ATTN: Technical Library, Bldg. 313 Aberdeen Proving Ground, Maryland 21005	1
NASA Sci. & Tech. Information Facility ATTN: Acquisitions Branch (S-AK/DL) P. O. Box 33 College Park, Maryland 20740	5
U. S. Army Edgewood Arsenal ATTN: Librarian, Tech. Info. Div. Edgewood Arsenal, Maryland 21010	1

	No. of Copies
National Security Agency ATTN: C3/TDL Fort Meade, Maryland 20755	1
Goddard Space Flight Center, NASA ATTN: Library, Documents Section Greenbelt, Maryland 20771	1
U. S. Naval Propellant Plant ATTN: Technical Library Indian Head, Maryland 20640	1
U. S. Naval Ordnance Laboratory ATTN: Librarian, Eva Liberman Silver Spring, Maryland 20910	1
Air Force Cambridge Research Labs. L. G. Hanscom Field ATTN: CRMXLR/Stop 29 Bedford, Massachusetts 01730	1
Springfield Armory ATTN: SWESP-RE Springfield, Massachusetts 01101	1
U. S. Army Materials Research Agency ATTN: AMXMR-ATL Watertown, Massachusetts 02172	1
Strategic Air Command (OAI) Offutt Air Force Base, Nebraska 68113	1
Picatinny Arsenal, USAMUCOM ATTN: SMUPA-VA6 Dover, New Jersey 07801	1
U. S. Army Electronics Command ATTN: AMSEL-CB Fort Monmouth, New Jersey 07703	1
Sandia Corporation ATTN: Technical Library P. O. Box 5800 Albuquerque, New Mexico 87115	1
ORA(RRRT) Holloman Air Force Base, New Mexico 88330	1
Los Alamos Scientific Laboratory ATTN: Report Library P. O. Box 1663 Los Alamos, New Mexico 87544	1
White Sands Missile Range ATTN: Technical Library White Sands, New Mexico 88002	1
Rome Air Development Center (EMLAL-1) ATTN: Documents Library Griffiss Air Force Base, New York 13440	1
Brookhaven National Laboratory Technical Information Division ATTN: Classified Documents Group Upton, Long Island, New York 11973	1
Watervliet Arsenal ATTN: SWEWV-RD Watervliet, New York 12189	1
U. S. Army Research Office (ARO-D) ATTN: CRD-AA-IP Box CM, Duke Station Durham, North Carolina 27706	1
Lewis Research Center, NASA ATTN: Library 21000 Brookpark Road Cleveland, Ohio 44135	1
Battelle Memorial Institute ATTN: Mr. Vern Ellzey, 505 King Avenue Columbus, Ohio 43201	25
U. S. Army Artillery & Missile School ATTN: Guided Missile Department Fort Sill, Oklahoma 73503	1
U. S. Army CDC Artillery Agency ATTN: Library Fort Sill, Oklahoma 73504	1
U. S. Army War College ATTN: Library Carlisle Barracks, Pennsylvania 17013	1
U. S. Naval Air Development Center ATTN: Technical Library Johnsville, Warminster, Pennsylvania 18974	1
Frankford Arsenal ATTN: C-2500-Library Philadelphia, Pennsylvania 19137	1
Div. of Technical Information Ext., USAEC P. O. Box 62 Oak Ridge, Tennessee 37830	1
Oak Ridge National Laboratory ATTN: Central Files P. O. Box X Oak Ridge, Tennessee 37830	1
Air Defense Agency, USACDC ATTN: Library Fort Bliss, Texas 79916	1
U. S. Army Air Defense School ATTN: AKBAAS-DR-R Fort Bliss, Texas 79906	1

	No. of Copies
U. S. Army CDC Nuclear Group Fort Bliss, Texas 79916	1
Manned Spacecraft Center, NASA ATTN: Technical Library, Code BM6 Houston, Texas 77058	1
Defense Documentation Center Cameron Station Alexandria, Virginia 22314	20
U. S. Army Research Office ATTN: STINFO Division 3045 Columbia Pike Arlington, Virginia 22204	1
U. S. Naval Weapons Laboratory ATTN: Technical Library Dahlgren, Virginia 22448	1
U. S. Army Engineer Res. & Dev. Labs. ATTN: Scientific & Technical Info. Br. Fort Belvoir, Virginia 22060	2
Langley Research Center, NASA ATTN: Library, MS-185 Hampton, Virginia 23365	1
Research Analysis Corporation ATTN: Library McLean, Virginia 22101	1
U. S. Army Tank Automotive Center ATTN: SMOTA-RTS.1 Warren, Michigan 48090	1
Hughes Aircraft Company Electronic Properties Information Center Florence Ave. & Teale St. Culver City, California 90230	1
Atomics International, Div. of NAA Liquid Metals Information Center P. O. Box 309 Canoga Park, California 91305	1

INTERNAL	No. of Copies
Headquarters U. S. Army Missile Command Redstone Arsenal, Alabama 35809	
ATTN: AMSMI-D	1
AMSMI-XE, Mr. Lowers	1
AMSMI-XS	1
AMSMI-Y	1
AMSMI-R, Mr. McDaniel	1
AMSMI-RAP	1
AMSMI-RBLD	10
USACDC-LnO	1
AMSMI-RB, Mr. Croxton	1
AMSMI-RBR	25
AMSMI-RSM, Mr. Wheelahan	1
AMSMI-RTR	1
AMSMI-SME	1
AMSMI-RFE, Mr. Kobler	1
AMSMI-R, Mr. Fagan	1
AMSMI-RR, Dr. Hallowes	1
AMCPM-NX, Dr. Lange	1
National Aeronautics & Space Administration Marshall Space Flight Center Marshall Space Flight Center, Alabama 35812	
ATTN: MS-T, Mr. Wiggins	5
DIR, Mr. Shepherd	1
R-RP-N, Dr. Shelton	1
I-PL-CH, Mr. Goodrum	1
R-P&VE-MM	1
R-P&VE-SE	1
R-P&VE-SS	1
R-P&VE-SA	1
R-QUAL-Q	1
R-ME-MW, Mr. R. V. Hoppes	100
R-ME-MM, Mr. W. A. Wilson	1

DOCUMENT CONTROL DATA - R & D

(Security classification of title, body of abstract and indexing annotation must be entered when the overall report is classified)

1. ORIGINATING ACTIVITY *(Corporate author)*
Battelle Memorial Institute
505 King Avenue
Columbus, Ohio 43201

2a. REPORT SECURITY CLASSIFICATION
Unclassified

2b. GROUP
N/A

3. REPORT TITLE

INTEGRATION OF NASA-SPONSORED STUDIES ON ALUMINUM WELDING

4. DESCRIPTIVE NOTES *(Type of report and inclusive dates)*
None

5. AUTHOR(S) *(First name, middle initial, last name)*
Koichi Masubuchi

6. REPORT DATE
9 May 1967

7a. TOTAL NO. OF PAGES
170

7b. NO. OF REFS
42

8a. CONTRACT OR GRANT NO.
DA-01-021-AMC-14693(Z)

b. PROJECT NO.

c.

d.

9a. ORIGINATOR'S REPORT NUMBER(S)
RSIC-670

9b. OTHER REPORT NO(S) *(Any other numbers that may be assigned this report)*
AD

10. DISTRIBUTION STATEMENT

Distribution of this document is unlimited

11. SUPPLEMENTARY NOTES
None

12. SPONSORING MILITARY ACTIVITY
Redstone Scientific Information Center
Research and Development Directorate
U. S. Army Missile Command
Redstone Arsenal, Alabama 35809

13. ABSTRACT

This is a report of a program to analyze and integrate data generated from NASA-sponsored studies on the welding of aluminum alloys.

Information in this report comes from the Marshall Space Flight Center, from visits to the Lockheed-Georgia Company, Marietta, Georgia; the Martin Company, Denver, Colorado; the Douglas Missile and Space Systems Division, Santa Monica, California; Harvey Aluminum, Incorporated, Torrance, California; The Boeing Company, Seattle, Washington; the Illinois Institute of Technology Research Institute, Chicago, Illinois; and the Air Reduction Company, Incorporated, Murray Hill, New Jersey.

DD FORM 1 NOV 65 1473 REPLACES DD FORM 1473, 1 JAN 64, WHICH IS OBSOLETE FOR ARMY USE.

14. KEY WORDS	LINK A		LINK B		LINK C	
	ROLE	WT	ROLE	WT	ROLE	WT
Aluminum welding						
Porosity of welds						
Test procedures						
Surface preparation						
Time-temperature control						
Gas contamination						
Inspection						